UNIVERSITY *of the*
WESTERN CAPE

PORE PRESSURE PREDICTION: A CASE STUDY OF SANDSTONE RESERVOIRS, BREDASDORP BASIN, SOUTH AFRICA

By

EKWO ERNEST UCHECHUKWU

A thesis submitted in partial fulfillment of the requirements for the degree of Master of Science (M.Sc.) in Applied Geology in the Department of Earth sciences, University of Western Cape, Bellville, South Africa.

Supervisor: Dr. MimonituOpuwari

May, 2014.

ABSTRACT

The Bredasdorp basin is situated off the south coast of the Republic of South Africa, southeast of Cape Town and west-south-west of Port Elizabeth. It covers approximately 18,000 sq. km beneath the Indian Ocean along the southern coast of South Africa, which is in the southwest of Mosselbay. Bredasdorp basin contains South Africa's only oil and gas production facilities and has been the main focus for oil and gas exploration in South Africa. It is one of the largest hydrocarbon producing block in South Africa, rich in gas and oil prone marine source rocks of kimmeridgian to berriasian age. The wells of interest for this study are located within block 9 which is made up of 13 wells but for this study the focus is only on 3 wells, which are well F-01,F-02 and F-03. The goal of this study is to predict as accurately as possible the areas within and around the sandstone reservoir intervals of these wells with abnormal pressure, using well logs and production test data. Abnormal pore pressure which is a major problem for drillers in the oil industry can cause serious drilling incidents and increase greatly drilling non-production time if the abnormal pressures are not predicted accurately before and while drilling. Petrophysics log analysis was done to evaluate the reservoirs. The intervals of the reservoir are the area of interest.Pore pressure gradient, fracture gradient, pore pressure and fracture pressure model were run. Pressures of about 6078.8psi were predicted around the zone of interest in well F-01, 7861 psi for well F-02 and 8330psi for well F-03. Well F-03 was the most pressured of the three wells. Abnormal pressures were identified mostly at zones above and below the area of interest and predicted pressure values were compared to actual pressure values to check for accuracy.

DECLARATION

I declare that Pore Pressure Prediction : A case study of sandstone reservoirs, Bredasdorp Basin, South Africa is my own work, that it has not been submitted before for any degree or examination in any other university, and that all the sources I have used or quoted have been indicated and acknowledged as complete references.

Name: Ekwo Ernest Uchechukwu.

Signature: 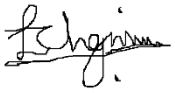

Date: 13-08-2014

ACKNOWLEDGEMENT

I would like to thank GOD for HIS Grace, Mercy and Strength to make this possible.

I would like to thank my supervisor Dr. Mimonitu Opuwari for his ever willingness to assist and support me, his friendliness which made him approachable anytime and his untiring effort to see that this work is a success.

Thank you also to my fellow graduate students Ayodele Oluwatoyin, Moses Magoba, and Hajiera Mosavel for their intelligent discussions, advice, friendship and support. You made this a fascinating and enjoyable experience.

Finally I would like to say thank you to my Parents for their support, upbringing and education, more especially my Mom, you have always encouraged me with love, understanding and patience. I owe much of my success to you.

DEDICATION

This project is dedicated to

My Mom, Mrs. B. Ekwo

For her love, understanding and patience.

She is one of the reasons why this is a reality. Love you dearly.

TABLE OF CONTENTS

Contents

LIST OF FIGURES

LIST OF TABLES

CHAPTER ONE

1.1 INTRODUCTION:

Pore Pressure is the pressure of fluids inside the openings of a reservoir, commonly hydrostatic pressure, or the pressure applied by a column of water from the formation's depth to sea level but it's not always the case. When impervious rocks such as shale formed as sediments are closely packed together, their pore fluids cannot always discharge and must then support the whole overlying rock column, resulting to anomalously high formation pressures.

When drilling, two kinds of pressure can be predicted which are; (1) Shale Pore Pressure (Paul et al.,2009) and (2) Reservoir Pressure. Pore Pressures in shale can be predicted and from that Sand and Shale Pressure can be projected.

Pore pressure of formations is one of the main worries of drillers in the exploration areas today. The pore pressure and fracture gradient, defines the mud weight that is required. Excess mud weight fractures the rock, too little mud weight lets formation fluids to enter into the well and can lead to blow-outs if not controlled.

Pore Pressure Prediction can offer timely warning of the possibility of a gas kick so that the driller can modify the mud weight well before a kick is allowed to happen. Gas kick results in delay in drilling practice as steps are taken to balance the pressure in the well and this can be very costly for the company. In extreme circumstances a gas kick can become a blow-out with much more disastrous consequences up to and including the loss of the well.

Pore Pressure Prediction also influences the decision of casing strings placement. The decision to place casing is determined by how stable the well at a particular level or levels is, and by the alleged risk of encountering a gas kick. For very expensive Deep Oil wells, a conservative method is used by the driller, in which optimum numbers of casing strings are placed. Placement of casing entails that drilling be stopped and the drill string removed from the well. With precise Pore Pressure Prediction one can minimize the total number of casing strings thus dramatically decreasing the cost of the drilling operation.

Accurate and well-timed Pore Pressure Prediction is a “Driller’s Tool”, as it is an aid to the drillers of a gas or oil well that lets them enhance the drilling process for time and cost, and even optimize the final implemented well design.(Real time pore pressure prediction ahead of the bit report by C. Esmersoy, S. Mallick ,2004)

Fracture Pressure is the pressure needed to crack a formation, which leads to the loss of mud from the wellbore into the crack made. When the true vertical depth is divided from the fracture pressure it results to the fracture gradient. “Fracture gradient is the maximum mud weight, thus, it is a vital factor for mud weight design in both drilling planning stage and while drilling. If the mud weight is greater than the formation fracture gradient, then the wellbore will have tensile failure (be fractured), leading to loss of drilling mud or even lost circulation. Fracture pressure can be measured unswervingly from down-hole leak-off-test (LOT)”(Jincai Zhang, 2011). Various methods exist in which fracture gradient can be calculated, e.g. Hubbert and Willis method, Mathews and Kelly method.

1.2: AIM OF RESEARCH:

The aim of this research is to predict as accurately as possible the areas within sandstone reservoir intervals of the wells with abnormal pressure using well logs and production test data.

1.3: STUDY AREA:

The Bredasdorp basin is located off the south coast of the Republic of South Africa, southeast of Cape Town and west-south-west of Port Elizabeth. It covers about 18,000sq km underneath the Indian Ocean beside the southern coast of South Africa, which is in the southwest of Mosselbay. It’s one of the four sub-basins of the Outeniqua basin. Bredasdorp basin which contains South Africa’s only oil and gas production facilities has been the focus area for oil and gas exploration in South Africa.

Hydrocarbon prospectivity is rated high in this basin which is 1 out of the 2 basins that contain almost all of South Africa's proven hydrocarbon. Numerous small oil and gas accumulations have been discovered in the Bredasdorp basin and some are under appraisal. Further exploration in this basin is expected to yield continued success. Bredasdorp basin is a basin that underwent a series of structural deformation during the breakup of Gondwanaland and the rest the continents within the southern hemisphere.

The structural deformation within the area with the addition of sediment influx from the coastal region was sufficient in the formation of average to good source rock. The area mainly consists of half grabens which dip somewhat towards the south with structural pinch-outs finishing the trapping mechanisms for hydrocarbons within the basin. The geologic elements essential for oil and gas accumulation in adequate quantities to create a sufficient pool to be worth producing are: Permeable and Porous reservoir rocks to stock the accumulated oil and gas, Organic-rich source rocks and a structure of seal and trap to stop the oil and gas from seeping away. Fine-grained sediment which in its natural condition has produced and released sufficient hydrocarbons to form profitable accumulation of oil and gas is known as Petroleum source rock.

Figure 1.1 Location Map of the Bredasdorp Basin (Petroleum Agency SA. (2008)).

The Bredasdorp basin is rich in gas and oil prone marine source rocks of Kimmeridgian to Berriasian age. Lower Cretaceous lacustrine source rock which is oil prone is present in the onshore Algoa sub-basin. Acknowledgedgas and oil source rocks which originate from deep marinearepositioned in a rift-drift sequence that is transitional. These are best developed in the bredasdorp basin. The entire source rocks are mature over a large extent. Sandstone reservoirs are available in both the synrift and drift areas; where the sandstones that are drift are deposits of deep marine turbidite, fluvial to shallow marine reservoirs exist (Burden, P.L.A., 1992). The trapping mechanisms within the synrifts are structural as well as truncational. The drift marine shales provide the main seals. Synrift seals also exist and are mainly tilted fault blocks.

The wells of interest for this study are located within block 9 .Block 9 is made of 13 wells but the focus of this work is on well FO1, FO2, and FO3

1.4: REGIONAL GEOLOGY OF BREDASDORP BASIN

The offshore basins of South Africa were split into three dissimilar tecto-stratigraphic units such as the western board passive margin basin that is linked to the opening of the South Atlantic in the Early Cretaceous southeastern offshore basin with a thin passive margin that was made due to the breakup of Africa Madagascar and Antarctia. The basin contains series of echelon sub-basin which is made up of half graben (Burden, P.L.A., 1992).

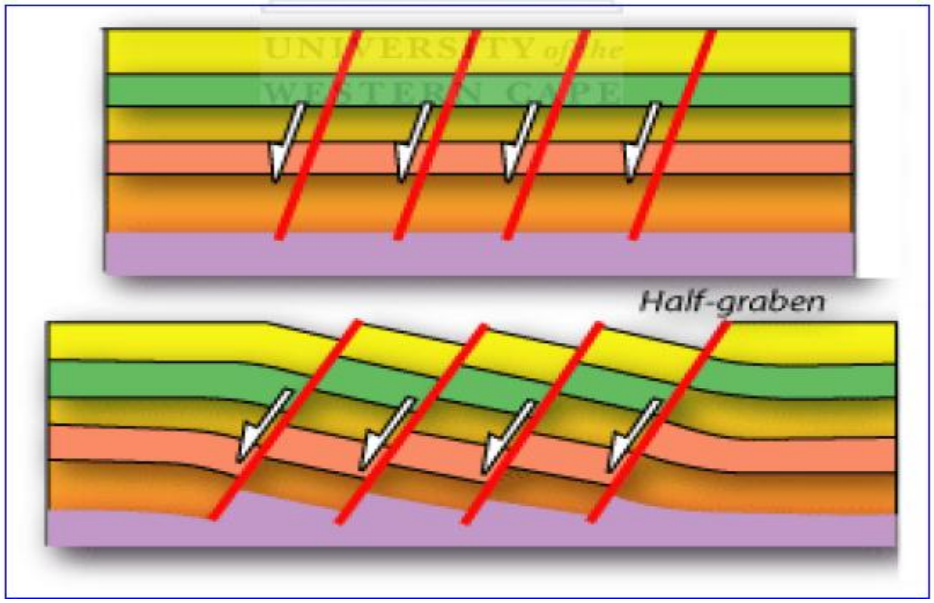

Figure 1.2 Development of half-graben from strings of normal fault plunging in a similar way (Burden, P.L.A., 1992).

The Outeniqua Basins, also called the southern margins, are per se reciprocal action and reaction of transformed margins and separated basins. The Outeniqua basin has the Bredasdorp, Algao, Gamtoo and Plemos as its sub-basins. They show a characteristic of rift half-graben superimposed by change in drift sediment thickness. (Burden, P.L.A., 1992).

In the sub-basin of south-central Bredasdorp basin offshore, the Mid- Cretaceous lowstand system tract which comprises of various sandstones thickness was discovered. The unconformity at the tertiary side is associated with the youngest faults. The Albian age experiencing a type1 unconformity is superimposed by these lowstrand tracts. The steepening of the gradient might have been caused by local tectonic activity that took place within a short period alongside faults next to the Agulhas fracture region.

The lower side of the post rift sequence might have been involved in the displacement of secondary generation drift onset unconformity. Interaction of reduced rift tectonic, contingent eustatic change in universal seal height, and thermal cooling dropped a distinct order of

deposition of sequences of recurring cycles. This is seen in different components of low stand system tracts. Potential reservoirs seem to be present in this sequences. Mounded, basin floor fan, sheet like submarine and submarine channel fill surfaces provided by canyons and cut valleys. Also witihn the area are coastal lowstand wedge, and a prograding delta.

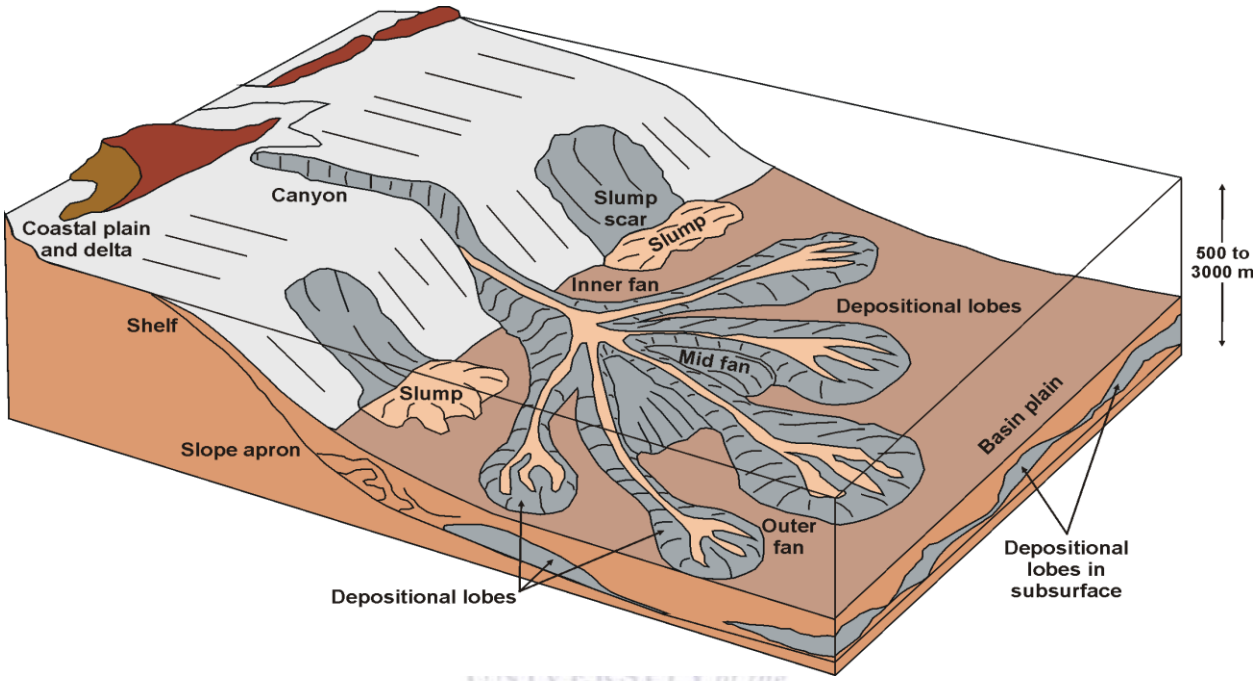

Figure 1.3: Evolution of the deposits of deep marine channel (Petroleum Agency SA. (2008)).

1.5 TECTONIC SETTINGS OF BREDASDORP BASIN

The faulting in the northern Agulhas-falkland fracture area is as a result of the separation in the east which led to dextral transtensional stress. Faults separating the infant arch and Agulhas arch trends northwest to southeast at the synrift phase. The faulting brought about half-graben & graben basins. (Brown et al., 1995, McMillan et al., 1997)

Sedimentation continued from horizon D – At1 (Fig 1.4) till around 126Ma from marine and continental source. Throughout this time rift faulting closed and activities after rift (erosion, deposition, and tectonics) started (Brown et al, 1995). Proof of different subsidence is obvious in the sedimentation due to graben have expanded units from horizon D – 1At1 and horst

structures have condensed units …the sedimentation has different subsidence because of the expanded units of the graben from horizon D-1At1 and the compacted units of the horst structures (Fig 1.4) (McMillan et al., 1997).

Within the rift stage, the sediments supplied into the bredasdorp basin was obtained from provenances in the northeast and the north including slates from Cape Super Group, orthoquartzites, shale and sandstone from the Karoo Basin Super Group (Mc Millan et al., 1997).

Materials were eroded from sandstones that are "high stand shelf which were moved into the middle of the basin by turbidity current from west to southwest because throughout the Early Aptian (112Ma) to Mid –Albian (103ma) the height of the sea plummeted." (Turner et al., 2000). These sediments created "stacked and amalgamated channels and lobes" (Turner et al., 2000) "that comprise of fine lobes of upward-coarsening nature with reservoirs comprising of deposit characterised by upward-finings" (Turner et al., 2000).

The fan lobes dominated the eastern side of the basin and the channels are dominant in the western to south-western zone (Turner et al., 2000). In the south of the basin source rocks of the Aptian age can be found, a 50km long and 5km wide submarine channel formed with tributaries up dip which serve as a medium of deeper sedimentation (McMillan et al., 1997) while having a type-1 component the organic material is predominantly type2 (Van Der Spuy, 2000). The uplift of the horst blocks and arches triggered the 1At1 unconformity which ended the sedimentation of the active rift. According to McMillan et al., (1997) 13A channel form the oil accumulation site.

Thermal subsidence formed the 1At1 – 13At1 sequences, continued the deposit of post rift on-lap-fill sequences and reactivated the normal faulting. Basin floor-fan sandstones are present in the 14A sequence in the middle of the basin that has some reservoirs bearing oil.

Uplift caused the onset of unconformity 6At1 (Brown et al., 1995). Sediment run to the middle zone of basin from 5At1 – 13At1 was dominated by turbidity current. Oxygen and water circulation was lacking in this area (McMillan et al., 1997). The occurrence of cycle6 -12 (3rd -

order) between 117.5 – 112Ma was given by the second supercycle of the post-rift phase. (Brown et al., 1995).

Sequence 6A was formed by rein subsidence at high rates, with sequence 7 taken away by 8At1 erosion throughout 116 – 115Ma, faulting and subsidence rates slowing down (115.5 – 112Ma) system tract 8 – 12 deposition occurred (Brown et al., 1950). Miocene rocks are superimposed by the unconformities in Late Pleistocene and Holocene (McMillan et al., 1997). Fig. 1.4 shows the chronostratigraphic log that displays these properties. It displays two synrift stages. One from Lower Cretaceous (112Ma) to Early Jurassic (157.1Ma) and the other shorter synrift stage inside Hautenvian (fraction of the Lower Cretaceous), divided by the initial type-1 unconformity (1At1). The biogenic clay was deposited and uplift of the arch over the southern area of the basin was marked by Early Miocene.

Erosion took place within this period which carved submarine valleys and canyons into pre-1At1 units, these provided passages for sediment transfer into the deeper basin zone from the west, southwest and northwest. (McMillan et al., 1997) The onset of unconformity 6At1 was caused by uplift. (Brown et al., 1995) Turbity current dominated the sediment flow into the central region of the basin from 5At1 to 13At1. This area lacked adequate water circulation and oxygen. (McMillan et al., 1997)Marked by 15At1, with slight warping and some uplift the late cenomanian (Fig. 1.4) showed erosion. (McMillan et al., 1997)

In the most eastern section of the basin erosion was at the extreme. A shale was found immediately above 15At1 (Fig. 1.4.) that contains a rich content of plankton and other organic materials, which has a source rock potential mostly in the south and absent in the north (McMillan et al,1997).With the little prospect source in the southern region the rock is too immature. Between the Mid- Coniacian time and Turonian, progradation took place. A domal structure was formed in the south eastern region of the Bredasdorp Basin around the latest Cretaceous period (Fig. 1.4.), which formed one of the few late structures forming in the basin (McMillan et al., 1997).

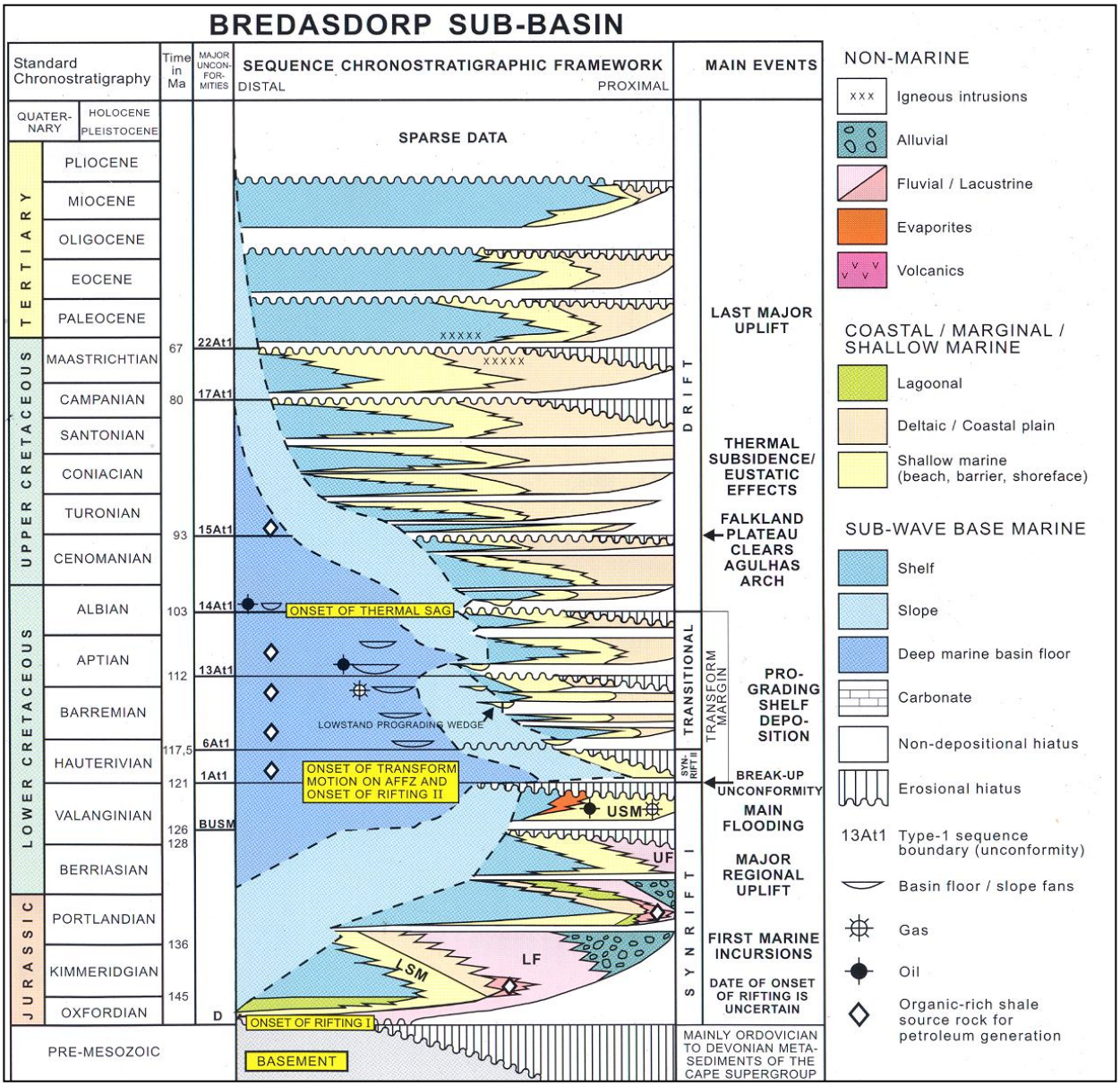

Figure 1.4 Bredasdorp Basin chronostratigraphy (Petroleum Agency SA. (2008)).

CHAPTER TWO

2.0: LITERATURE REVIEW

Drilling is a key component of the petroleum industry. Pore pressure is a property of the formation that has direct impact on drilling and completion of wells. Pore pressure which is the pressure exerted by fluids in the pores of a reservoir, normally hydrostatic/pressure exerted by the column of water from the depth of the formation to sea level is a major issue faced by drillers in the exploration sector. Abnormal pore pressure can lead to very serious drilling incidents like well blowouts, fluid influx and could greatly increase non-productive drilling time if not predicted accurately while and before drilling. Over pressure is a common drilling hazard that presents safety risk and economic problems to the industry on a yearly basis. Knowing the pore pressure is important to decide the mud weight to be used when drilling and also crucial for evaluating exploration risk factors including seal integrity and migration of formation fluids. In the bore hole, drilling mud creates hydrostatic head to balance the formation pressure during drilling. Overburden pressure is the pressure at any depth that results from the joint weight of the fluids in the pore space and the matrix of the rock superimposing the formation of interest.

Overburden pressure rises with depth and is also known as the vertical stress. As overburden pressure increases with depth, when water is ejected from shale mudrocks compaction continues, the vertical effective stress increases and the grains are driven closer, thus the pore space reduces. When the porosity decreases, the permeability diminishes too. When the permeability reduces such that the water can no longer be effectively expelled, the pore pressure starts to assume some of the load borne by the grain contacts, taking the pore pressure above normal pressure and giving the shale mudrock over pressure.

Resistivity, density and sonic velocity of a normal pressured formation will normally build with profundity of entombment and the manner in which such rock properties contrast with entombment under typical pore pressure settings is known as normal compaction trend.

2.1: CAUSES OF ABNORMAL PORE PRESSURE

The major variance between ordinarily and anomalous pressured rocks is that in anomalous pressured regions the pore liquids no more correspond 100% capably with the water-table (surface correspondence). Some component is giving a seal or top to hamper the liquid segment and keep it from achieving normal hydrostatic balance. When the progression of the liquid section has been broken, the pore liquids could be followed up on in various ways. Using Ian's analogy for instance, on the off chance that we took the zone of anomalous pressure as a compartment, it might exist in three circumstances ; 1) it may be impeccably closed like a balloon, 2) it might gradually seep like a punctured tire, or 3) it may be leaky to the point that it holds pressure for a brief period of time (these exceptionally broken seals are not regularly purposely drilled yet have other topographically critical roles, for example, being the reason for significant landslips and slope failure.)

The efficacy of the seal is determined by

- The amount of differential pressure,
- Thickness,
- The duration at which the pressure variations took place,
- Permeability.

The best seal would be perfectly impervious, pliable rock, able to keep its form and typify a rock that is porous and loaded with liquid. Salt is a sample of such a lithology. As such, loads of stern pressure issues may be interfaced to salt. The seals most generally drilled are shales and clay stones. Not all shale/clay stone series are impervious even the densest, however a great blend of low penetrable and satisfactory thickness can maintain significant overpressures, especially if the rock still has enough elasticity.

To a certain degree, due to low permeability, there might be a pressure aura surrounding the anomalous pressured area which extends further to the following variety in vertical permeability. The slow seepage of pressure demonstrates that overpressures are extremely transitory, except the pressure is consistently renewed by an alternate charging process. Research by Bradley 1975, found that “there just needs to be a spillage of one "drop" of water

for every square centimeter consistently for 300 years to drain off a differential pressure of 1000 psi. This is inside the permeability range of numerous shales.” (Bradley, 1975)

Therefore bigger anomalous pressures are prone to be met where the procedures that structured them are fresh or still dynamic and seal proficiency is still high. To portray the distinctive pressure forming mechanisms (some just assumed and some demonstrated) some basic analogies are needed." "The easiest is a barrel loaded with water. The barrel has a settled volume, certain rigidity and a fixing proficiency dependent on how immovably the cover is secured on. To alter the inward pressure in the barrel one of the following can be done; 1) change the volume of the fluid or 2) change the volume of the barrel. It is additionally significant to think on the fluid without any gas top (like a half vacant soda container) since gas has a high compressibility and a low hydrostatic impact, which can result in extremely differing pressures at the highest point of the compartment from those that might have been experienced without gas.

Let’s consider first, frameworks where the compartment size alternates, however not in harmony with the liquid (i.e. no liquid leaves or comes in), then contrast them and frameworks where the compartment size does not change, despite the fact that these are not simple differentiations to achieve.

As we consider these processes and the land setting in which they take place, we shall find that information of how pressure abnormalities start truly can help the well planner to foresee trouble regions. (Ian Hillier, BH, 2007)

Lower Pressure Environments

Changing compartment size:

In the event that the pressure in the compartment diminishes, the compartment will loosen up and swell (if flexible). Liquid effectively inside the framework are necessary to fill a large space if no fluid can enter the system any longer, so the pressure drops.

Geological setting:

Zones where the thickness of the overburden has been incredibly uprooted by disintegration, the sediments which are more flexible (like claystones and shales) may loosen up enough to experience a pore volume increase. This increment in volume might pull in liquids from close-by and interbedded porous rocks (lenticular sands) making the pressure in those sands to lessen. On the off chance that the liquid in the zone is not enough, the entire framework, including clays, will be underpressured. In underpressured compartment the seal is completely supported by the matrix.

Compaction Disequilibrium:

Compaction disequilibrium has to do with sediments being unable to expel their pore fluids in response to sediment loading, which leads to fluid overpressure.

In normal sediment compaction, formation porosity decreases as pore liquids are discharged. Throughout entombment, expanding overburden stress is the primary driver of liquid removal. In the event that the sedimentation rate is slow, normal compaction happens, i.e. harmony between the overburden increasing and capability to dislodge liquids is sustained (Mouchet and Michell, 1989). This normal compaction produces hydrostatic pore pressure in the formation. At the point when the sediments subside quickly, or the formation has very low penetrability, liquids in the sediments can be released partly only, and the liquid left over must carry all or some of the weight of overburden sediments. This leads to anomalous high pore pressure. For this situation the porosity decreases less quickly than it ought to be with depth, and formations are in compaction disequilibrium or under-compacted." Sometimes it could be identified "by higher than anticipated porosities at any given profundity and the porosities diverged from the normal porosity pattern."(ips.org.uk/origins of abnormal pressure)

Changing fluid volume:

Depletion of aquifers and reservoirs via production are the well-known cause of underpressure. Therefore encountering underpressured sands in mature fields are not unusual. Where there is no seal supported by matrix, there will be compaction of the surface subsidence and reservoir as the full load is taken by the matrix.

Low water table:

A water bearing rock with an outcrop under the water table or water table which is low will bring about underpressure. Underpressure is not as catastrophic as overpressure, but the subsequent loss of circulation and resulting loss of hydrostatic pressure control in the well can even be more disastrous than a basic kick from overpressure, and might be far harder to oversee.

Tectonics:

Tectonics has to do with the methods which control the properties and structure of the Earth's crust, and its development over time which in its self is over pressure dependent, short of "the lubrication" of colossal overpressured rock masses, liquids couldn't move like they used to at the bottom of the thrust. Aggregate absence of twisting along numerous thrust exhibits the effectiveness of the liquids in the faulting process, it is conceivable to bore into a thrust whose pressure is still high, yet usually their effect is two-fold. (Ian Hillier, BH, 2007)

1. It can raise compartments to more elevated amounts without cracking. The point before thrusting can additionally cause pressure. In the foreland basins of Active Mountain building thrust belts the horizontal stress can get to double the overburden before faulting happens, any of that stress which acts straightforwardly on the pore liquids should absolutely prompt excess pressure. (Ian Hillier, BH, 2007)

2. It may stack the sediments lying under and if seals exist, perpetrate additional pressure on the enclosed pore liquids. The pressure might be changed if the geothermal gradient is sufficiently changed.(ips.org.uk/origins of abnormal pressure)

Clay Diagenesis:

The digenetic varieties that happen in a few sorts of clays are generally known to be the reason, either by implication or straightforwardly, of overpressure. Over the last two decades the exact nature of this mechanism has been ardently debated. The essential thought of this mechanism is that the surficial, more youthful argillaceous sediments are consistently rich in smectite clay called montmorillonite. The primary characteristic of the smectite group is its high surface territory. These clay platelets are held together by a frail electromagnetic power (van der Waal's bonds), and there is a sizeable measure of zone to which up to ten layers of water can bond. This brings about low density swelling clay, much like bentonite (a smectite mud), which is a key element of drilling fluids.

Smectite clays experience various transformations with profundity. At the outset, increasing pressure will push out the inexactly bound water (a methodology like typical compaction), however as the amount of layers decrease, the pressure needed to discharge the water left over increments. At last, just chemical processes and high temperature will discharge the last layer, which might be bound with metallic cat ions.

Virginia Colton- Bradely (1987) mulled over "absolutely physical dewatering of smectites and its potential part in the generation of overpressure." She established that "smectites in the pore spaces of sand, under hydraulic pressure, find it incredibly hard to lose their last two water layers. At the point when smectites inside shale are subjected to lithostatic pressure and a temperature of 67 – 81 degrees centigrade the penultimate layer will be dislodged. A further climb in temperature to 172 – 192 degrees centigrade is obliged to drive off the last layer which is nearly bound between the mud plates.

The climb in these serious temperatures is influenced by nearby overburden and despite the fact that the past dewatering may really bring about a few overpressures, the ensuing

additional hydrostatic pressure will likewise have a tendency to avoid further dewatering. Subsequently, under most circumstances the basic dewatering process won't bring about intemperate overpressure, as there is a negative input circle at work. In any case, there is additional chemical diagenesis to bear in mind." (Bradely, 1987)

The limit temperature at which hydrocarbons are produced is about the same for the loss of the penultimate water layer. At this stage the smectites can transform into illite muds. Reliant upon the sort of smectite (K or Na smectites respond more rapidly than Ca or Mg smectites), the availability of existent cat-ions like K^+ will be okay for the surface charges replacing water and breakdown the mud into the more smaller illite-type.

The water left over is dislodged into the new porosity made by the decrease in mud volume. Theoretical studies have as of late moved down speculations that this last water is truly dense and unsettled on its ejection.

Osmosis:

Osmosis is the process whereby water particles move down to the angle of water concentration (i.e. fresh – saline). The particles move continuously until the salinities adjust or pressure hinders further development. That pressure is known to be up to 4000 psi in the subsurface, where shales can be the semi-permeable membranes. (ips.org.uk/origins of abnormal pressure)

Imposed pressure:

Sometimes a framework may be present with no pressure aberrance yet with a sensible seal. Past pressures may have seeped away, abandoning a compartment prepared to get pressure from an outer source. Formations like this could be reenergized from various sources, from faults and even by drilling. During production man-made charging takes place, as liquids are pumped into a reservoir in place of the removed hydrocarbon. (ips.org.uk/origins of abnormal pressure)

Aquathermal Pressuring:

In actuality when "a tin of water is set over a flame it will pop its cover." Change in temperature, related to cooling can prompt reduction in pressure. A rock has to move to a higher geothermal gradient for it to be heated. The gradient is capriciously zoned, where some inner basins are cool and some active continental margins are hot." The resultant increase in pressure and rate of expansion in aqueous brines was reported by Barker in 1972, and was reprimanded by Danies in 1980. The contention was "does water expand" or "does the expansion cause pressure" yet "can the seal truly hold the pressure?". (ips.org.uk/origins of abnormal pressure)

The increase in volume needed to generate pressure is in the order of 0.05%, well inside the seepage or elastic abilities of all except the hardest, stiffest, and most impervious seals. It is more probable that aquathermal pressuring is an additional drive that breaks seals, moves liquids and pressures, usually keeping the frameworks dynamic. The convection of liquids is additionally determined by redistribution particles that can influence diagenesis, and temperature, in the upper part of numerous basins.(ips.org.uk/origins of abnormal pressure)

Faults:

By and large faults are discontinuity in a volume of rock or planar crack, crosswise over which there has been critical shift along the cracks due to the movement of the earth. They are frequently brought on by or connected with overpressure. When moving and enlarging, pressure can basically be exchanged. This can bring about moving liquids to a past low potential or draining pressure off, bringing it back to hydrostatic. Faults are likewise great sidelong seals.

Basin structure:

Most deep basins seem to be broken into two areas. From the surface to 10,000 ft., the frameworks are convective, boundless and hydrostatic, with mixtures of a several insitu systems bringing about overpressure." This shows up usually as a form of compaction disequilibrium.

Beneath 10,000 ft, the basins are compartments with boarders or layered cells that slice through lithological and stratigraphic boarders. It is in this deep basin condition, at high pressures and temperatures that the seal seismic pumping works (instead of basic fault charging).

As the basin lessens, hydrocarbon develop, amass and are discharged with hot liquids frequently pumped upwards to produce the regional seals, territories of anomalous hot liquid and sidelong seals. Some hydrocarbon presence has been identified with openings in the parallel seals (following in zones of high pressure potential hydrocarbons tend not to aggregate). At the point when a compartment is cracked, it tends not to be the water that leaves but the hydrocarbons.

Gas hydrates and pingos:

Avariety of conditions exist where critical overpressures can be generated in cold, deep seas and in the Polar zones. Gas hydrates are solidified consolidations of methane inside crystalline water. Due to the arrangement of methane inside the ice, it can store more than 160 times a greater number of gases for every unit volume than free gas. Once drilled, they can cast out colossal measures of gas. Biogenic and leaking gas can likewise amass beneath permafrost. "Pinto" is a well-known evidence of water overpressure brought on by ice, a type of mud-lump in the tundra, these anticlinal- looking hills develops in the winter because of the solidifying of shoaling lakes, trapping the water and compacting it. (ips.org.uk/origins of abnormalpressure)

Evaporite Deposits:

Evaporite deposits can assume a major part in the development of geopressures by the part it plays in sealing. Evaporites are completely impervious, they get to be nearly perfect seal to liquid movement. This hindrance to the vertical release of liquids from underlying sediments, together with restrained sidelong seepage can create overpressured zones in formations underlying evaporite successions. The movement of these formations, for example, halite, additionally implies that any crack that generates can be fixed immediately, keeping up the salt's efficiency as a seal. This movement can have the inverse impact by making "openings" in the formation where the salt was and permitting some liquid run out. (ips.org.uk/origins of abnormal pressure)

Tectonism:

Pore pressure might be influenced by the mobility of salt domes in many ways;

1. Osmosis could be of great importance if sediments comprising of diverse pore liquid salinities are brought nearer, detached by a semi-pervious mud membrane.

2. Lateral seepage might get inhibited and Pierced formations may get secluded.

3. While retaining their original pore pressure, secluded rafts of pervious rock may get stuck inside the salt dome and likewise be moved to greater levels.

4. Formerly sediments lying deep might be pushed nearer to the surface while retaining their original pore pressure. They are no more "ordinary" when compared to neighboring formations.

Hydrocarbon Gradient:

Disparities in the pore liquid gradient, and thus in the greatness of the pore pressure is brought on by the vicinity of hydrocarbons in the pore liquid section. Oil and gas have lesser fluid densities than water and their existence will produce less than anticipated pore pressure gradients. Where gas exist as a free gas top, superimposed by impervious rocks, its

compressibility can cause a higher than anticipated pore pressure gradient, until the water or oil section is gotten to. The pore pressure might then come back to normal.

Sulphate Diagenesis:

In a way like that of montmorillonite, dehydration sulfate diagenesis can help in the making of geopressured areas. The precipitated type of calcium sulfate is gypsum. Change to anhydrite happens a little bit early in the burial process, normally over 40 degrees centigrade (this temperature will be brought down to about 25 degrees centigrade if salt is available, with pressure a fundamental variable). The conversion from gypsum to anhydrite consists of the production of free water into pore spaces. On the off chance that this is restricted and sidelong seepage is inhibited, then it could prompt rise in pore pressure. Water adding up to 38% of the first capacity may be ousted, yet since the variation regularly happens at shallow profundities, it is by and large plausible for majority of the discharged water to seep.(ips.org.uk/origins of abnormal pressure)

Hydrocarbon Migration and generation:

A distinct element in generating overpressure is the breakdown results of organic particles, especially in profound and exceptionally shallow conditions. The pressures they produce are for the most part unrelated to compaction, and owing to this the systems used to determine geopressures created by compaction disequilibrium won't work fine. The mix of this, alongside the developing number of deep wells, which require on location pressure monitoring, is one of the most astounding tests for the "pressure engineer" today (ips.org.uk/origins of abnormal pressure).

Biogenic Methane:

An organic material confined inside sediments, without being oxidized at first, is a major focus for bacterial rot and steady cooking. This rot makes pockets of shallow gas since, much like the production of marsh-gas, the temperatures are normally excessively low to generate any oils and the organic matter is likely to be of terrestrial inception (lignites, peat). The microscopic organisms (bacteria) in existence in the ground water acts to create

this methane gas. Some shallow gas may have coined out at more terrific profundities and has leaked out as a crest into the surface sediments, where it gets stuck under the surface muds or permafrost.

Cellulose might be broken down into both carbon dioxide and methane

$C^6H_{10}O_5$ -> CO_2 + CH_4

The carbon dioxide and methane, in the event that they break to the surface, could be the source of calcareous knobs on the seabed and may structure mounds or diapirs where the fluid has been relocated from the current deposited muds by the gas. This will make the muds to have additional buoyancy linked to their surroundings. Any further gas seepage will result in gas tufts into the ocean. Where the gas leakage does not affect the muds, the outcome might be deep carters and pock-marks in the seabed. Shallow gas can generate significant drilling risks. On account of the low fracture gradients inside the sediments, dynamic kill or diverter lines approaches are normally utilized. Prevention of shallow gas by close consideration regarding high resolution seismic, or other counterbalance information is essential." The utilization of MWD resistivity instruments and drilling of little diameter pilot gaps can upgrade detection and repress issues from developing.

2.2: METHODS USED FOR PORE PRESSURE AND FRACTURE PRESSURE PREDICTION

BEN EATON METHOD

Eaton Resistivity:

Under compaction is the primary driver of overpressure in young sedimentary basins e.g North Sea, Gulf of Mexico. Eaton (1972, 1975) gave the accompanying mathematical statement for pore pressure gradient prediction in shales utilizing resistivity log;

Ppg = OBG – (OBG – Png) (R/Rn) ^n

Ppg = Pore pressure gradient

OBG = Overburden gradient

Png = Hydrostatic pore pressure gradient (typically 0.45 psi/ft or 1.03 Mpa/km, reliant on the salinity of water).

Rn = Shale resistivity at ordinary (hydrostatic) pressure

n = an exponent which differs from 0.6 to 1.5, and normally n = 1.2.

R =shale resistivity acquired from well log

This approach is applied essentially for young sedimentary basins, where the normal shale resistivity is calculated correctly. Assuming that the normal shale resistivity is constant, is one methodology, accurate determination of the normal compaction trend line is an alternate method of determining pore pressure.

Eaton Interval Velocity and Transit time;

The following observational mathematical statement was displayed by Eaton (1975) from sonic compressional travel time for pore pressure gradient prediction;

Ppg = OBG – (OBG – Png) (Dtn/ Dt) ^3

Where Dtn = sonic travel time at the normal pressure

Dt= sonic travel time in shales gotten from well log, and could be gotten likewise from seismic interval velocity.

This methodology is usable in some petroleum basins, however unloading impacts are not put into consideration. This hinders its utilization in complicated topographical zone, in the same way as formation uplifts. The normal travel time (Dtn) must be identified for one to utilize this method.

EQUIVALENT DEPTH METHOD;

The Equivalent depth approach is an example of the analysis utilizing trend line. A depth section is first assumed in this method where the pore pressure is hydrostatic, and the sediments are generally compacted due to the deliberate rise in effective stress with profundity. Normal Compaction trends (Ncts) might be shown as straight lines fitted to the data over the ordinarily compacted interim after the log of a measured quality are plotted as a function of profundity. Pore pressure at any profundity where the measured value is not on the NCT (Normal compaction trend) could be calculated from the equation below as the value of the measured physical property is a distinct function of effective stress. (ips.org.uk/origins of abnormal pressure)

$Pb = Pd + (Sz – Sa)$

Where Pb = Pore pressure at b

Pd = Pore pressure at d

Sb = Stress at b

Sd = Stress at d

b = depth of interest

d = depth along the normal compaction trend at which the measured parameter is the same as it is at the depth of interest

Effective stress is a linear function of profundity, this is the main significant presumption needed when the equivalent depth system is utilized.

RATIO METHOD:

Here, pore pressure is computed based on the supposition that for resistivity, sonic delta-t, and density singly, the pore pressure is as a result of the normal pressure increased (multiplied) or separated by the degree(ratio) of the measured value to the normal value for the same profundity (depth).

$P_p = P_{hyd}\Delta T_{log} / \Delta T_n$,

$P_p = P_{hyd\rho n} / \rho_{log}$, and

$P_p = P_{hydRn} / R_{log}$,

The subscripts n and log indicate the normal and measured values of resistivity, density, or sonic delta-t, Phyd is the normal hydrostatic pore pressure and Pp is the real pore pressure. Calibration of this approach needs knowledge of the right typical value of every parameter. It is vital to perceive that in distinction of trend line systems, the ratio approach doesn't utilize effective stress or overburden explicitly thus is not an effective stress methodology. This can result in unphysical conditions, where the overburden is lower than the computed pore pressure.

BOWERS METHOD:

Miller's sonic methodology portrays a relationship between effective stress and velocity that could be utilized to associate seismic/sonic travel time to formation pore pressure." An input parameter maximum velocity depth, dmax, determines if unloading has happened or not utilizing this approach. Unloading has happened, If dmax is short of what the depth (Z) is, the pore pressure can be gotten utilizing the equation;

P = SV – 1/^ ln(Vm– Vml/ Vm – Vp)

Where Vm= sonic interim velocity in the shale matrix (asymptotic transit time at infinite effective stress, Vm = 14,000 – 16,000 ft/s)

Vp = the compressional velocity at a given profundity

^ = experimental parameter that characterizes the rate of increase in velocity with effective stress (usually 0.00025)

dmax = the profundity at which the unloading has happened.

SV = overburden stress

On the off chance that dmax> or = Z, then unloading behavior is assumed, the pore pressure in the unloading case is ascertained from the equation

Pulo= SV – 1/^ ln[am(1 – Vp – Vulo/ Vm – Vml)]

Where am = the ratio of slopes of unloading and virgin loading velocities in the effective stress curve sul(normally am = 1.8) and am = Vp/ Vulo

sulo = the effective stress from unloading of the sediment

Vulo = velocity at the beginning of unloading.

TAU METHOD:

Shell proposed a pore pressure prediction technique that depends on velocity as it introduced a "Tau" variable in the mathematical statement of effective stress (Lopez et al., 2004; Gutierrez et al., 2006);

Se =AsTBs

Where As and Bs= the fitting constants

T = the Tau variable, and T = (C – Dt)/ (Dt – D)

Dt = the compressional travel time either from seismic velocity or sonic log

C = the constant associated with the travel time (mudline) (typically C = 200 ms/ft)

D = constant associated with the travel time (matrix) (normally D = 50ms/ft.)

The pore pressure can be computed from the equation below;

P = Sv – As (C – Dt/ Dt – D)Bs

Miller's method and the Tau model are like the Bowers' method. The playing point Tau method and Miller's approach have is that both the impacts of the matrix and mudline velocities are put into consideration predicting the pore pressure.

FIELD METHOD:

This is utilized for the most part when formation pressure is due to under compaction. The formation liquid underneath the boundary must support the rock matrix, formation liquids and overburden, in the event that it is assumed that compaction does not take place beneath the boundary depth. The pressure is computed as;

P = df psi/ft (DB) + OVB psi/ft (Di – DB)

Di = profundity(depth) of interest beneath the boundary, ft

DB = profundity of boundary, ft.

P = pore pressure at Di, psi

df =density of formation liquid, psi/ft.

OVB = overburden stress gradient, psi

FRACTURE PRESSURE:

Fracture pressure is the pressure needed to rupture the formation causing loss of mud from wellbore into the induced crack. Dividing the true vertical profundity by the fracture pressure gives the fracture gradient. The facture gradient can be taken as highest mud weight.

Various hypothetical and field-created mathematical statements have been utilized to estimate fracture pressure/gradients. The vast majority of these are suitable for quick

application in a given zone, while a hindsight method based on density or other logging measurements gotten after the well have been drilled." Some of the fracture pressure prediction methods are;

Mathews and Kelly Method:

Mathews and Kelly created the accompanying mathematical statement for computing fracture gradients in sedimentary formations after they understood that the cohesiveness of the rock matrix is regularly identified with the matrix stress and differs just in the level of compaction;

F = (P/D) + (Ki Sm/ D)

Where, P = formation pressure at the area of interest, psi

D = depth of interest, ft.

Sm = matrix stress at the area of interest, psi

Ki = matrix stress coefficient

F = break inclination at purpose of investment, psi/ft

Di = the depth for which the matrix stress is normal.

The value of Di is utilized to get the value of Ki utilizing the Mathews and Kelly matrix stress coefficient plot.

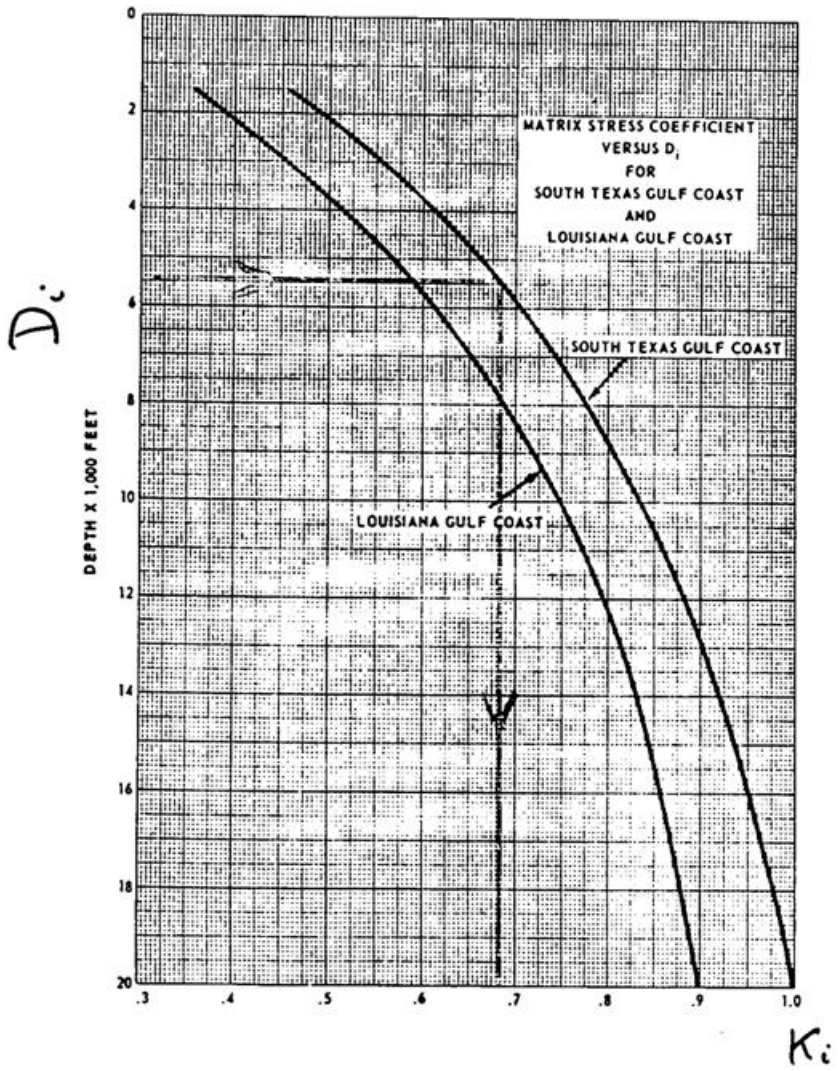

Figure 2.1 Matrix stress coefficients of Mathews and Kelly (Eaton, B.A., 1972)

Hubbert and Willis method:

Hubbert and Willis investigated the variables included in starting a crack in a formation. They accepted the fractured gradient is a function of formation pressure, overburden stress, and a relationship between the vertical and horizontal stress. They accepted the stress relationship to be within ½ to 1/3 of the aggregate overburden." The fracture gradient is in this manner dictated by;

Fmin = 1/3 (1 + 2p/ D)

Fmax = ½ (1 + P/D)

Where P = pore pressure, psi

D = Depth

Fmin , Fmax = least and greatest fracture gradient

NB: for quick solution the graphical method can be used also to determine the fracture pressure/gradient using the Hubbert and Willis graph.

Ben Eaton Method:

Ben Eaton amplified the ideas offered by Mathews and Kelly to bring Poisson's ratio into the equation for the fracture pressure gradient;

$F = (S – P)/D \times v/ (1 – v) + P/D$

Where P = pore pressure, psi

D = depth, ft

v = Poisson's ratio

S = overburden stress

F = fracture gradient, psi/ft

Eaton also has a quick solution graph to calculate overburden stress;

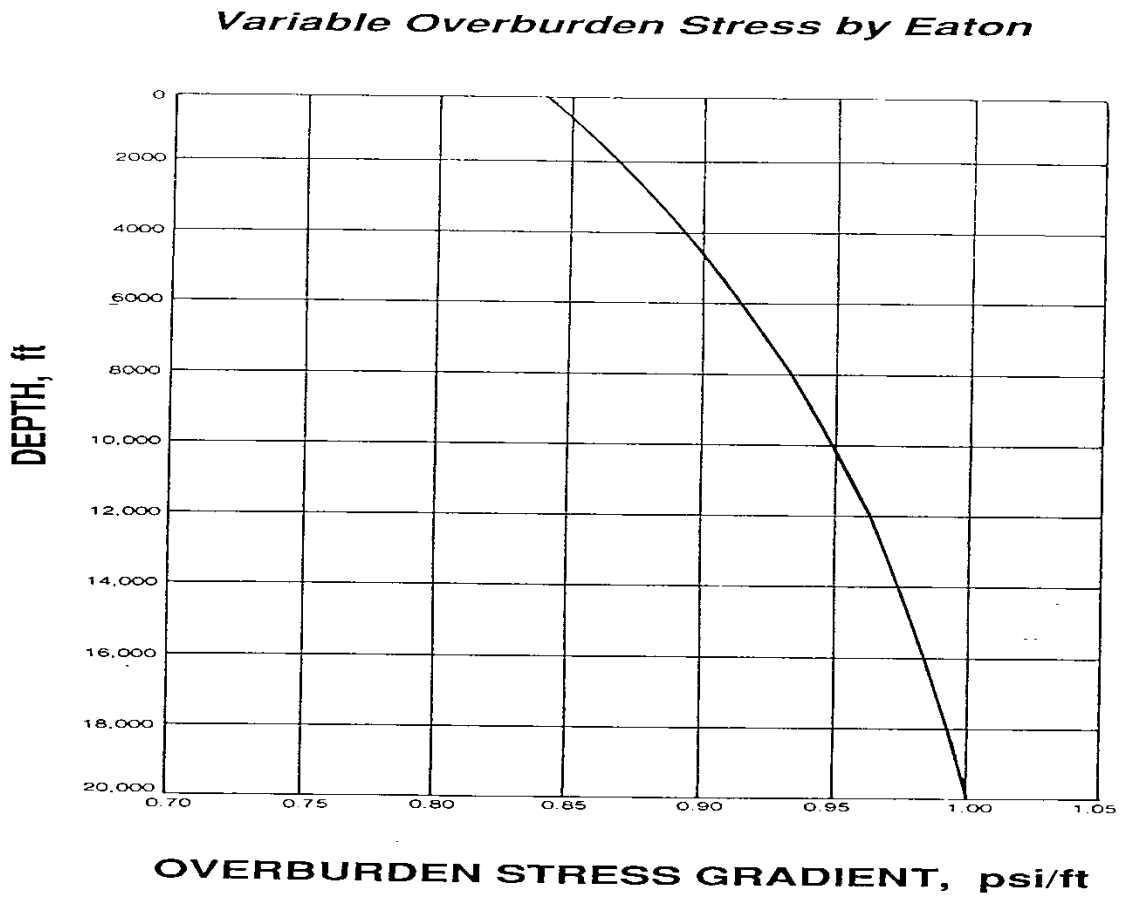

Figure 2.2 Eaton Overburden stress graph (Eaton, B.A., 1972).

The Poisson's ratio value can be gotten using the Poisson's ratio graph;

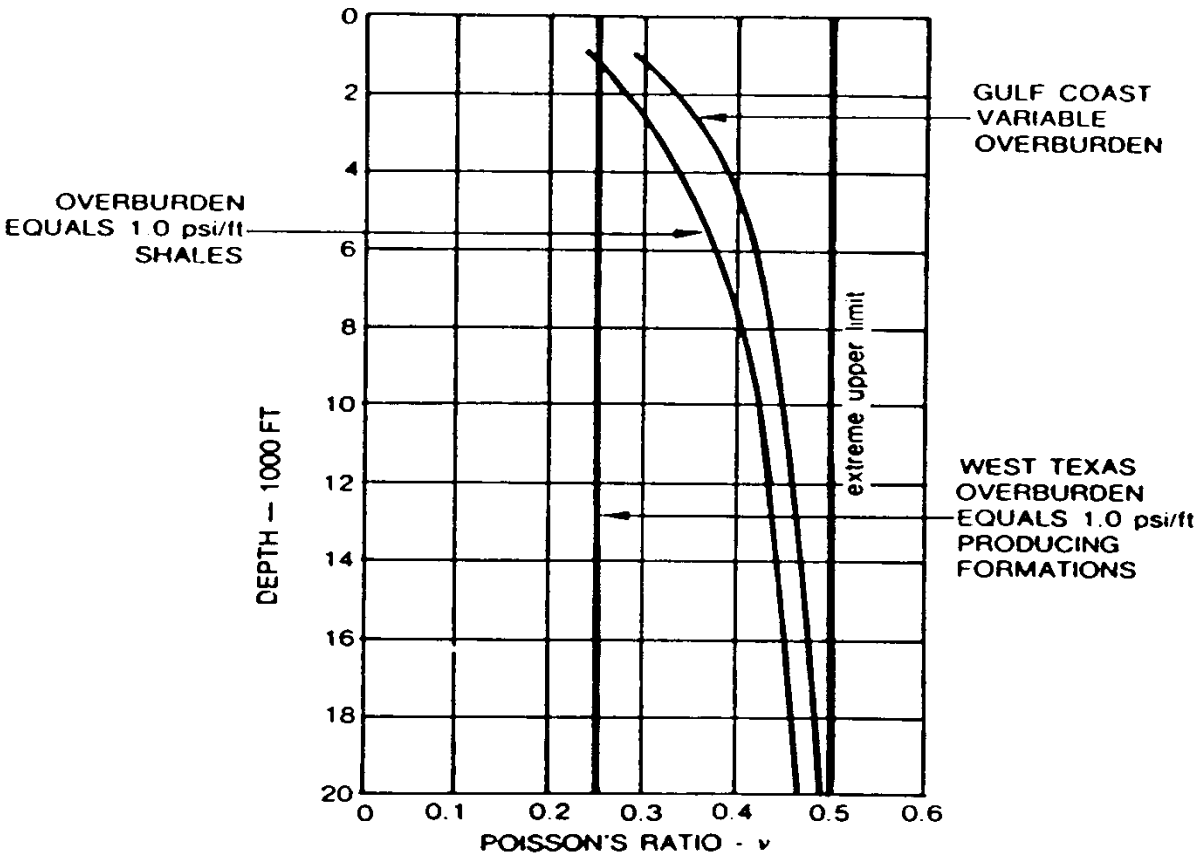

Figure 2.3 Poisson's Ratio Graph

2.3: INTERACTIVE PETROPHYSICS 4.0 (IP)

Interactive Petrophysics (IP) is a petrophysics computer application which is useful for geologists who wish to check the nature of their log information, and accomplished petrophysicists who do petrophysical field analysis on multi-zone and multi-well. It is a simple log analysis instrument. For the individuals who are specialists in IP, it offers a portion of the sophisticated interpretation modules in the business like:

- Statistical Prediction: A suite of modules to anticipate log curves, rock type or facies, core data. Add value to limited datasets by anticipating missing data. Improve your combination of the petrophysics and static reservoir model.

- Rock Physics: Modeling of elastic impedance, fluid substitution, shear sonic estimation and QC, creation of seismograms and additionally with better adjustment to the logs, more value from seismic information is gotten.
- Pore Pressure Prediction; Predict pore pressure utilizing log information and other geomechanical information thereby reducing hazard as over pressured areas which might cause operational and security issues are recognized.
- Real Time Data; get connected with a remote information server and load real time drilling information and log curves in IP .Automated analysis workflows can spare important operational time with quick interpretation.
- nDpredictor; This module predicts log curves, facies and rock types, core data. It is great in anticipating petrophysical properties from mudlogs. This is economical as logging programs are lessened.
- Monte Carlo Analysis; Monte Carlo recreation of a complete workflow to enhance your understanding of parameter sensibility and the instability in the petrophysical interpretation.
- Saturation Height Modeling; Model saturation as a function of height utilizing core capillary pressure information and decrease instability in the petrophysical elucidation and give vigorous functions to dynamic reservoir simulation models.
- Formation Testing; LWD and wireline, Formation analyzer pressure-time information analysis, to comprehend the reservoir better. Fluid gradients and contacts determination, compartmentalization and reservoir connectivity identification.
- image Processing and Analysis; A complete work stream for handling and translating any Wireline or LWD picture log, including “state of the art" picking tools, exceptional connections between picks, and statistical analysis of the outcomes. Save money, enhance data quality and extract more value by doing your LQC and interpretation.

IP is owned by SYNERGY and is utilized by more than 500 organizations, in excess of 70 nations worldwide.

CHAPTER THREE

3.0: METHODOLOGY:

Petrophysics log analysis was done to evaluate the reservoirs.

The summary of the data used for this study is as follows:

Table 1. Summary of Data used

Well name	Conventional Log	Conventional Core	Completion Report	Special Core Analysis	DST	RFT	Petrography
F-01	X	X	X			X	
F-02	X	X	X			X	
F-03	X	X	X				

Schlumberger ran the conventional suite of open-hole wireline logs in all the wells. Some of the vital measurements for this study gotten from all the wells are;

- ✓ Gamma-Ray, Bit size, Caliper
- ✓ Resistivity Logs- Deep Induction, Spherical Focused laterolog/shallow resistivity log, Micro Spherical focused laterolog/medium resistivity log
- ✓ Porosity Logs- Density, Neutron, Sonic

Data acquired was reviewed, edited where necessary and loaded into the petrophysics software used for this study for petrophysical modeling.

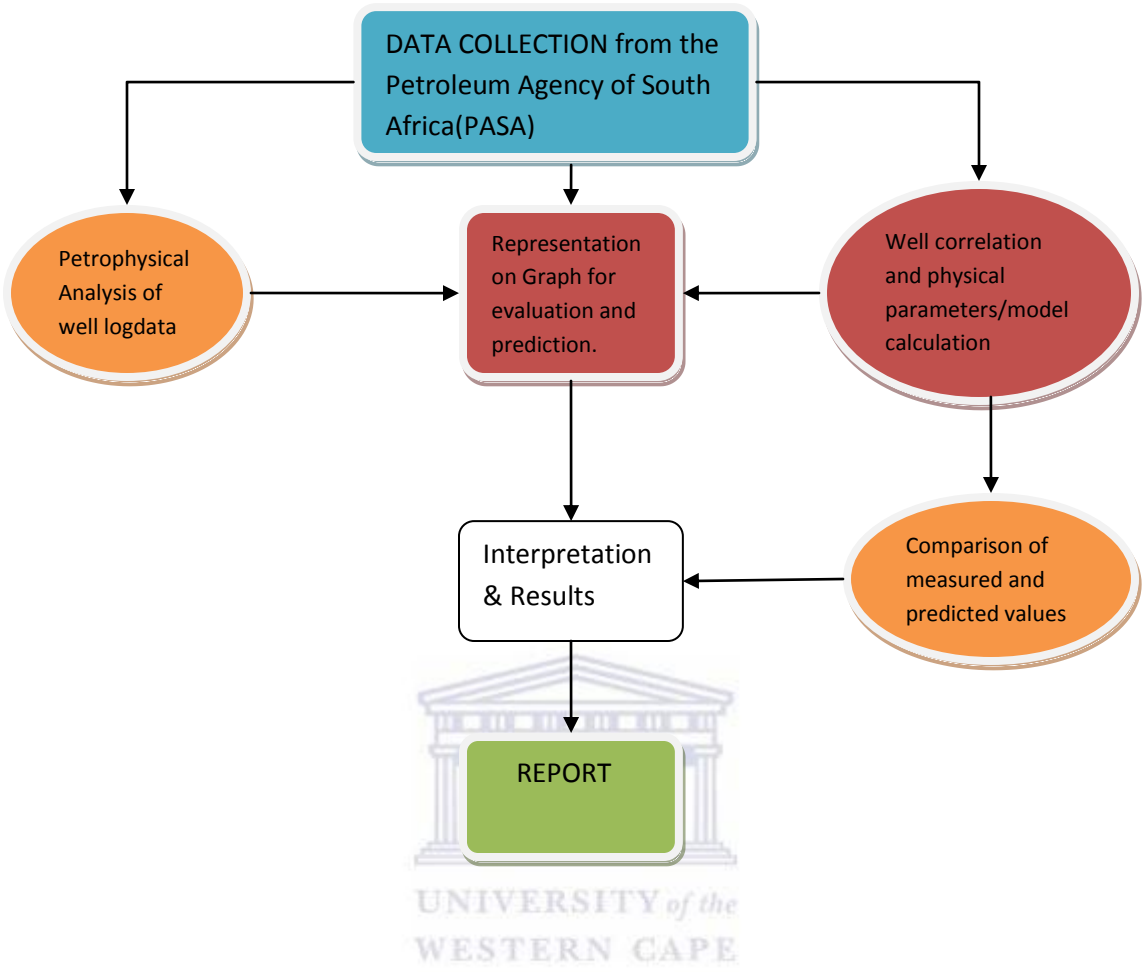

Figure 3.1 Research methodology flow chart

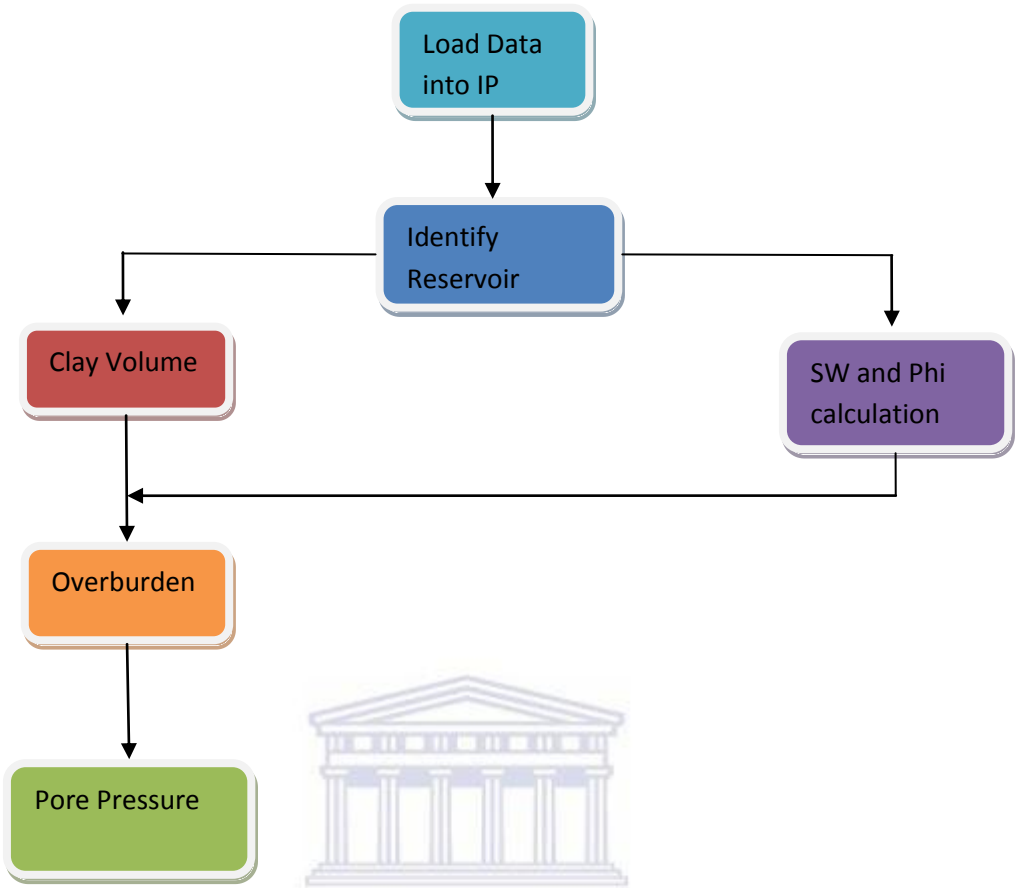

Figure 3.2 Petrophysical modeling Flow Chart

After data was acquired, it was loaded into the Interactive Petrophysics software (IP 4.0). Identification of the reservoirs for each well was done. Evaluation of the reservoirs was carried out using the well logs so as to know their characteristics. The intervals of the reservoir are the area of interest.

Using the well logs, the gamma ray curve was used to identify the sandstone reservoirs. A sharp decrease in value of the gamma ray curve indicates clean sandstone while a sharp increase in value or high gamma ray reading is assumed to be shale.

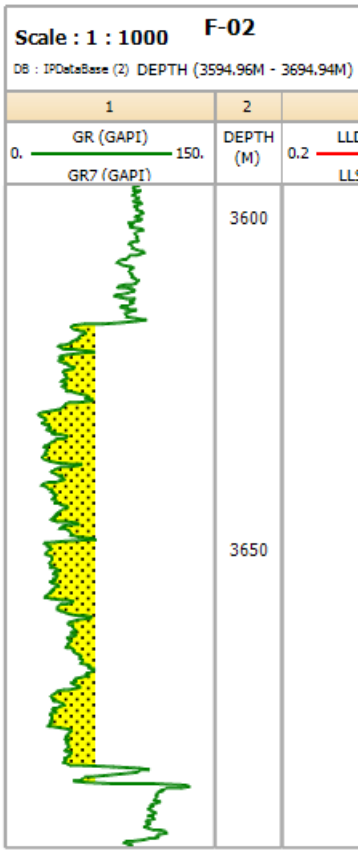

Figure 3.3 Gamma ray curve showing a sandstone reservoir in the F-02 well

The Caliper and Bit size (BS) curve was used as confirmation as they showed porous and permeable areas. When displayed together on the same track, if there is a reduction in the Caliper size or value i.e. it tilts to the left or right depending on which side has the lowest value of the scale. It is assumed that the area where the caliper curve crossed the Bit size curve moving to the lower scale is possibly permeable. Since a reservoir has to be permeable, this helps a lot in the analysis and supports the claim. The scale is usually 6 -16 for both curves.

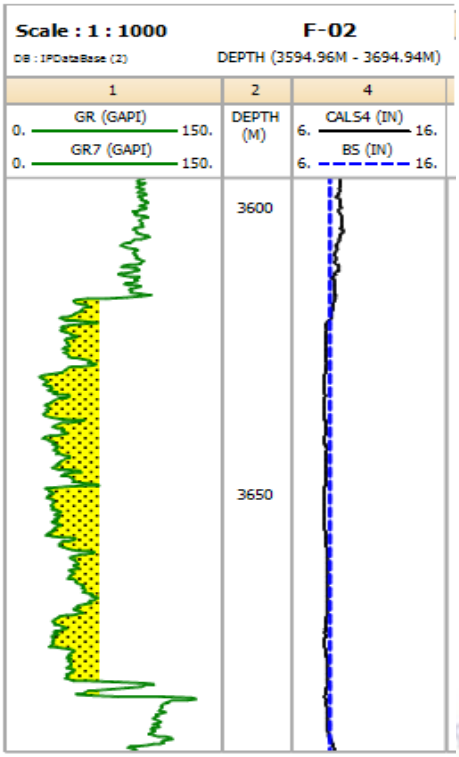

Figure 3.4. Well log showing the caliper curve (in black) and Bit size curve (in broken blue) cross

The resistivity curve, Density and Neutron Porosity curves were used to determine the type of fluid that was present in the reservoir. The resistivity of a substance is a measure of its ability to impede the flow of electrical current. For water bearing zone low resistivity is expected due to its high conductivity. High and higher resistivity values are associated with gas or hydrocarbon bearing zones. For the Neutron and density porosity curves, a crisscross(crossover) of both curves where the Neutron moves from the higher side of the scale to the lower side and the density porosity curve moves from the lower to higher side indicates presence of gas (Gas effect). When the density and Neutron porosity curves come closely together, with the resistivity curve showing a high value, this indicates a possible presence of hydrocarbon.

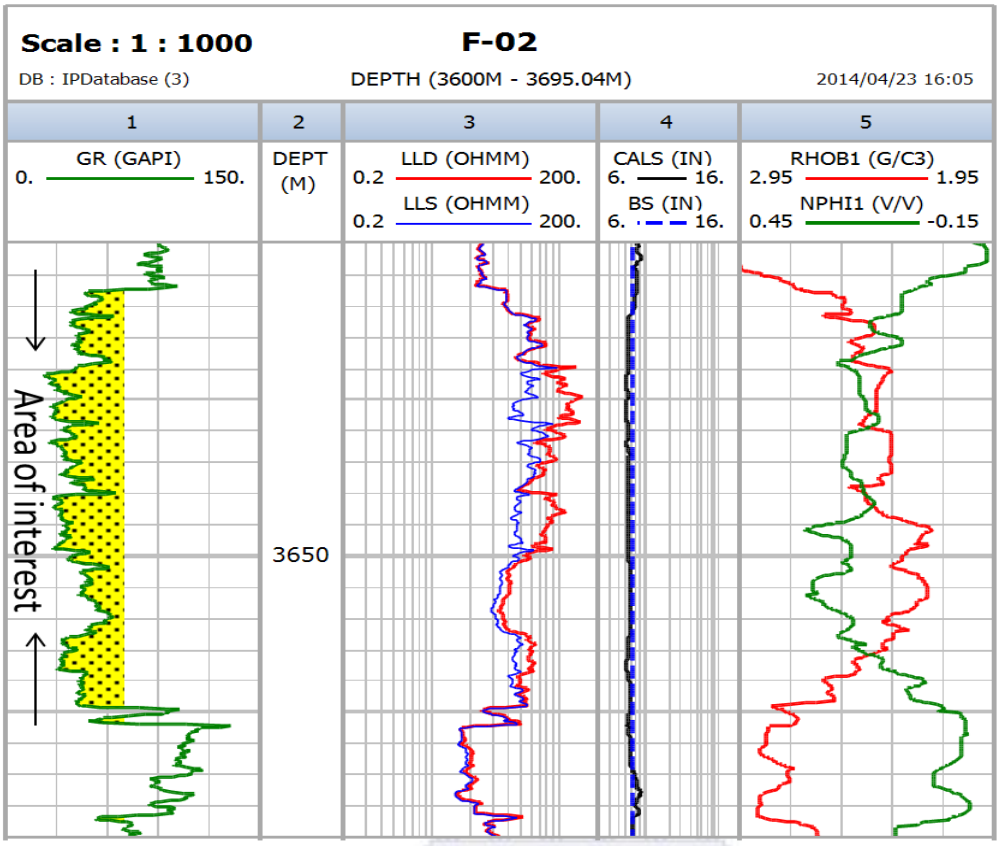

Figure 3.5 Well log showing the Resistivity Curve (LLD4) and the cross of Density and Neutron curve (RHOB & NPHI)

Clay Volume was also calculated using the common equation;

IGr = GRlog – GRmin / GRmax – GRmin

Where IGR = the gamma ray index

GRmin = the minimum gamma ray reading (normally the mean minimum through a clean sandstone or carbonate formation)

GRlog = the gamma ray reading at the depth of interest

GRmax = the maximum gamma ray reading (usually the mean maximum through a shale or clay formation)

From which Volume of shale (Vsh) or clay is determined from the Vsh-GR chart. Clay volume model was also run on IP to determine the volume of clay.

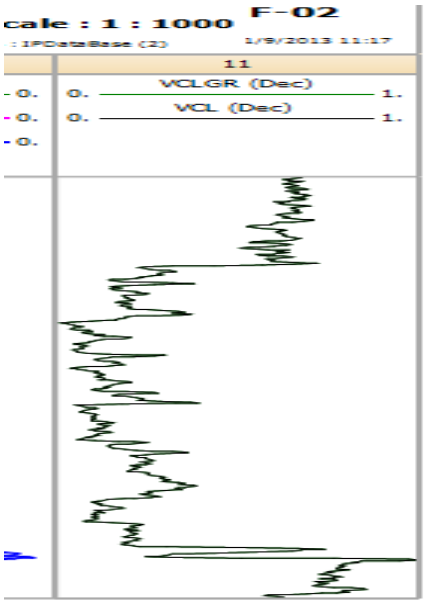

Figure 3.6 Volume of clay curve on the well log

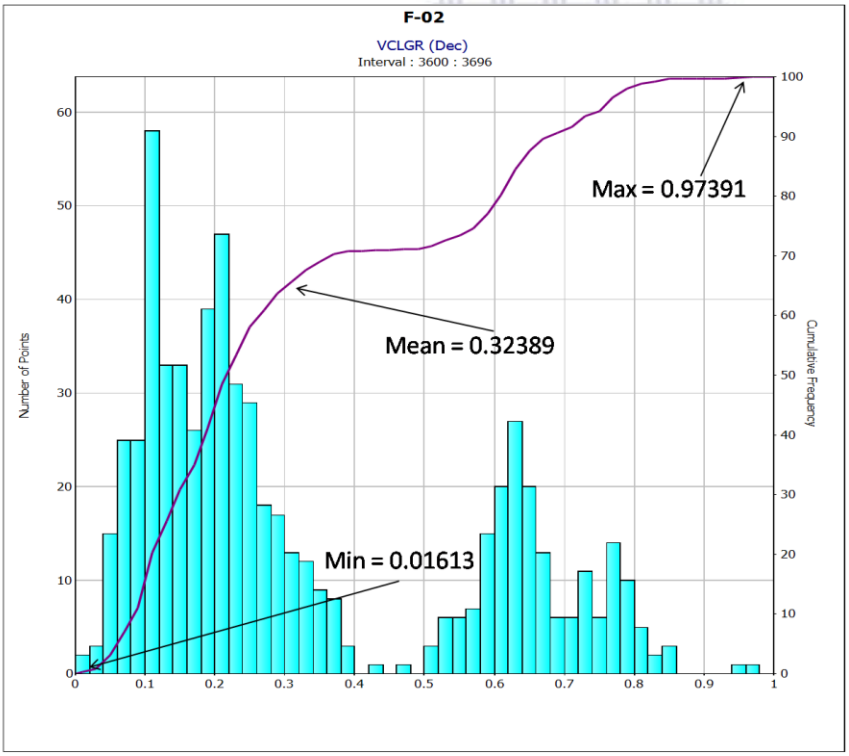

Figure 3.7 Volume of clay histogram showing the min, max and mean values

Porosity and Water saturation models were also run to give an idea of the porosity of the reservoir and the water saturation.

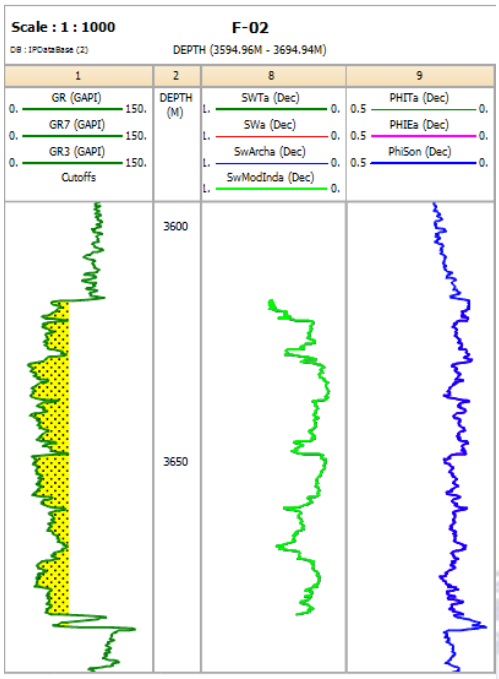

Figure 3.8 Well log showing the Gamma ray (GR), water saturation (Sw) and porosity (PHI) curves.

After which the overburden pressure at the reservoir zone was calculated using the pressure calculation tool available from main Advanced menu→ pore pressure calculation→Overburden pressure calculation.

On the overburden gradient window the depth curve was selected, the KB height was picked up automatically from the Well header info (but for cases where it is not detected and the box is blank, it can be inputted manually). The water depth was also picked up from the well header info automatically (can be inputted manually if box is blank), the density curve to be used for the calculation was selected and the top and bottom depth of the area to be covered was inputted on the result section and then the model was run by clicking the “ok” button at the bottom of the window.

Overburden gradient can be calculated manually using various equations like;

Po = Dw x Psw + RHOB x (D- Dsb) / D

Where Po= Overburden gradient (g/cc)

Psw= Specific gravity of seawater (1.03g/cc)

D= Depth measured from KB (m)

Dsb= Depth of sea bottom (m)

Dw= Water depth (m)

RHOB= Average bulk density of overburden (g/cc)

OR…

S ($^{kg/cm3}$) = Pb(g/cm3) x (TVD(m)/10)

S(kpa) = Pb(g/cm3) x TVD(m) x 9.81

S(psi) = Pb(g/cm) x TVD(m) x 0.433

Where; S = overburden pressure

TVD = True vertical depth

Pb = Average bulk density

The equation S(psi) = Pb(g/cm) x TVD(m) x 0.433 was used because the result comes out directly in psi and the overburden pressure/gradient used for the analysis is in lbs/gal and psi which makes it easier to convert.

Then the pore pressure gradient, fracture gradient, pore pressure and fracture pressure model was run. Different pore pressure models were ran for comparisons;

- Ben Eaton : resistivity & sonic
- Mathews & Kelly model
- Bowers method

The methods used for calculating pore pressure are as follows;

Eaton:

Resistivity: $P/D = S/D - (S/D - P/Dn) \times (Rsh\ observed / Rsh\ normal)^{1.2}$

Sonic: $P/D = S/D - (S/D - P/Dn) \times (DT\ shale\ normal / DT\ shale\ observed)^{3.0}$

Drilling Exponent: $P/D = S/D - (S/D - P/Dn) \times (Dxc\ Observed / Dxc\ normal)^{1.2}$

where; S/D = Overburden stress gradient

P/D = Formation pore pressure gradient (psi/ft)

P/Dn = Normal pore pressure gradient (psi/ft)

Rsh = Shale resistivity (ohm)

DTshale = Shale travel time (usec/ft)

Dxc = Drilling exponent in shale.

For the fracture gradient/pressure the following models are used ;

- Eaton
- Mathews & Kelly
- Baker & wood
- Modified Eaton
- Davies.

For this study Eaton Resistivity & Eaton Sonic models were used for pore pressure and pore pressure gradient calculations while the Mathews & Kelly model, Eaton(resistivity & sonic) model were used for fracture pressure and gradient calculation.

An RFT plot was made to confirm or determine the fluid contacts and available fluids and their gradients in relation to the pore pressures at various intervals of the zones of interest.

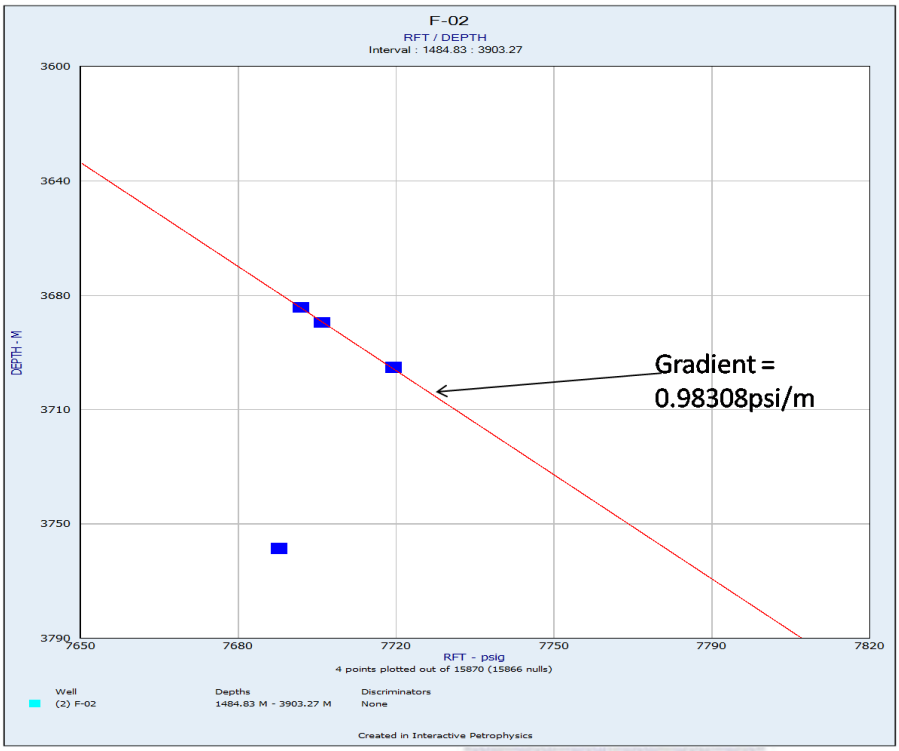

Figure 3.9 Repeat Formation Test cross plot versus Depth

Table 2. Reservoir fluids and their gradients

Fluids	**Gradient (psi/ft)**
Salt water	0.444 psi/ft to 0.460 psi/ft
Fresh water	0.433 psi/ft
Oil	0.30 psi/ft to 0.43 psi/ft
Gas	0.05 psi/ft to 0.30 psi/ft

The Normal Compaction Trend (NCT), Resistivity log and Sonic log was used to determine normal pressured zones and abnormal pressured zones. The sonic logs are considered to provide the most reliable quantitative estimates of pore pressure. The sonic log measures the transit time (DT) for a compressional sonic wave to travel through the formation from transmitter to receiver. Interval transit time (ITT) is the time it takes to travel through one meter (or one foot).

In an area presenting a normal compaction profile (normal pressure); the transit time should reduce with depth because of the increased density and decreased porosity. Abnormally pressured zones are likely to have lower density and high porosity than normally pressured areas at the same depth. Therefore the interval transit time will be high in value.

Shale resistivity increases with depth in normally pressured zones as the porosity decreases. An increase in porosity and therefore higher pore water content is an indication of abnormally pressured shales and will lead to lower resistivity.

Making a plot of interval transit time curve (DT) versus depth and the normal compaction trend line (NCT), abnormally pressured zones will show an increase in interval transit time above the normal compaction trend line value at the depth of interest. For the shale resistivity log, a decrease in shale resistivity value away from the trend line indicates abnormal pore pressure.

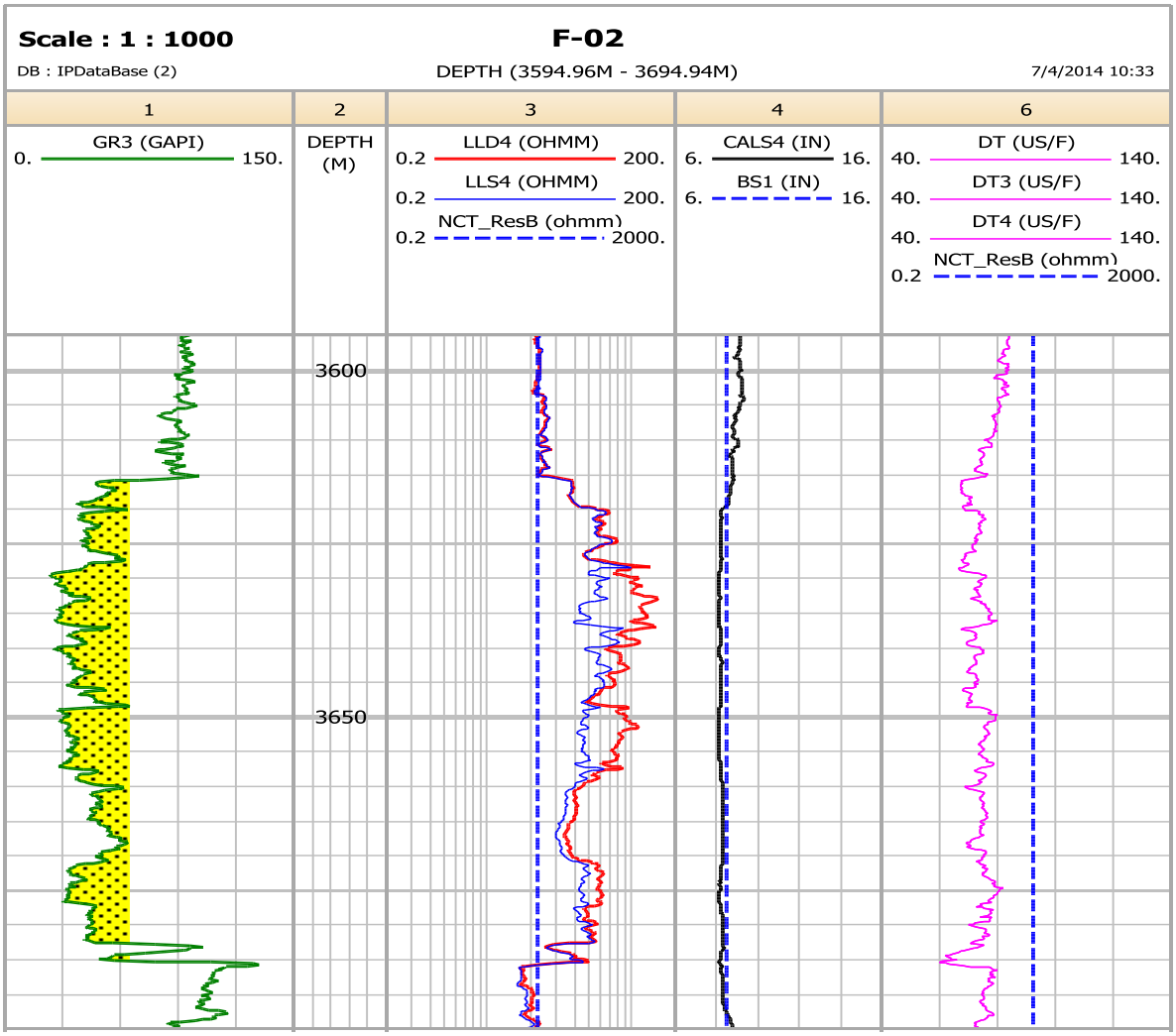

Figure 3.10 Normal compaction trend line (NCT) and resistivity curve plot, normal compaction trend line and sonic log (DT) plot.

CHAPTER FOUR

4.0: RESULT

4.1.0: RESERVOIR EVALUATION

4.1.1: WELL F-03

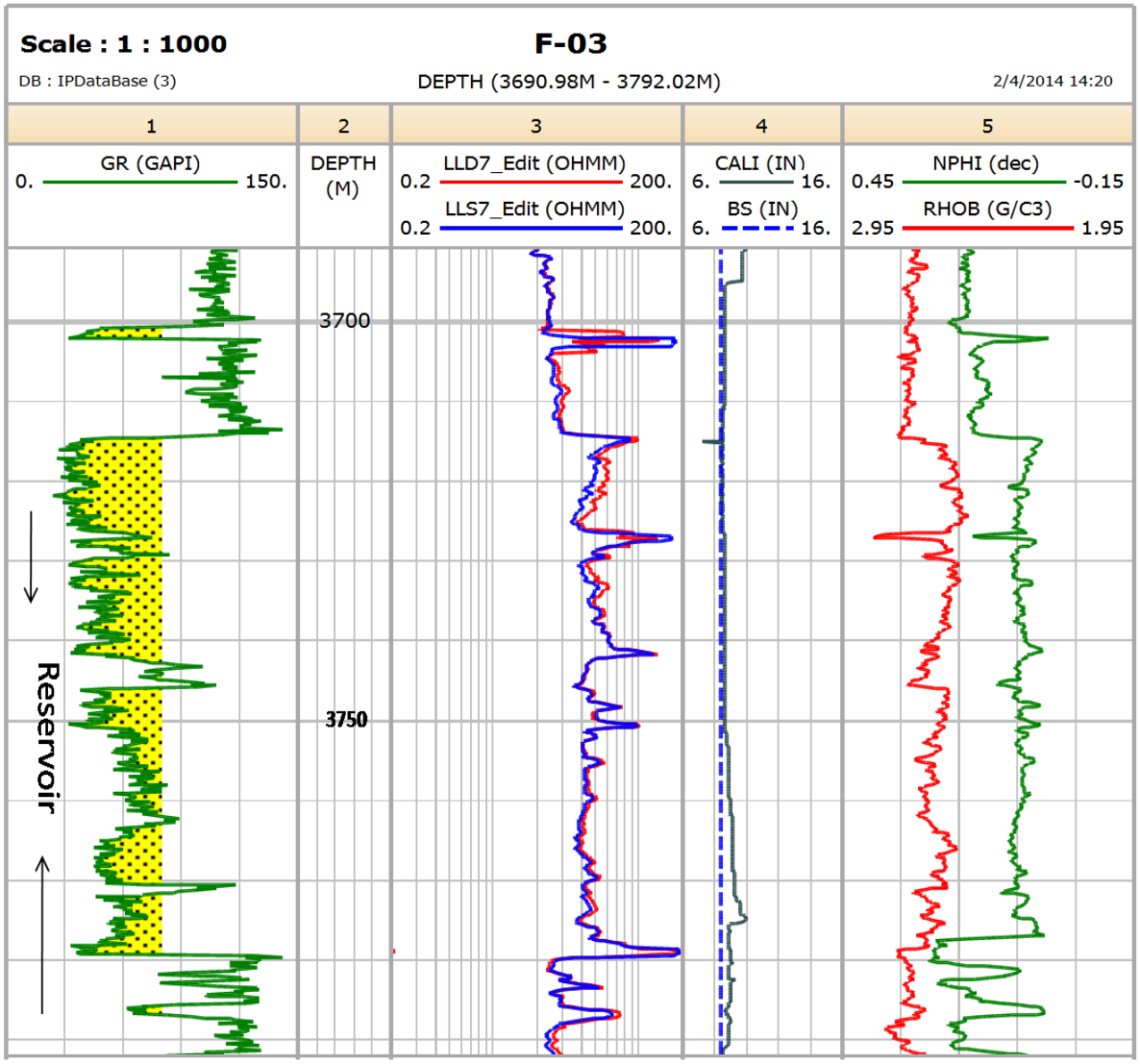

Figure 4.1 Resistivity(LLD7) and the deviation of the Caliper (CALI) curve

Looking at the figure above, at 3750m the caliper curve crosses back to the right of the bit size curve indicating a less permeable/not permeable area. The resistivity also decreases showing

absence of hydrocarbon or gas and presence of may be water as water is a good conductor, hence the low resistivity reading.

The caliper curve continues to go further right at 3756m to 3780m indicating how less permeable that area was.

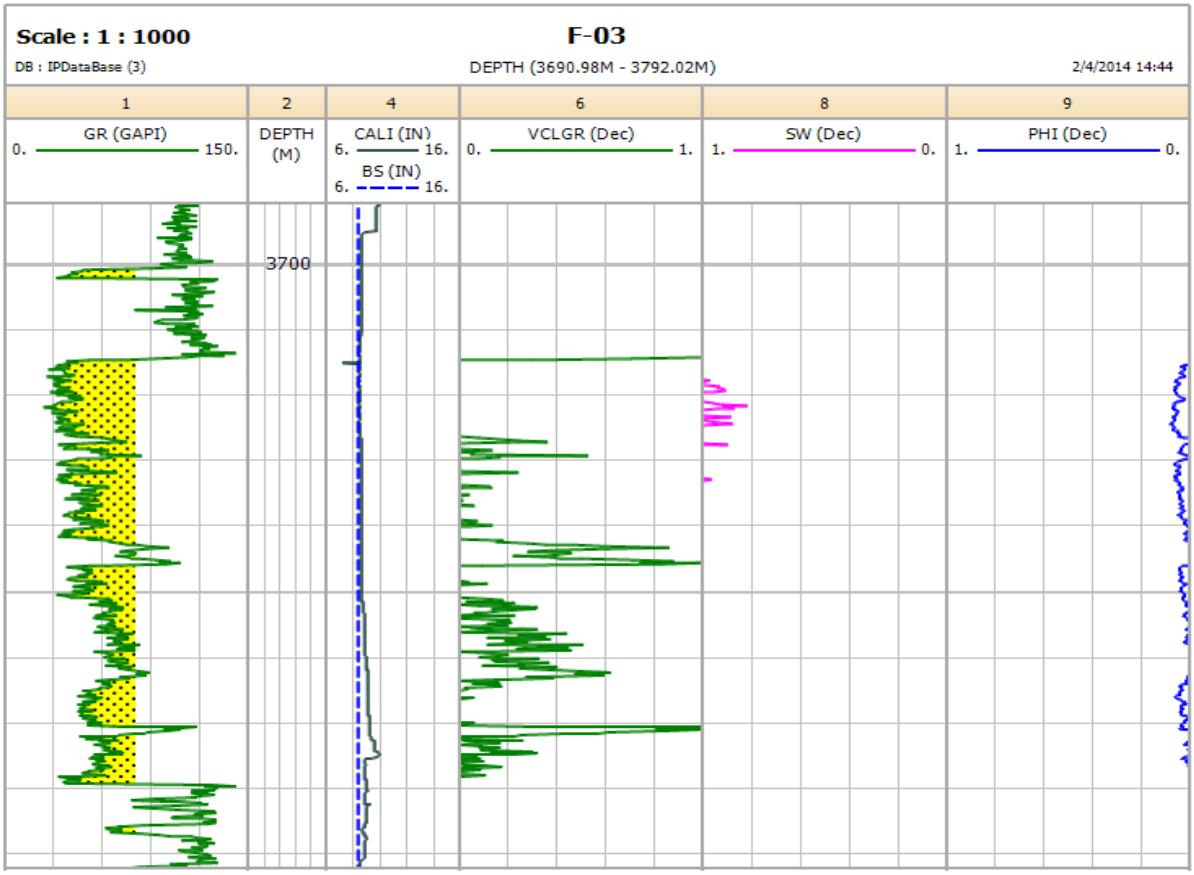

Figure 4.2 Gamma ray (Gr) curve, porosity (PHi) and water saturation curve (SW).

The figure above confirms from the SW curve 60% – 70% water saturation at the zone with a little bit permeability (3719m – 3746m). Outside that zone gives a 100% water saturation reading, meaning that this reservoir is water saturated thereby making it a bad reservoir. The porosity curve also shows that it is not porous with an average porosity reading of 0.05dec (5%).

Table 3. Reservoir properties and percentage values.

Properties	Percentage Values	Remark
Volume of clay	40% or >	Non Reservoir
Porosity	0.1 (10%) or >	Reservoir but anything less is a Non reservoir
Water Saturation	0.65(65%) or <	Reservoir but anything above that is a Non reservoir.

4.1.2: WELL F-02

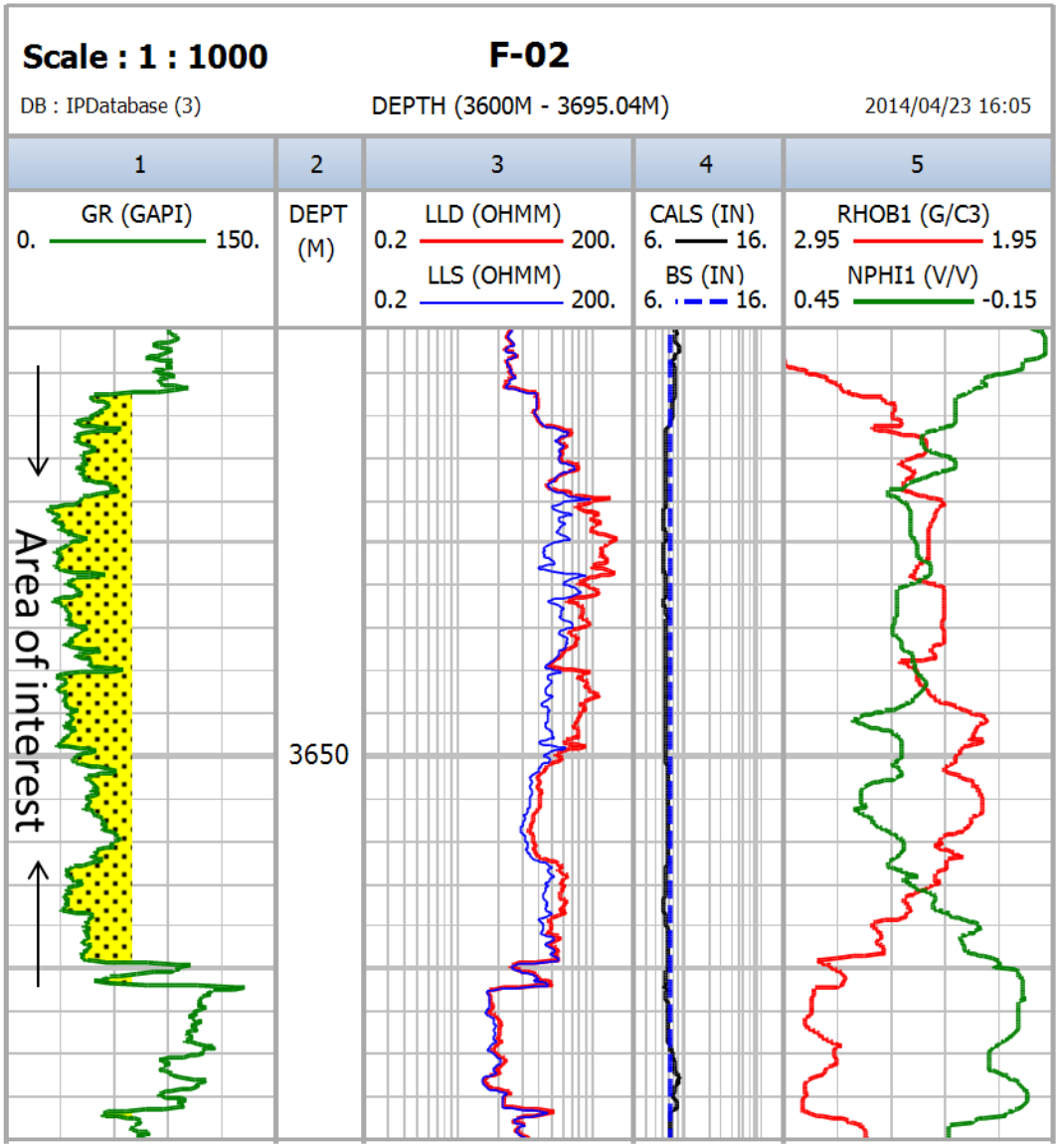

Figure 4.3 Neutron and Density Porosity curve cross for well F-02

The BS and CALI track in the figure above shows us that the reservoir is permeable as the CALI curve crosses to the left of the BS curve. The neutron porosity and density porosity track gives us an idea of the formation fluid contained or encountered at the reservoir and its surrounding area. The neutron and density porosity curves move close to each other at 3611m down to 3661m which indicates a presence of fluid, hydrocarbon or water. But with the increase and

high reading of resistivity in that range(3611m-3661m) we are made to believe that the fluid present at that range is not water due to its association with low resistivity reading (i.e. water is a good conductor).

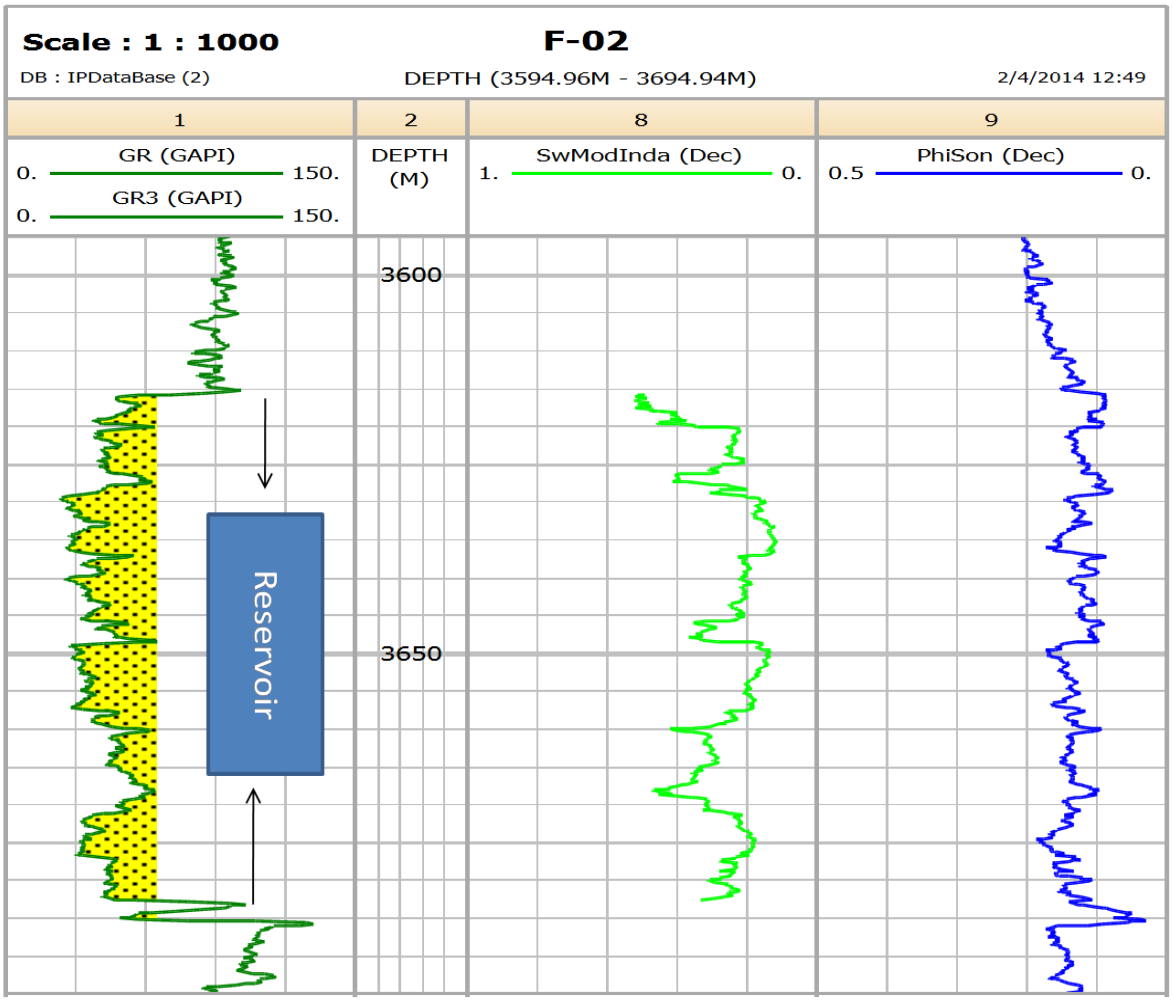

Figure 4.4 Porosity(PHi), water saturation(Sw), Bit size(BS),Caliper(CALI) and volume of clay(Vcl) curve of well F-02

The water saturation (Sw) track above shows us that the reservoir is not water saturated, with the Sw curve giving us an average reading of 0.251-0.294dec (25%-29%) on track 8. This shows that the reservoir qualifies as a reservoir first of all, but with a porosity reading of 0.1 to

0.13dec (i.e. 10% - 13% porosity) from the porosity curve (PHI) on track 9, it shows that it is not that good a reservoir.

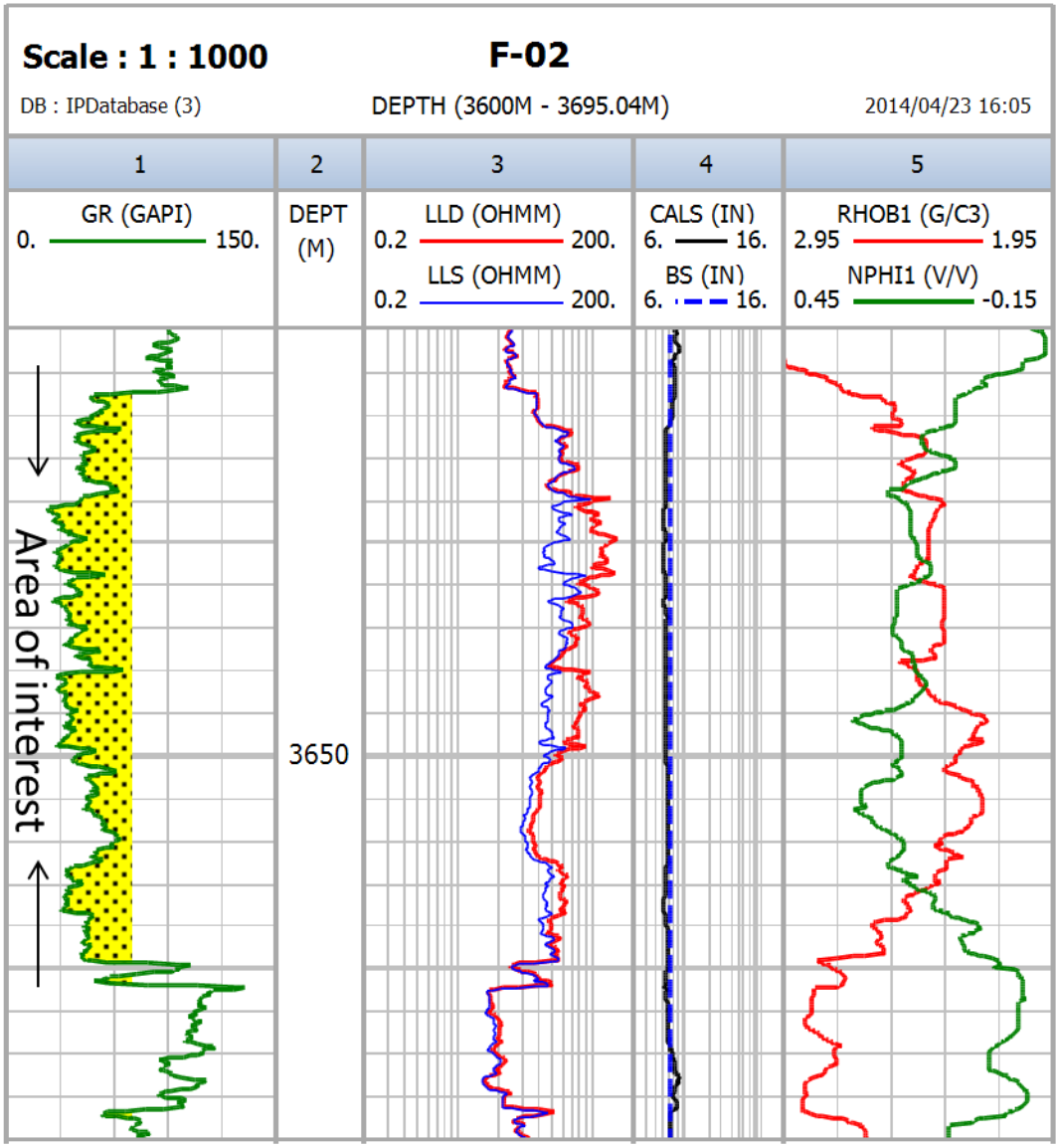

Figure 4.5 Neutron Porosity and Density Porosity curve cross in well F-02

There is also presence of gas from the neutron porosity and density porosity curve cross on the NPHI, RHOB track. On the neutron and density porosity track, the density porosity curve deviates to the left crossing the neutron porosity curve and giving a high density reading while the neutron porosity moves to the right of the density porosity curve and the scale thereby

giving a low neutron porosity reading. This cross or criss-cross as some people call it below 3661m, 3662m is known as a Gas effect. This indicates that gas was encountered at this zone.

The RFT plot below confirms this as the gas line goes through points with a gradient of 0.98308psi/m(0.29964psi/ft) below this zone and also shows there was no gas-water contact.

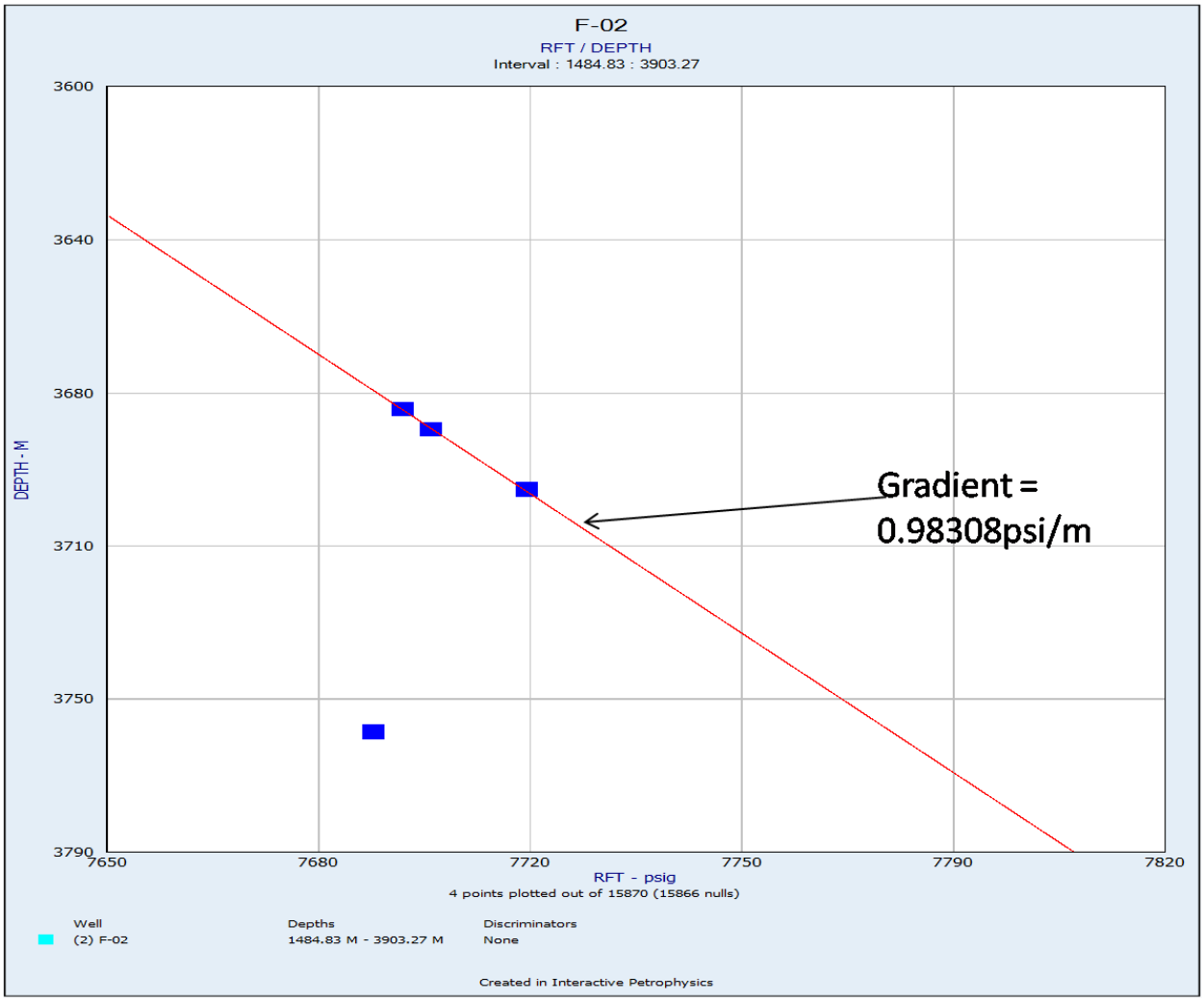

Figure 4.6 Repeat Formation Test pressure versus depth plot of well F-02

4.1.3: WELL F-01

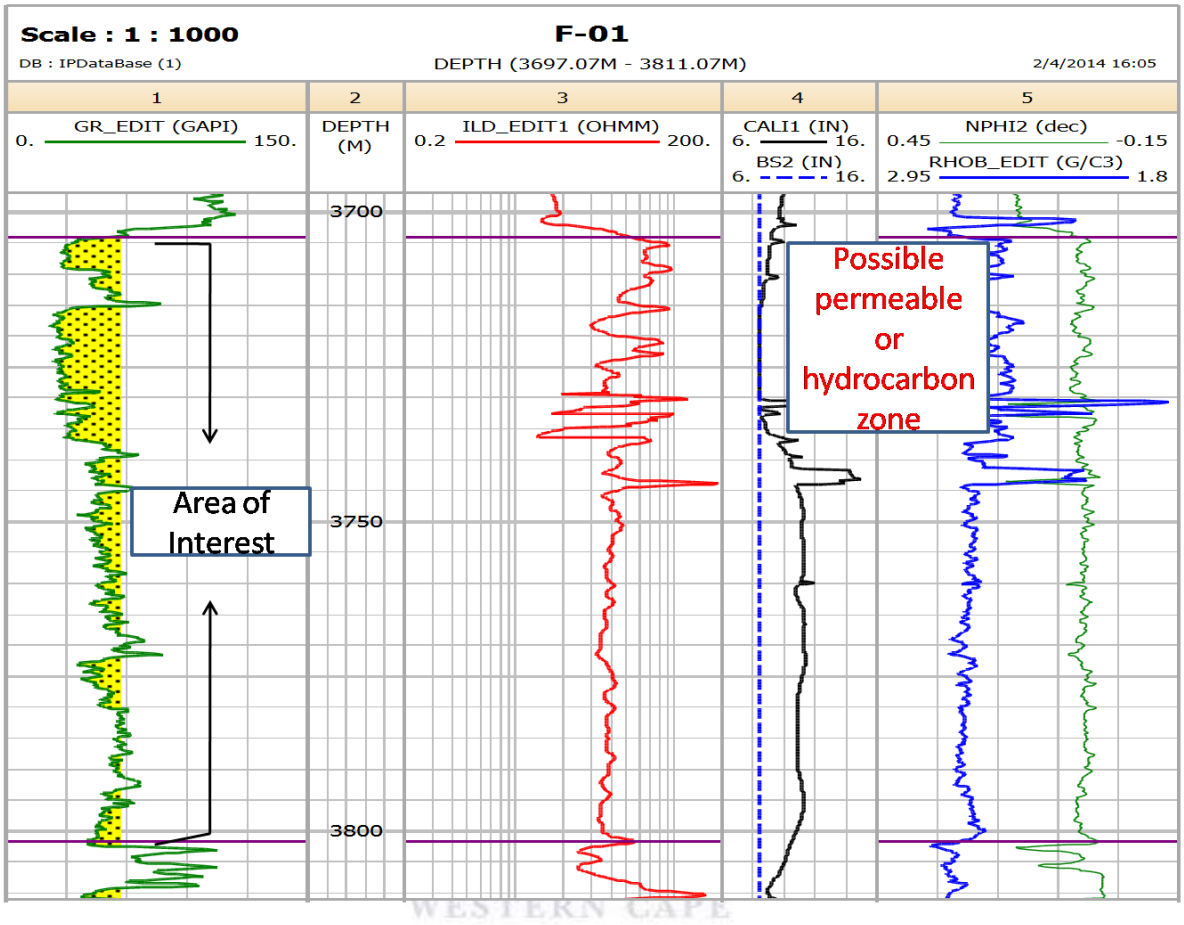

Figure 4.7 GR, ILD, BS&CALI and NPHI&RHOB curves in relation to the reservoir in well F-01

At the reservoir zone the resistivity curve (ILD) on track 3 increases significantly at 3701m, 3702m to 3745m before dropping. The caliper curve moves back to the right of bit size curve at about 3729m, 3730m down to 3800m showing the range below 3728m is not permeable or has very low permeability.

At the upper part of the reservoir, the neutron porosity and density porosity curves shows us there is a possible presence of gas at that zone (3702m – 3728m) as the density porosity curves gives a high density reading as it deviates to the left of the neutron porosity curve and the neutron porosity curve gives us a low neutron porosity reading as it moves to the right.

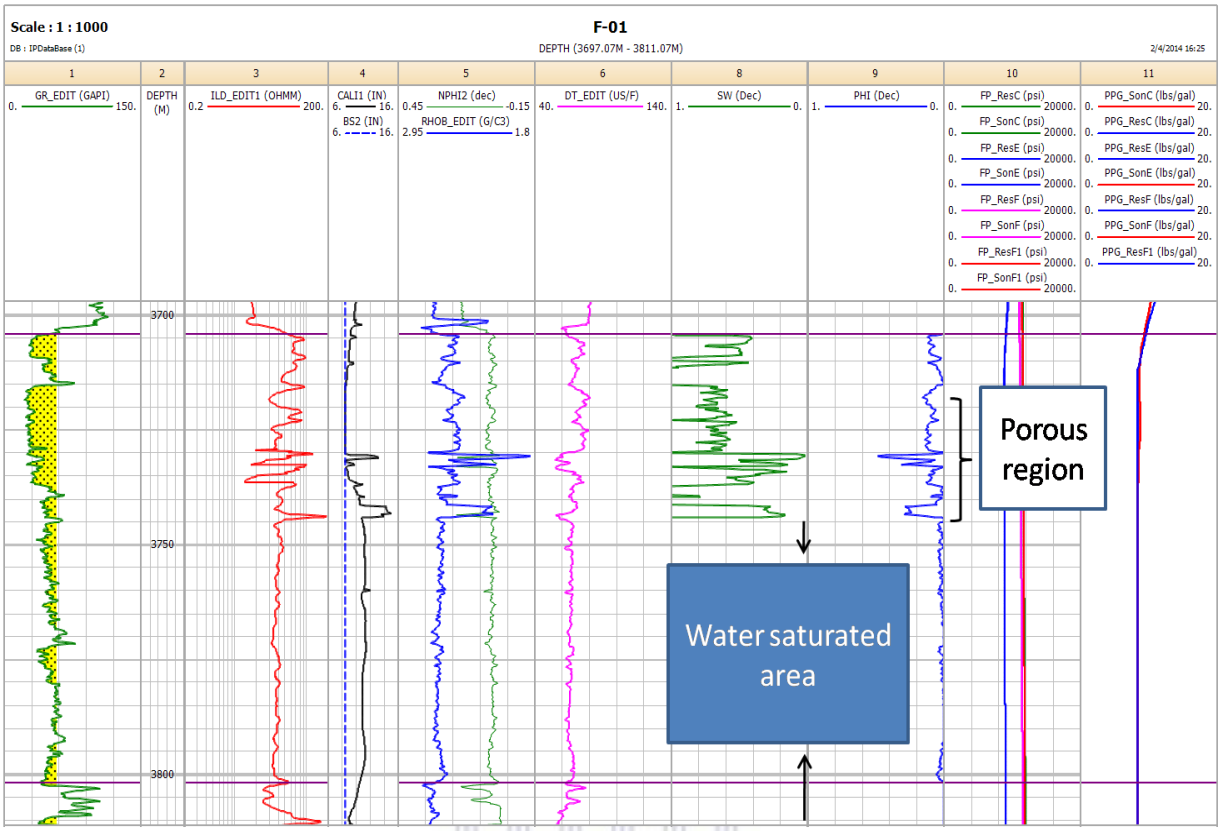

Figure 4.8 Well log of well F-01

The water saturation curve (Sw) in green on track 8 gives us an average reading of 24.2% at the upper part of the reservoir (3702m -3727m) indicating that this part of the reservoir is not water saturated. Below 3728m though seems to be water saturated as the SW curve gives an average reading of 85% and 90% respectively.

The porosity curve(PHI) in blue confirms that 3702m – 3727m is more permeable as it gives an average reading of 10%, 11% within this zone. Below 3739m, 3740m, the porosity drops below 10%.

Table 4. Gradients of reservoir fluids

Fluids	**Gradient (psi/ft)**
Salt water	0.444 psi/ft to 0.460 psi/ft
Fresh water	0.433 psi/ft
Oil	0.30 psi/ft to 0.43 psi/ft
Gas	0.05 psi/ft to 0.30 psi/ft

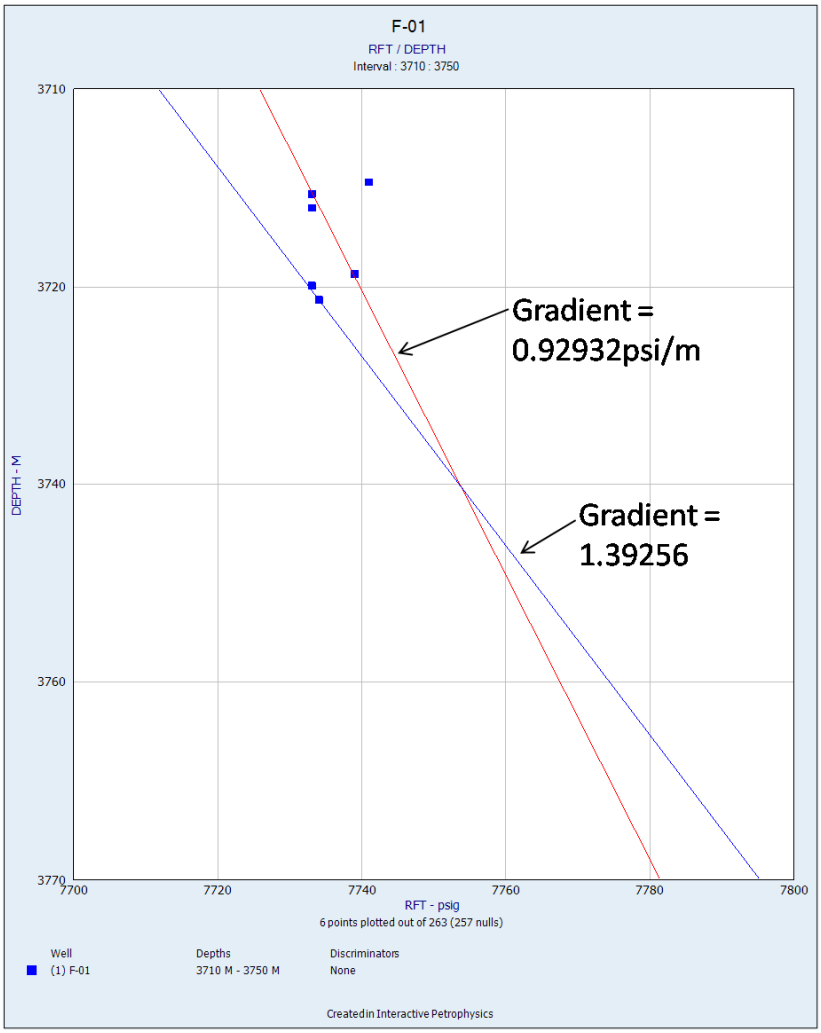

Figure 4.9 Repeat Formation Test plot of well F-01

4.2: PORE PRESSURE

4.2.1: WELL F-01

The figure below shows a drop in the pressure gradient from a higher value above 3704m to a lower value of 8.92ppg at 3707m, 8.6ppg at 3713m and later maintained this value down to 3810m. This is probably because of gas or shale zone which might be tight/not porous enough thereby exerting more pressure on the formation fluids or pores. On reaching 3704m which seems to be a little porous and permeable zone, looking at track 11 there is a drop in pressure which could be because the fluid has some space now to move thereby easing the pressure on the pores.

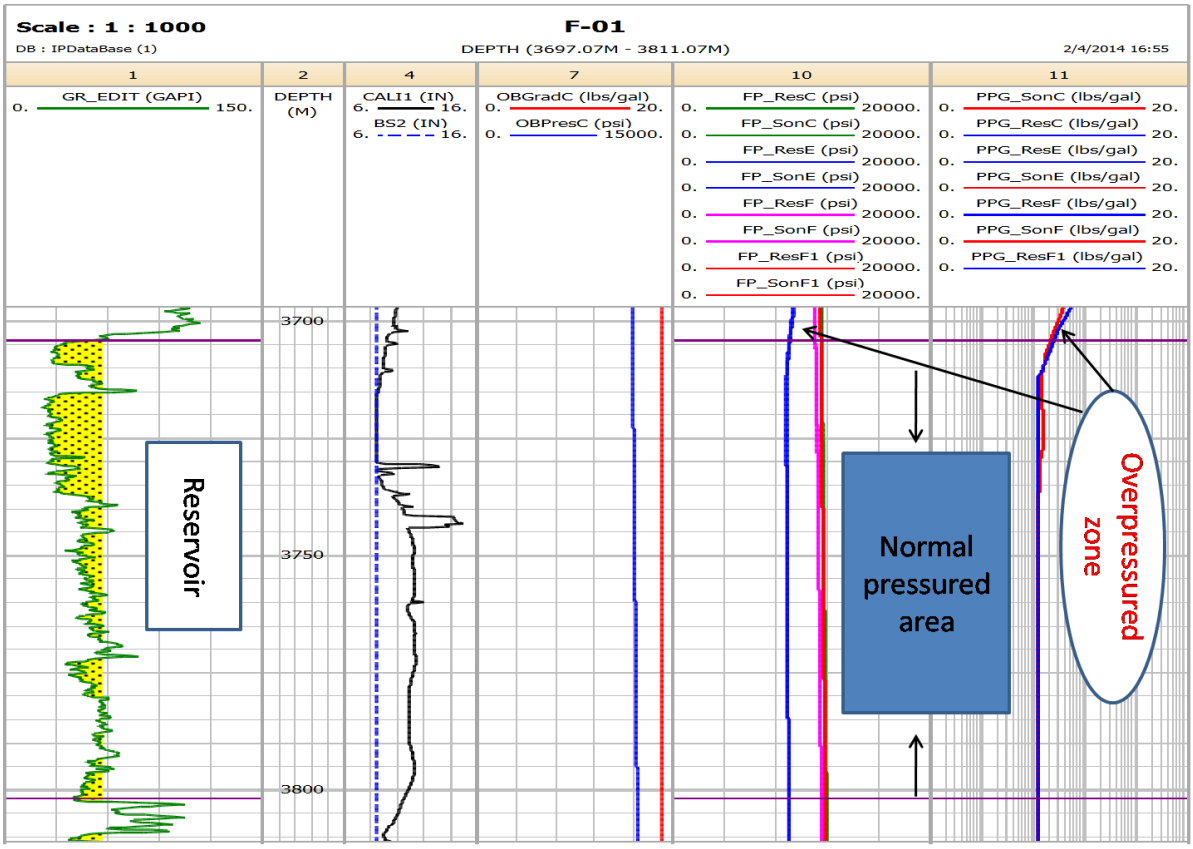

Figure 4.10 Fracture gradient (FG) and Pore pressure gradient (PPG) curves for well F-01

Looking at the pressure and depth plot (Fig.4.11), there was minimum drop and rise in pressure going down to 3680m but at 3682m a sharp increase in pressure was observed. This brings in the doubt that this could be caused by shaly tight non permeable or porous formation and puts

into consideration the fact that it might be formation fluids encountered at that zone especially gas.

The figure also shows that from 3704m the pressure begins to drop steadily and smooth and as it got to 3710m it stabilizes before increasing very slowly at 3720m, 3722m area as if it is being controlled. The pressure curve seems to be steady like almost a straight line which could be because the pressure was controlled by the engineers, they probably employed a higher mud weight to balance the pressure (as expected) and also reduced the mud weight when necessary.

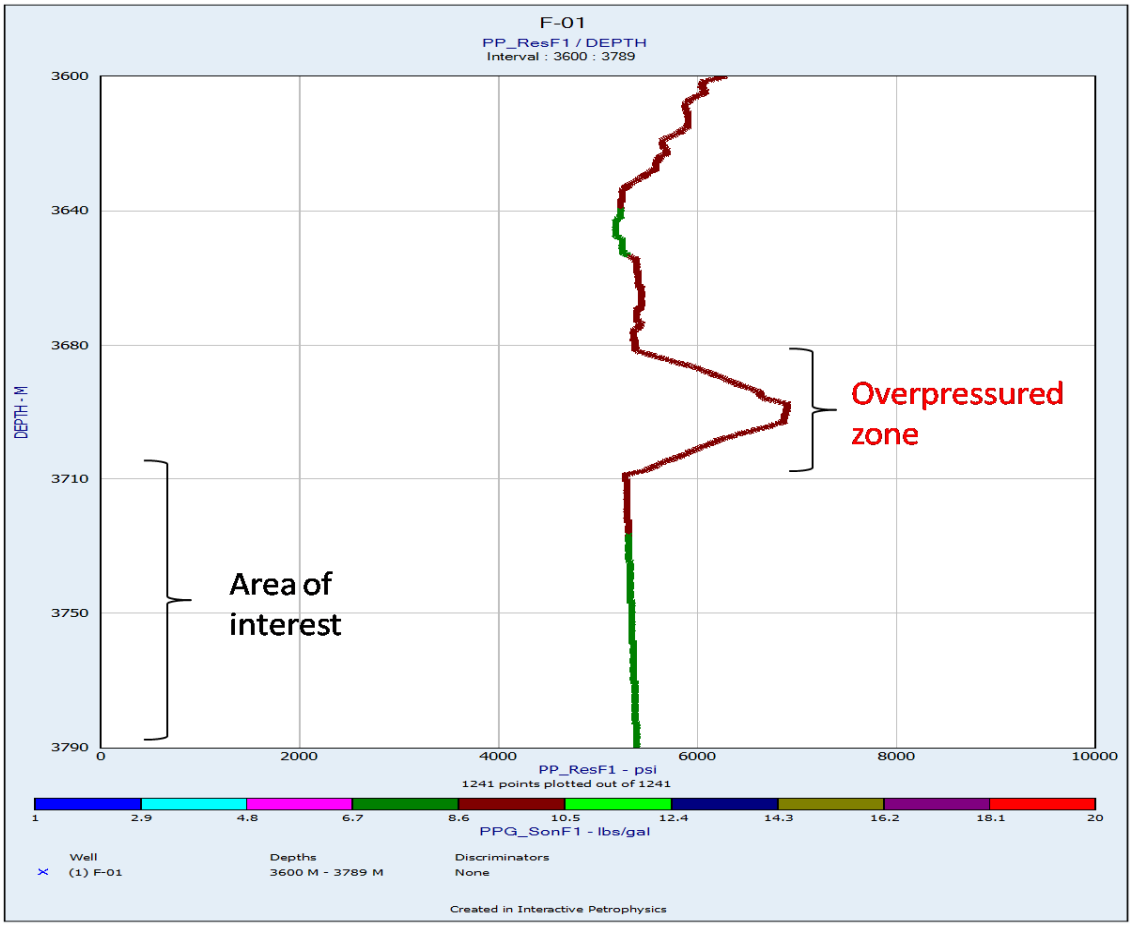

Figure 4.11 Pressure Vs. Depth plot of well F-01

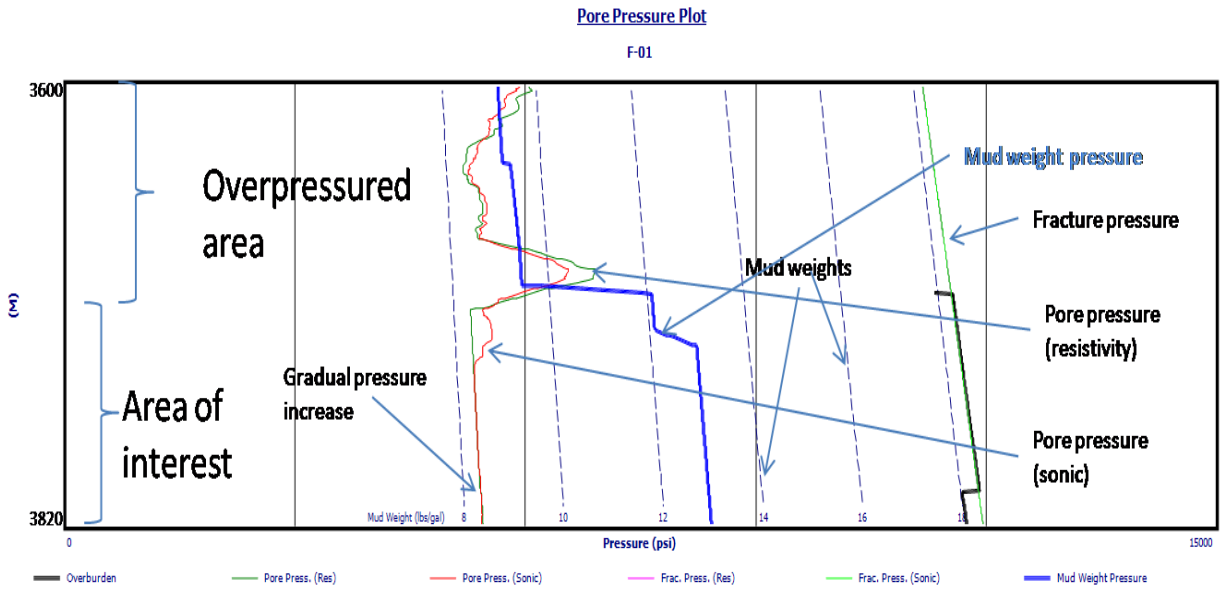

Figure 4.12 Cross-plot of Pore pressure, fracture pressure, overburden pressure and mud weight of well F-01

Looking at the pressure curves (green for resistivity pressure and red for sonic pressure curve) (Fig.4.12), abnormal pressure (overpressure) was observed around the 3700m-3703.6m area. And the mud weight (blue line/curve) was increased to maybe balance the pressure. This increased mud weight was probably maintained to the last depth.

The Repeat Formation Test plot confirms the presence of gas at the reservoir with gas line (line in red color) giving us a gradient of 0.97026 psi/m (0.29psi/ft) as it goes through points at 3718m down to 3730m. Gas-water contact (GWC) was also observed, with the water line (Line in green color) giving a gradient of 1.19662psi/m (0.36psi/ft).

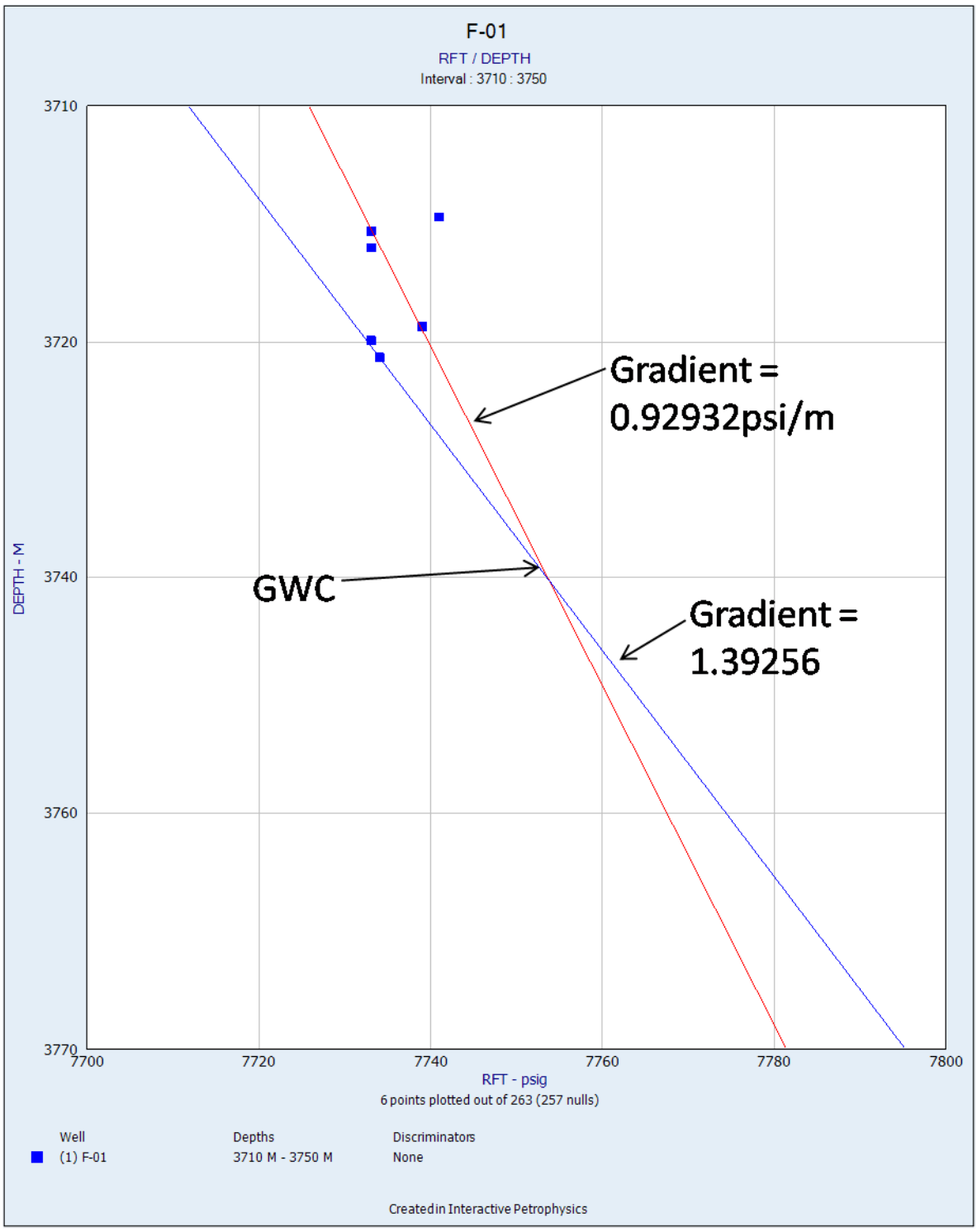

Figure 4.13 Repeat Formation Test plot of Well F-01

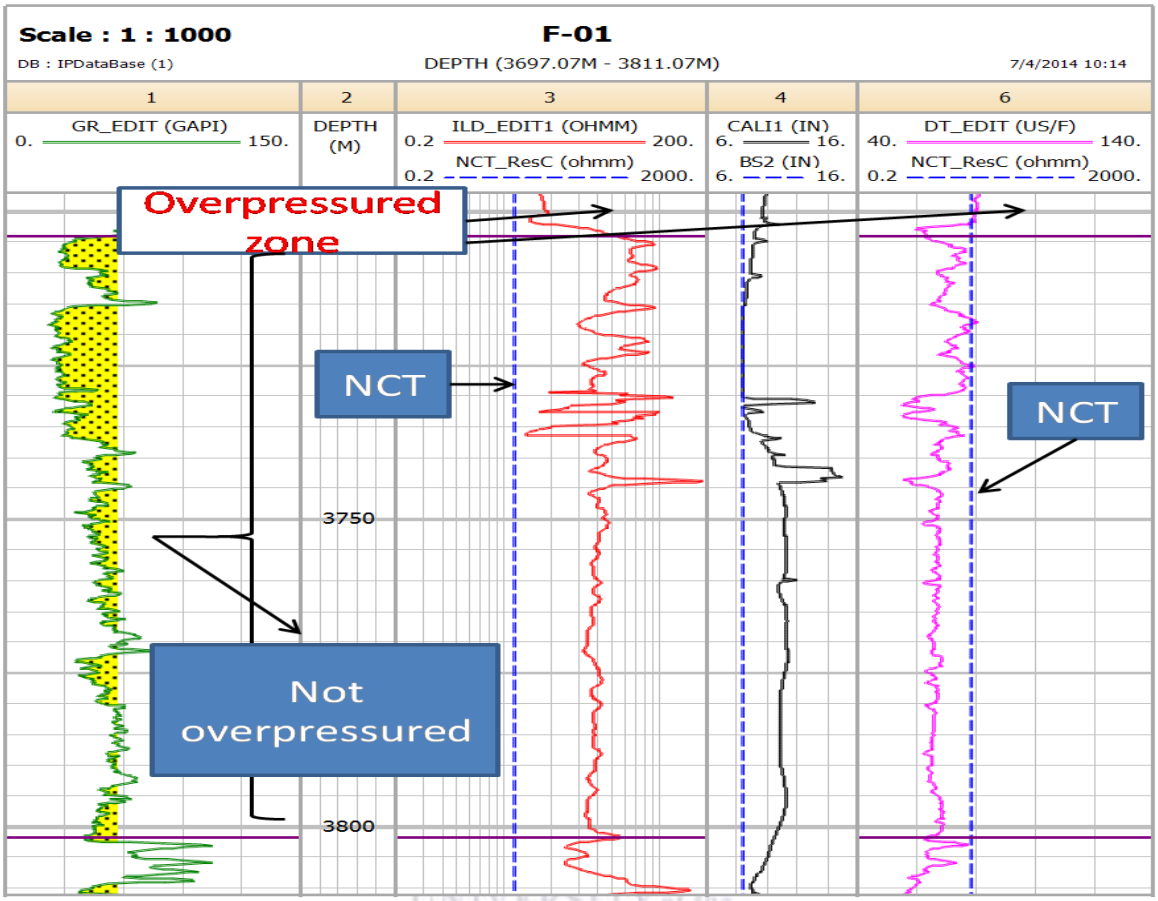

Figure 4.14 Normal compaction trend line (NCT) in relation to the resistivity curve(LLD) and sonic curve (DT) for well F-01

The above figure shows that at 3700m there is an increase in resistivity value moving away from the normal compaction trend line (NCT) in track 3 which continued all through the depth of interest indicating a normal pressure. The interval transit time curve (Dt) showed a decrease around 3700m too as we can see in track 6 from the figure above. This also continued down to 3800m.

Before 3700m the interval transit time curve (Dt) showed a higher value indicating overpressure, then moves away from the normal compaction trendline as it decreases from 3700m downwards indicating normal pressure.

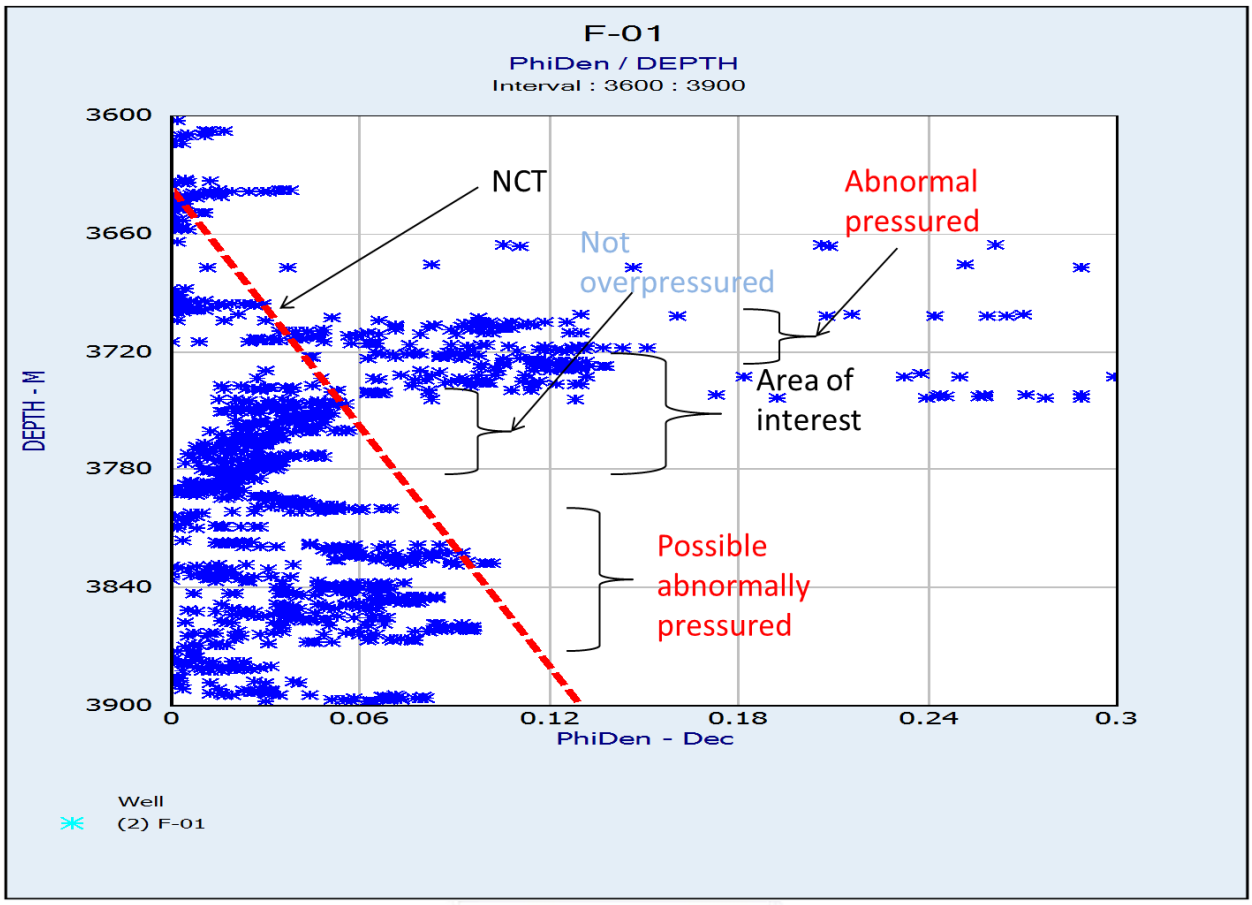

Figure 4.15 Shale porosity from density log vs depth plot of well F-01

Dutta (2002) in his work inferred that overpressured formations exhibit several of the following properties when compared with a normally pressured area at the same depth (1) lower bulk densities (2) higher temperature (3) higher porosities (4) higher Poisson ratios (5) lower velocities (6) lower effective stress.

Shale porosity was estimated from density log. The plot of shale porosity from density log (and the normal compaction trend) versus depth shows that from about 3740m – 3820m there is normal compaction which is usually associated with normal pressure. Compaction acts to reduce the porosity of sediments as they are buried, a process which continues only as long as fluids in the decreasing pore space are allowed to move out, which is the case in normal pressured zones where the fluids are in communication up to the sea floor. Also from the figure

above at about 3680m – 3710m the shale porosity remains constant with depth, a situation associated with undercompaction which leads to abnormal pressure(Fig. 4.15).

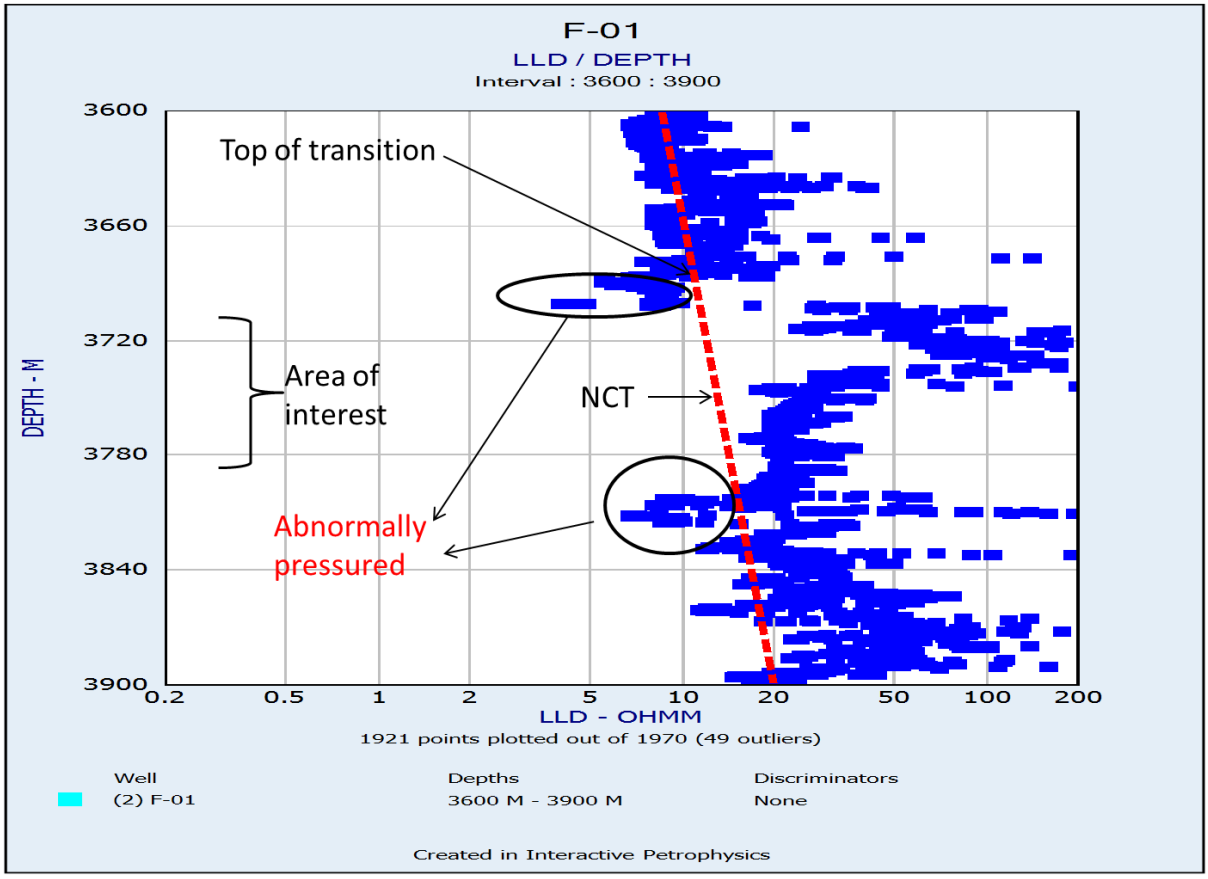

Figure 4.16 Resistivity vs depth plot of well F-01

The resistivity versus depth plot above indicates that there was abnormal pressure at about 3680m – 3710m and 3785m – 3800m. Shale resistivity increases with depth in a normal compaction and normal pressured zone, which is the case at 3720m – 3770m. However there is significant decrease in resistivity around 3785m – 3800m and 3680m – 3710m which is a characteristic of an overpressured zone.

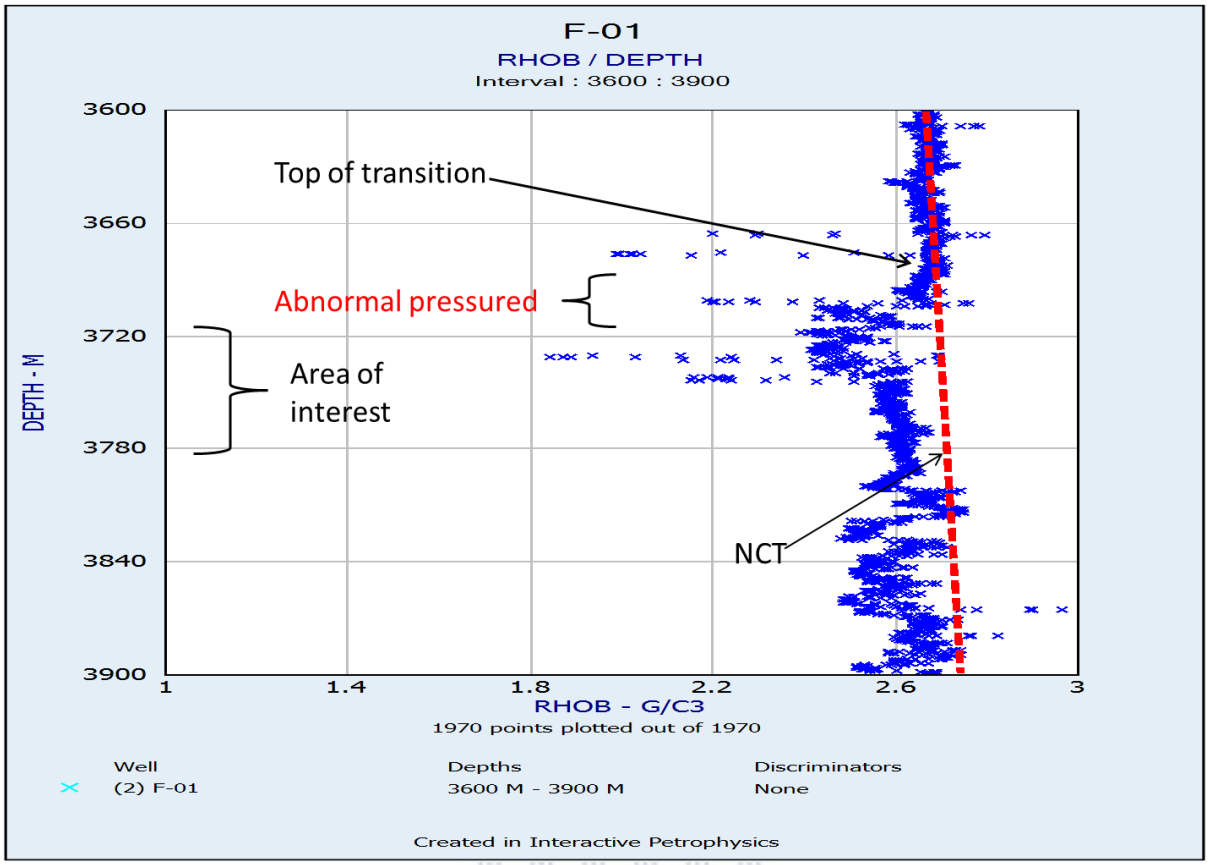

Figure 4.17 Density vs depth plot of well F-01

In a normal pressured formation, density increases with depth and in an abnormal pressured formation density decreases with depth which is associated with undercompaction (Chunduru, R., Ghosh, A., Kumar, M., 2009). At about 3690m – 3740m the upper part of the reservoir, there is a decrease in bulk density which signifies undercompaction. Another decrease occurred at about 3786m – 3800m at the lower part of the reservoir.

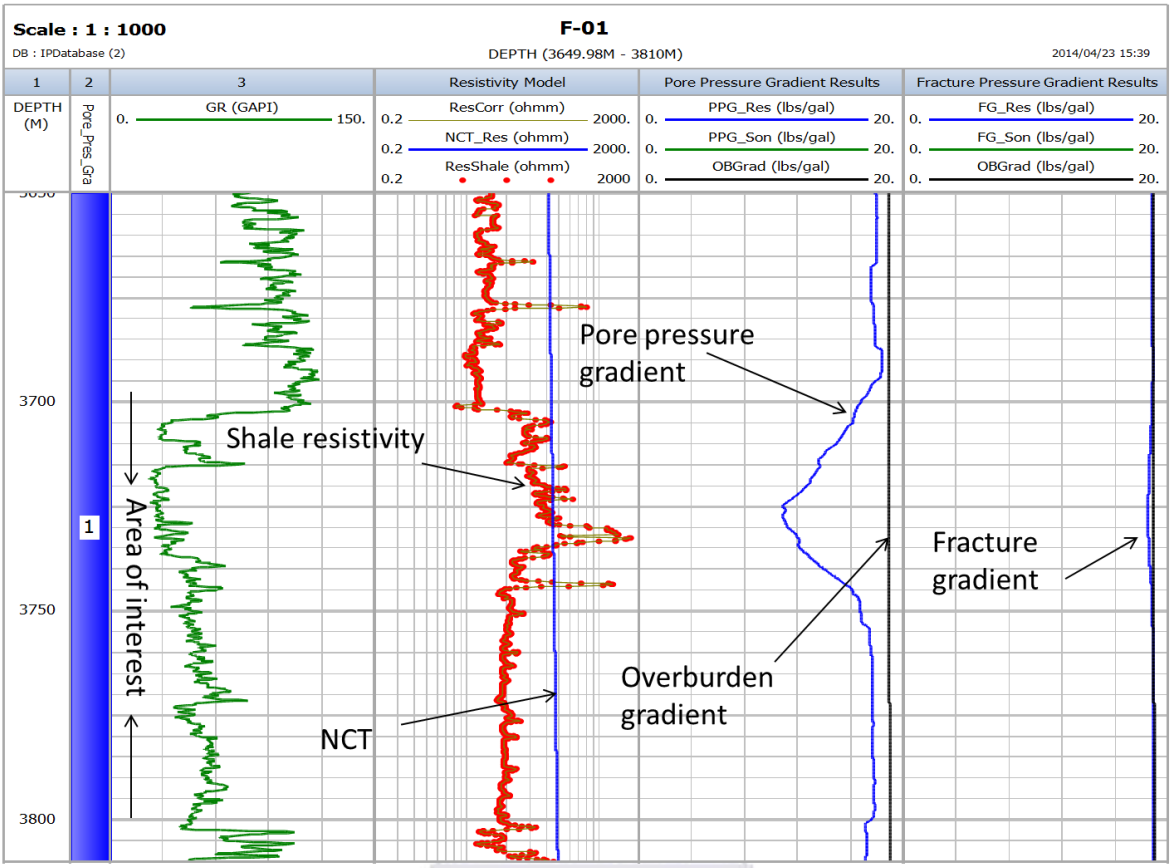

Figure 4.18 Pore pressure relationship with resistivity for well F-01

The diagram above shows the relation of shale resistivity to pore pressure. The pore pressure gradient decreases as the shale resistivity increases. And also as it deviates from the higher scale (right) of the NCT (normal compaction trend) to the lower scale (left), the pore pressure gradient increases.

4.2.2: WELL F-02

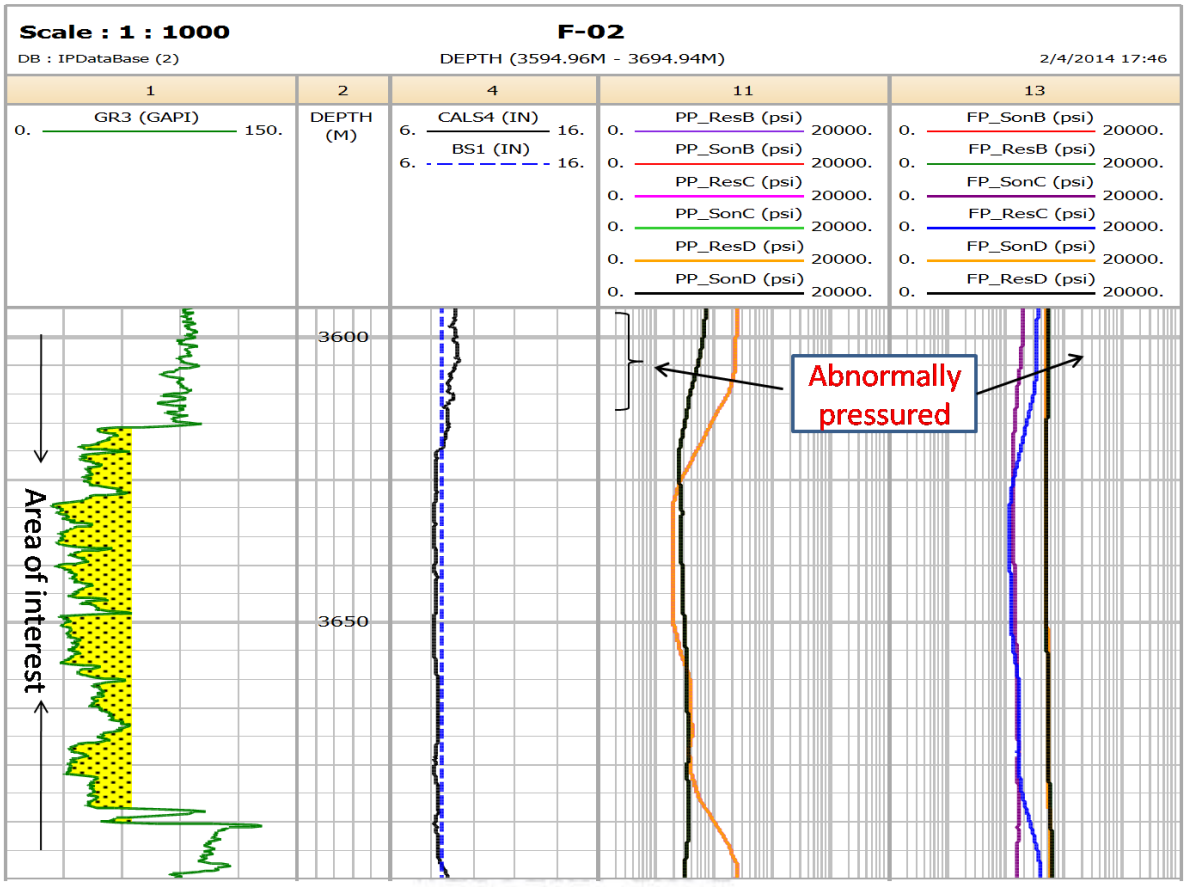

Figure 4.19 Pore pressure curve and fracture pressure curve in relation to the reservoir

In well F-02 an abnormal pressure of 9649psi was encountered at 3590m, 3600m probably due to the gas present or tighter, less porous and permeable formation reached at 3600m. We notice a pressure drop from 3609m looking at the figure above, this could be because a more porous and permeable zone was reached at that depth or may be the mud weight/ formation fluid was increased to balance the pressure.

The cross plot of pressure Vs. depth of the reservoir at 3600m-3700m (area of interest) shows us that the pressure gradient (15.57ppg) was high at 3600m area which might be because of the gas encountered in that area looking at Fig 4.21 which shows us the neutron porosity and density porosity curve crosses.

From the neutron porosity and density porosity curves track, between 3630m to 3660m the curves were moving closely to each other not making strong/wide significant cross which gives a sign of the presence of hydrocarbon. This might be the cause of the drop in pressure at that range (i.e. if the engineers didn't modify the mud weight) because of the permeable sandstone. There was abnormal pressure again at 3692m due to gas encountered in the well. The neutron and density porosity curves confirm this with a high density porosity reading and a low neutron porosity reading and a significant crossover showing the gas effect (M.F.Quijada, R.R.Stewart, 2007).

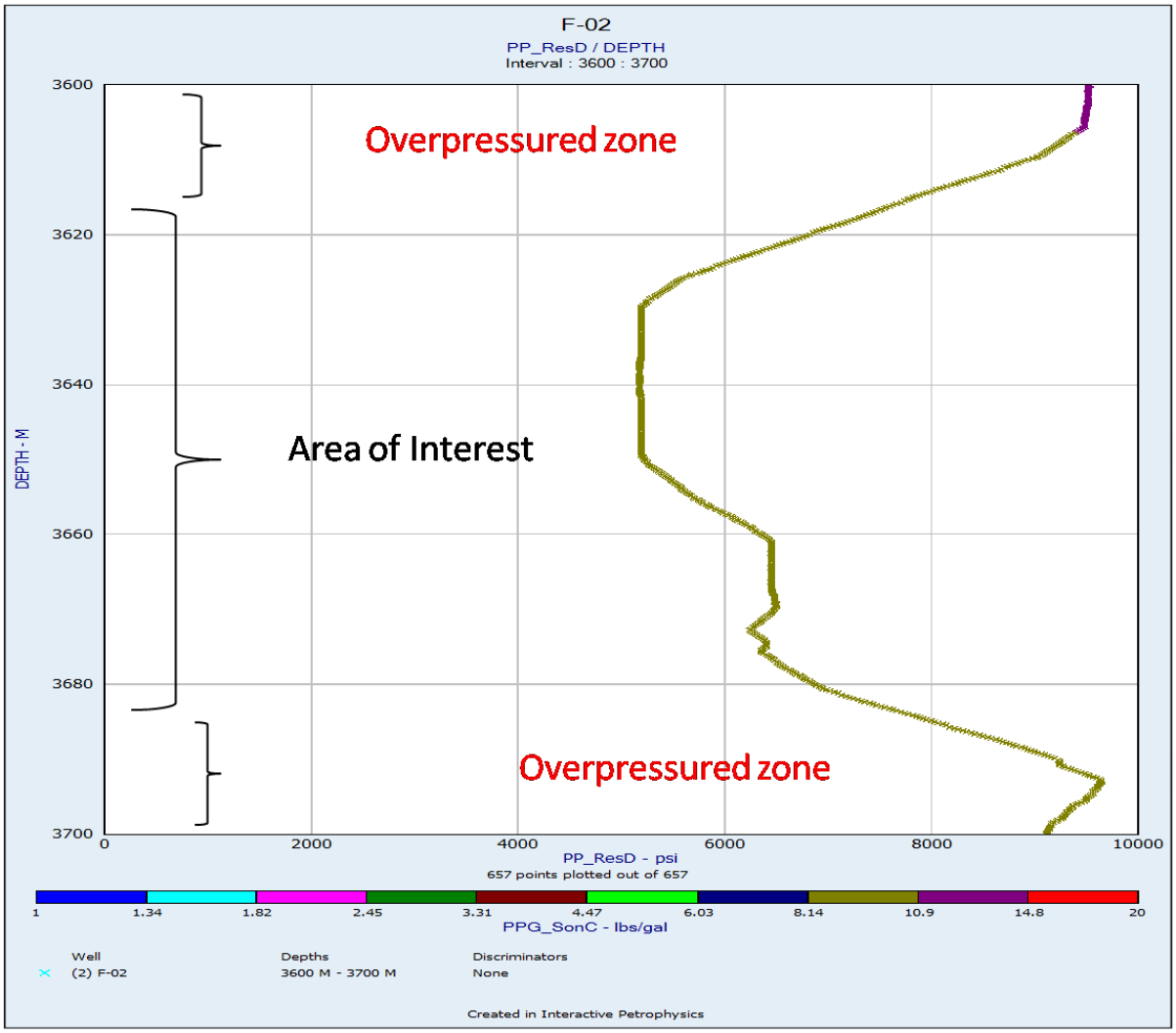

Figure 4.20 Cross plot of pressure Vs. depth of well F-02

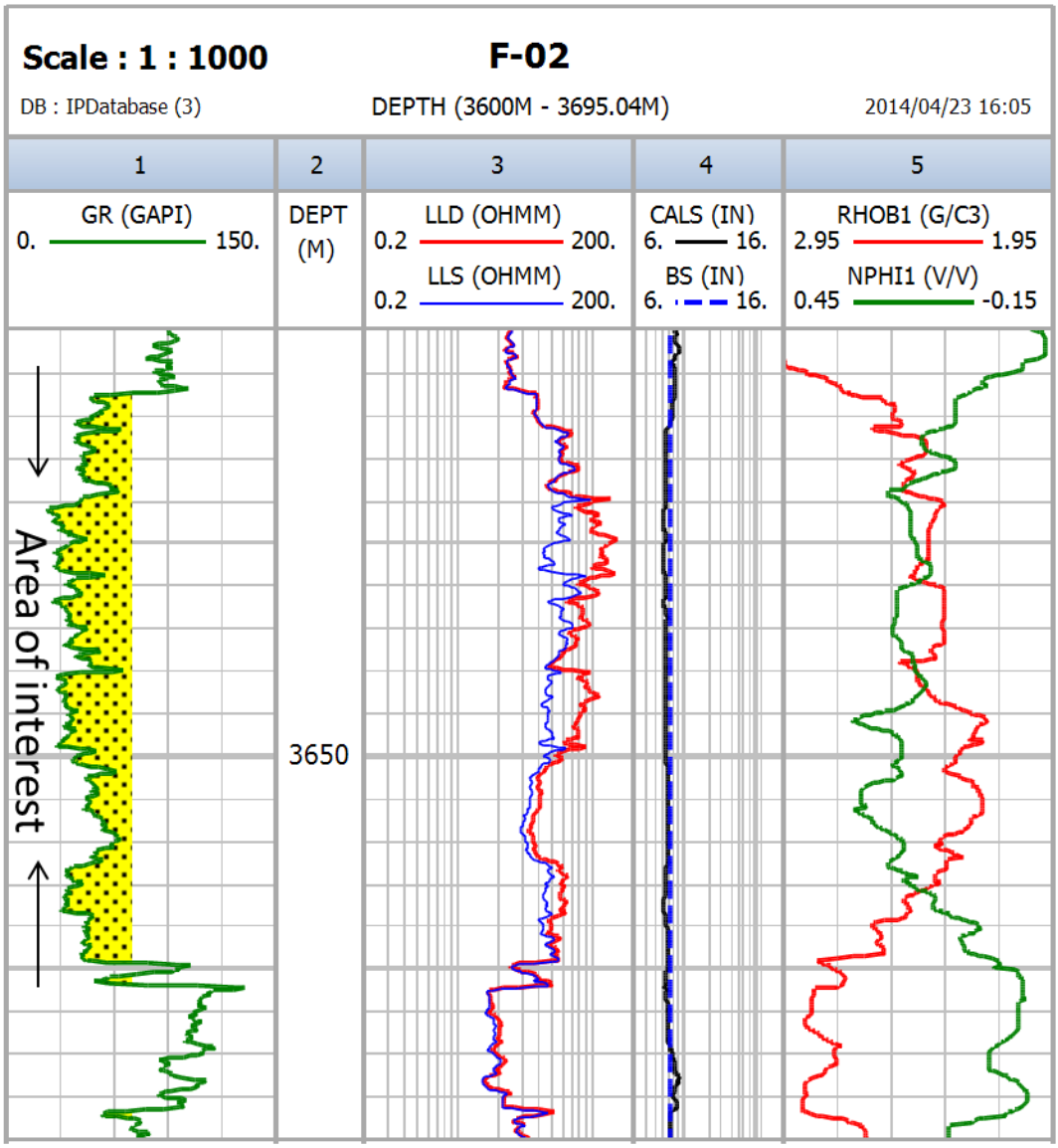

Figure 4.21 Log of well F-02 showing the density porosity and neutron porosity curves close movement.

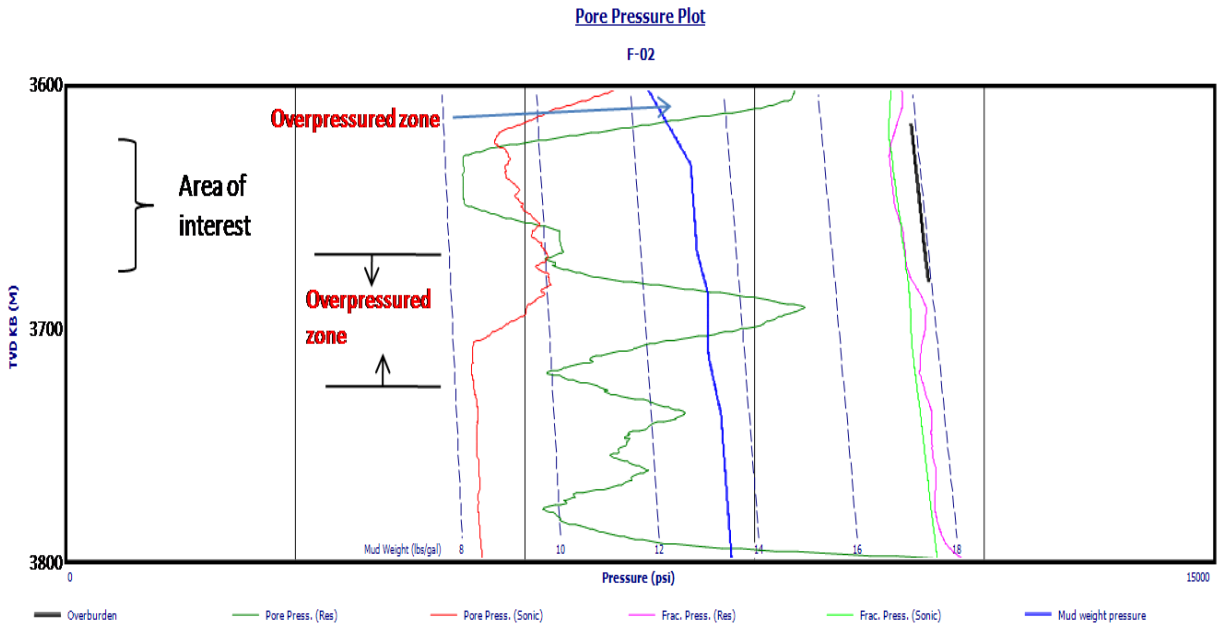

Figure 4.22 Cross plot of pressure vs. depth for well F-02

Figure 4.22 gives an idea of the workings inside the formation in relation to the mud weight and formation pressure. Mud weight increased around the 3602m zone and was maintained till around 3650m to 3665m area before the formation pressure spiked up(increased sharply) again at 3692m. As the formation pressure drops slowly after the spike, a gradual increase in the mud weight was noticed looking at the curve. This mud weight was probably maintained to total depth (TD) looking at smoothness of the curve.

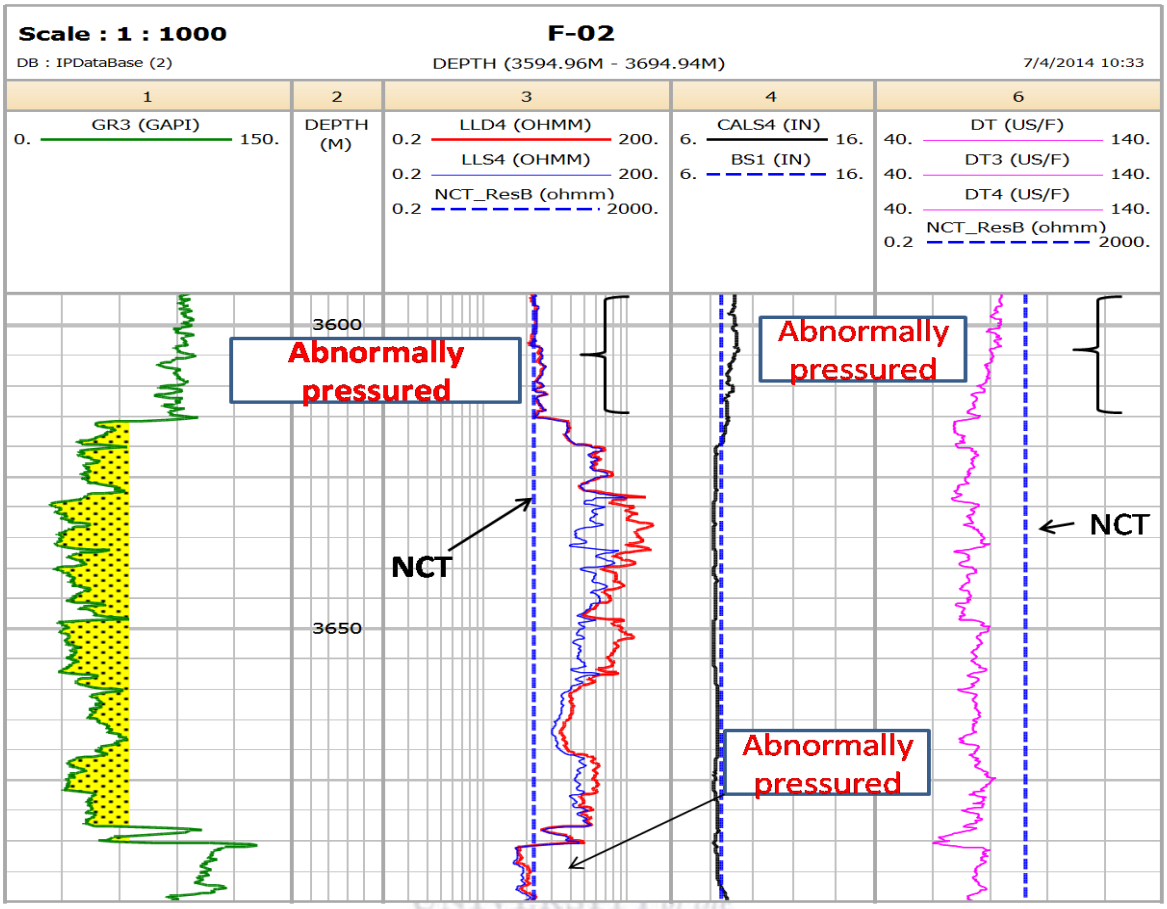

Figure 4.23 Normal compaction trend line (NCT) in relation to the resistivity curve(LLD) and sonic curve (DT) for well F-02

In the Figure above, the interval transit time curve (Dt) begins to decrease as it moves away from the Normal Compaction Trend line(NCT) approaching the area of interest and continues down to 3692m.This denotes normalcy in pressure in the area. The resistivity curve on the other hand increases at 3613m ,the top depth of the area of interest. It continued to increase downward from the Normal Compaction Trend line(NCT) until around 3693m. This also showed normal pressure at that range(3615m-3692m).

With the low resistivity value and high Dt value(interval transit time) at 3600m and 3693m,it shows that those regions are overpressured. The area of interest doesn't seem to be

overpressured from the higher resistivity reading on track 3 and low interval tansit time(Dt) reading on track 6 gotten at that zone.

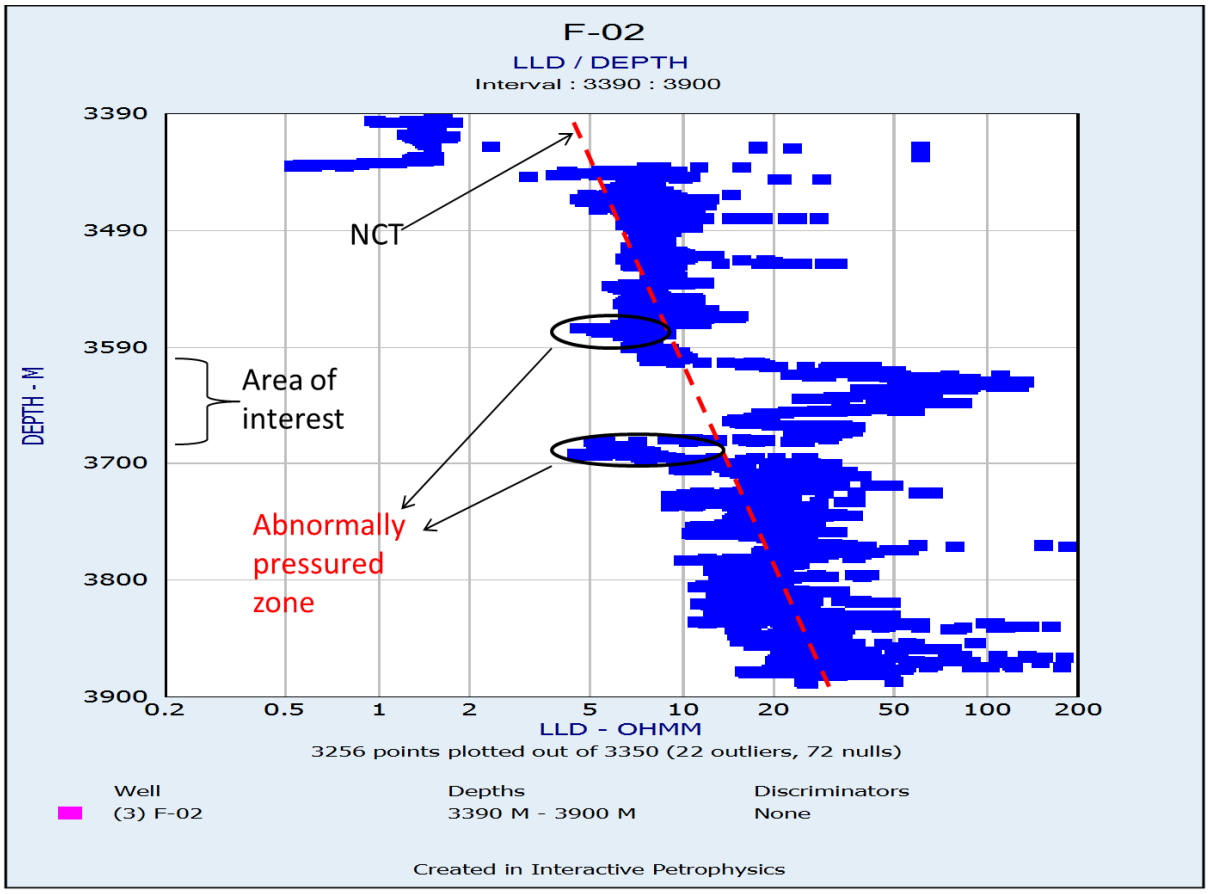

Figure 4.24 Resistivity vs depth plot of well F-02

From the figure above there is significant increase in resistivity at about 3620m – 3680m which lies within the area of interest. This characteristic (increase in resistivity) is associated with normal compaction and normal pressure, which infers that the reservoir is normal pressured (Chunduru, R., Ghosh, A., Kumar, M., 2009). At 3680m – 3700m there was significant decrease in the resistivity which is an indication of abnormal pressure.

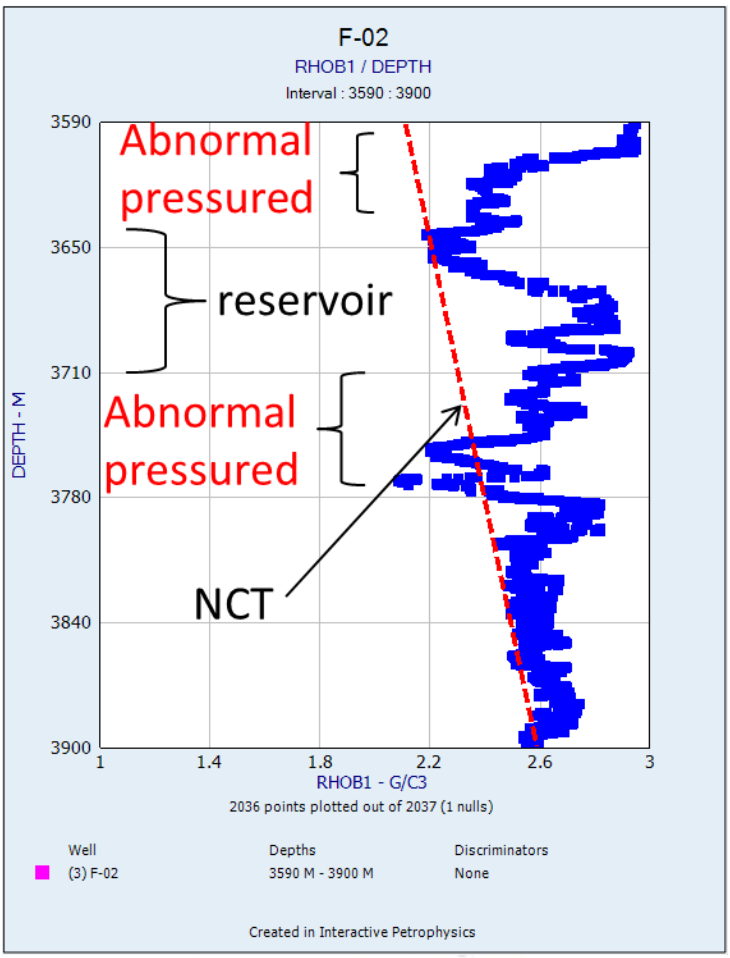

Figure 4.25 Density vs depth plot of well F-02

The density log versus depth plot above and sonic log versus depth plot below infers that 3620m – 3680m is not overpressured. Looking at the density curve increases at about 3620m – 3680m (normal pressure) before decreasing at about 3681m – 3700m (indication of abnormal pressure). Another significant decrease occurred at about 3704m.

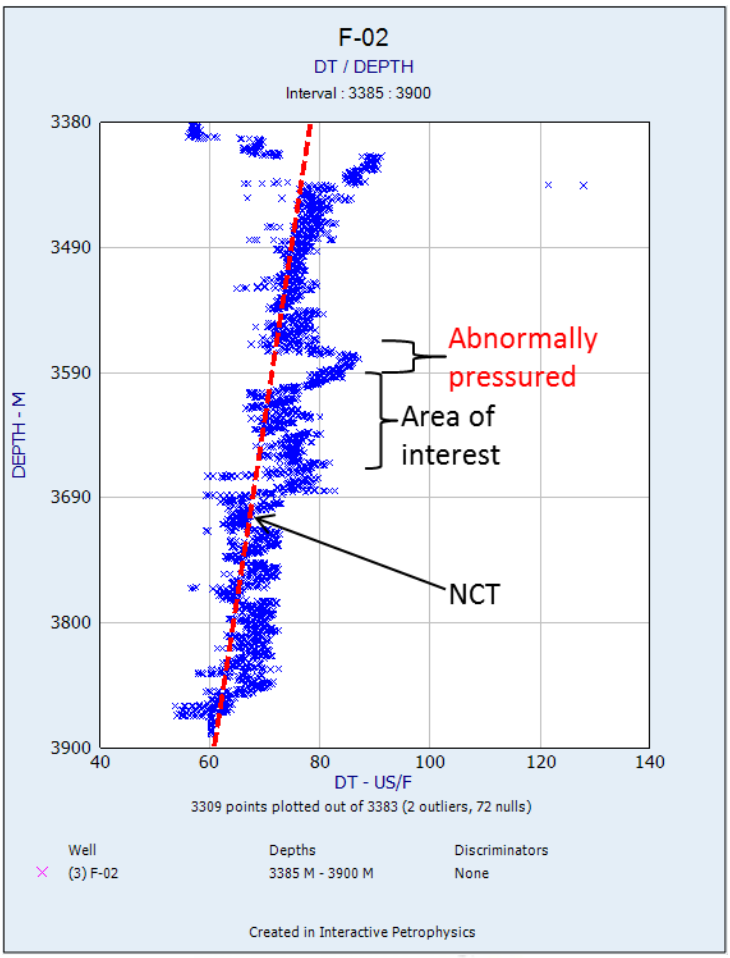

Figure 4.26 Sonic log vs depth plot for well F-02

The sonic log on the other hand increases at about 3550m which is at the top of the reservoir, an indication of abnormal pressure. It begins to decrease at about 3610m.

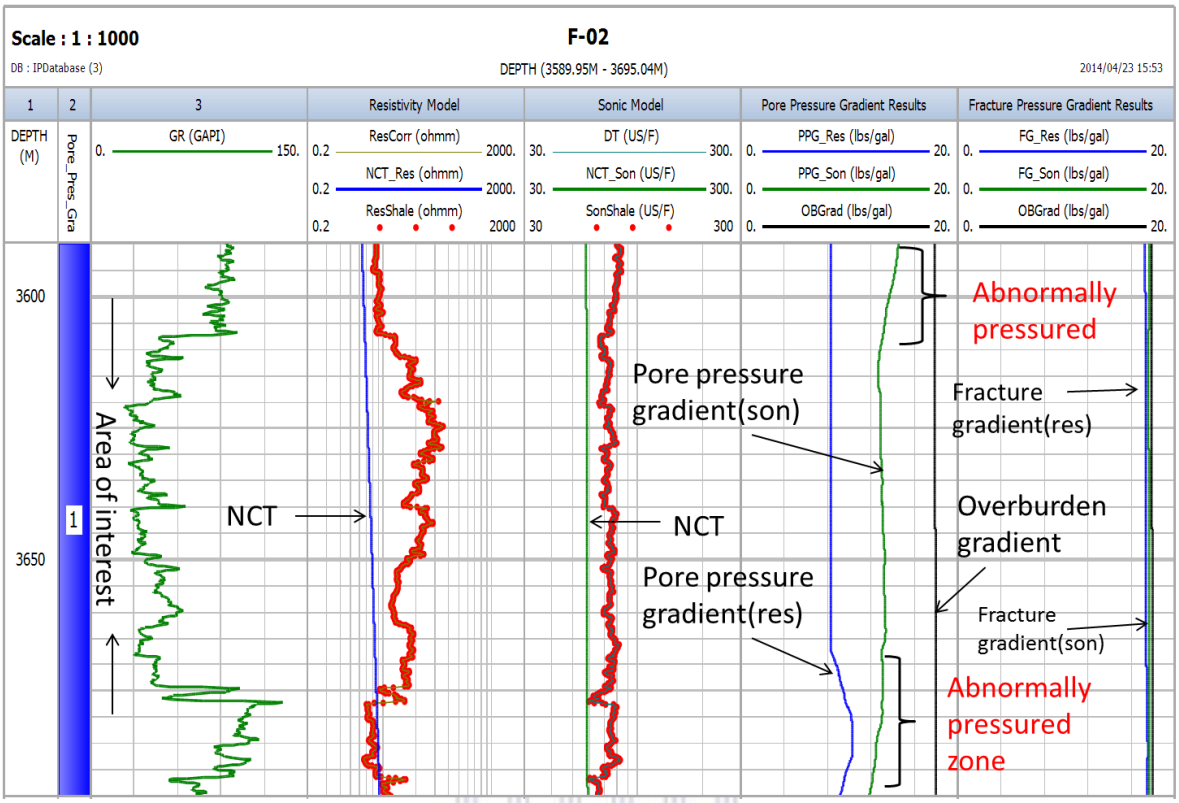

Figure 4.27 Pore pressure relationship with resistivity and sonic log for well F-02

4.2.3: WELL F-03

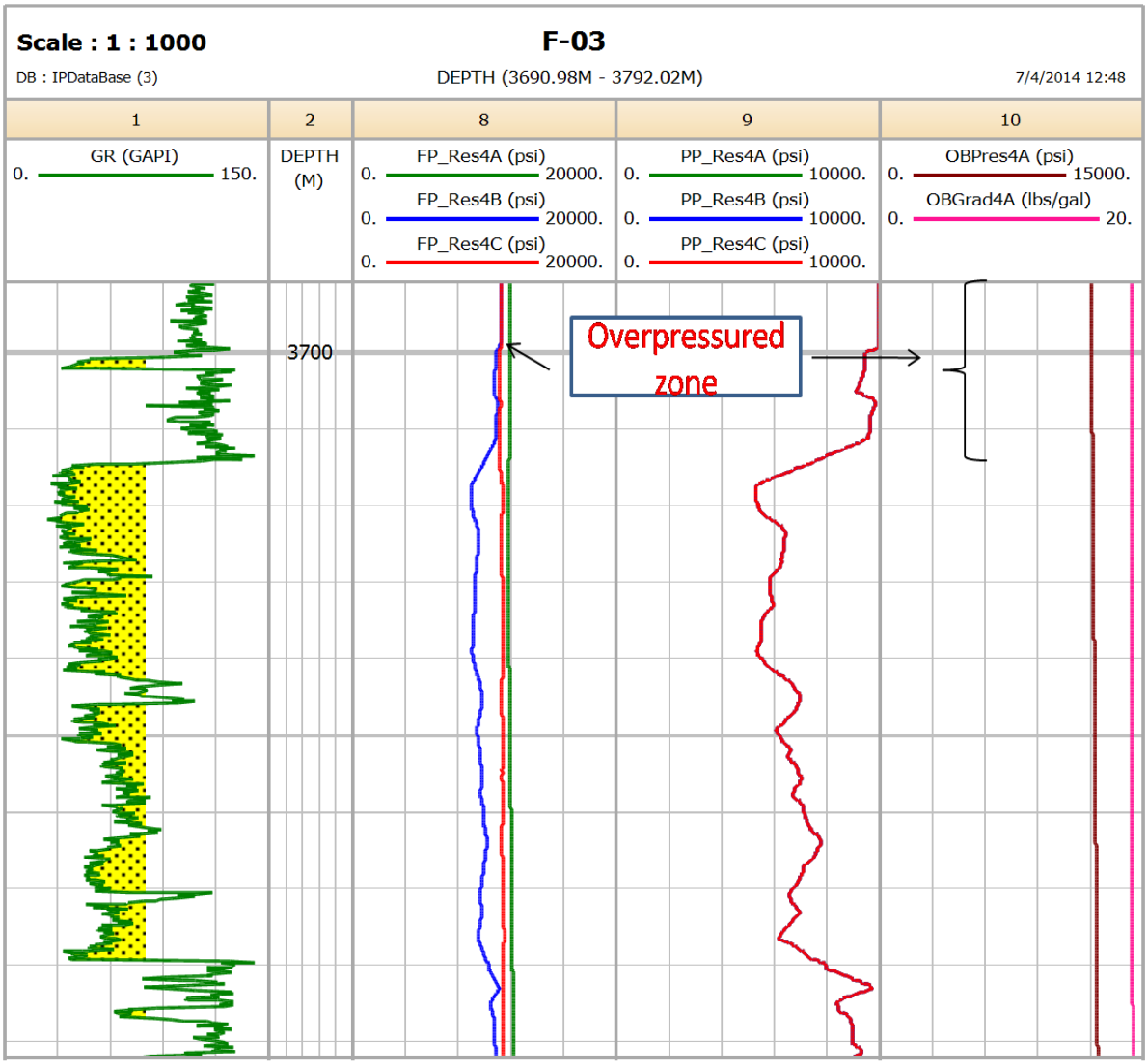

Figure 4.28 Fracture gradient and Pore pressure gradient curve in relation to well F-03 reservoir.

In well F-03 3719m – 3739m seems to be the only permeable zone around the area of interest with a 67% water saturation and very poor porosity. Looking at the pore pressure gradient curve at the Figure above, between 3719m-3739m there was a drop in pressure. This could be because of the permeability of this area as explained above for well F-01 and F-02. As the formation at this point is permeable this enables fluid to flow, releasing the stress on the pores

and formation. Note an increase in pore pressure gradient again below that zone (3719m-3739m).

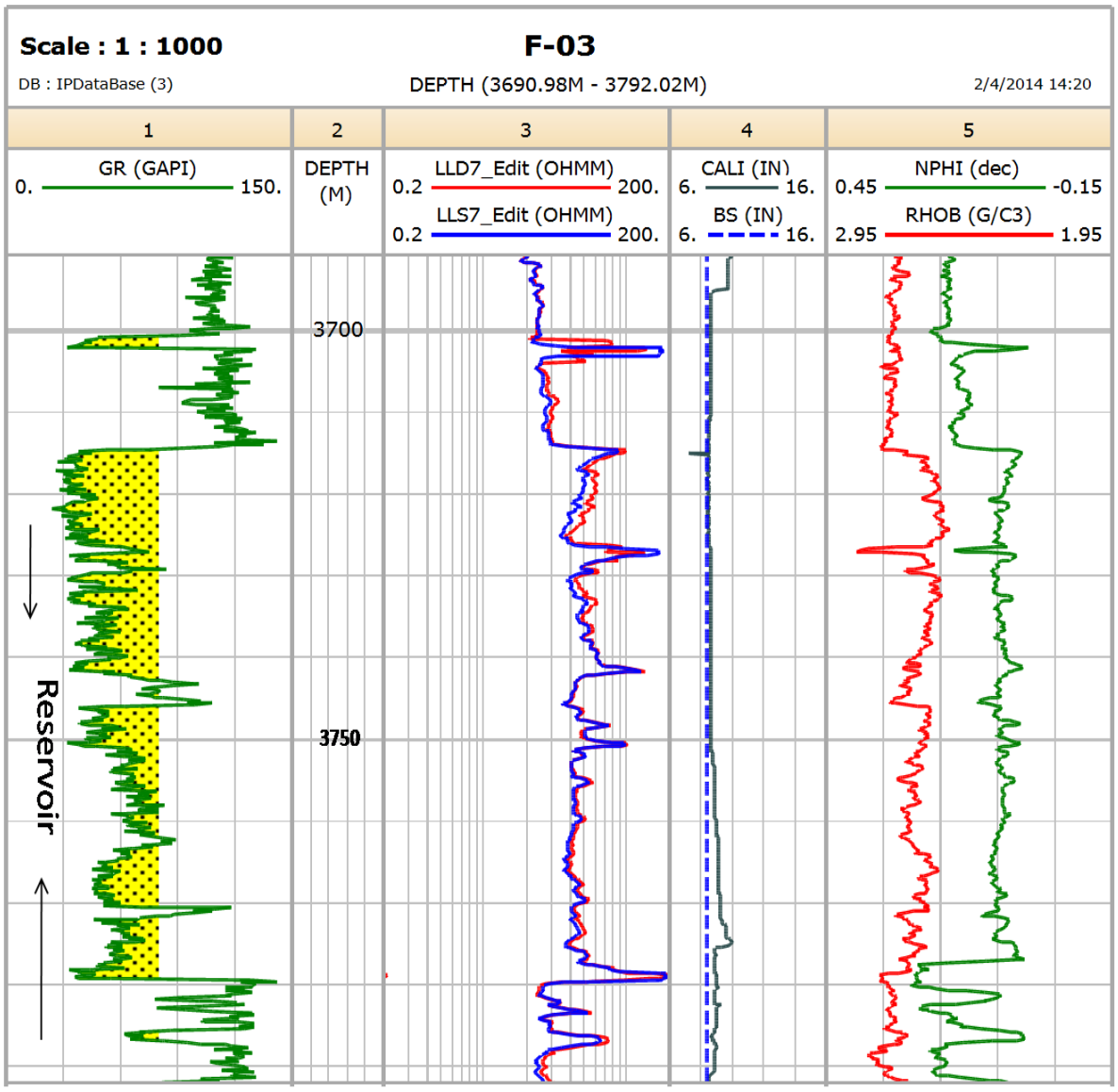

Figure 4.29 Bit Size (BS) and Caliper (CALI) curve cross of well F-03

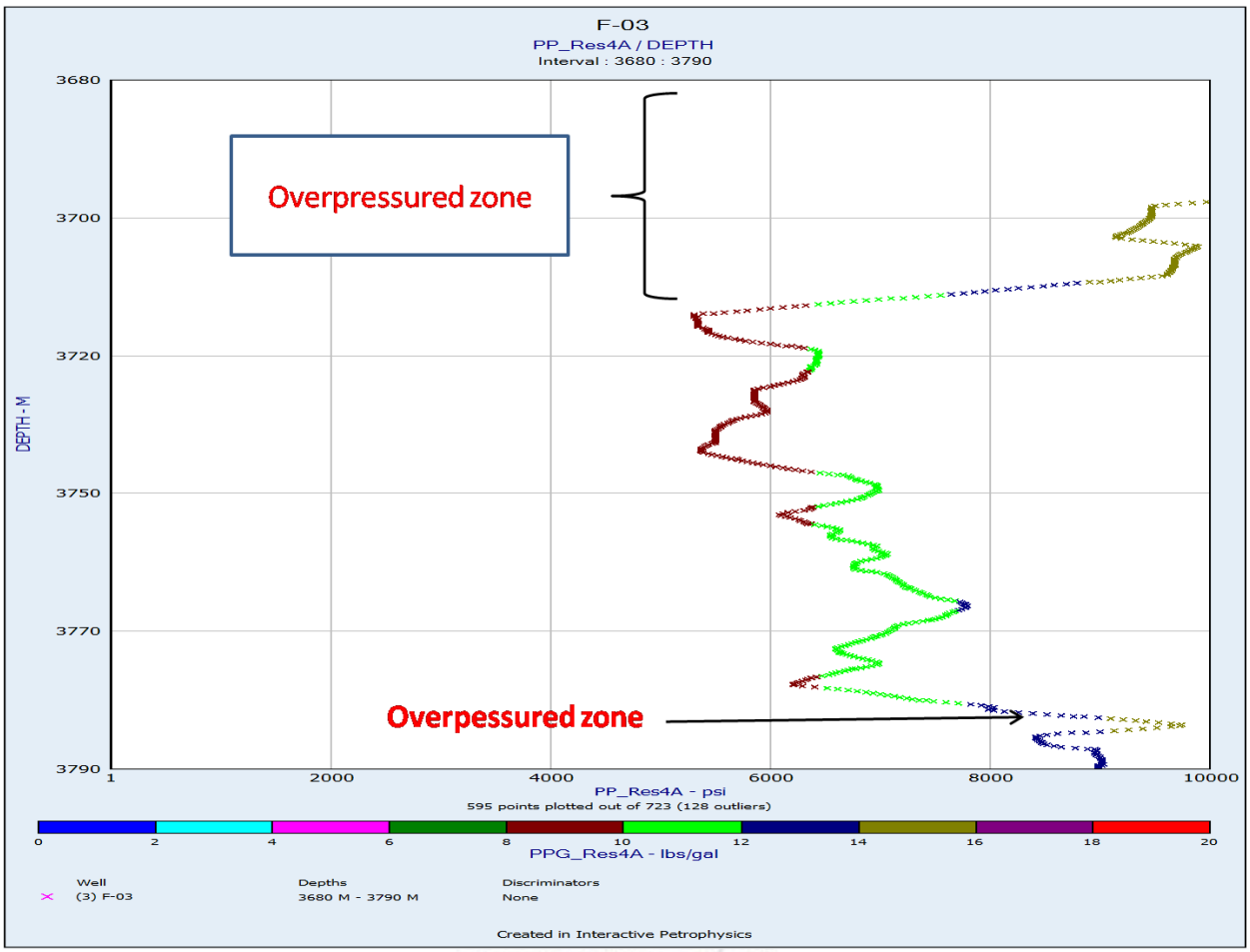

Figure 4.30 Cross Plot of Pressure vs. Depth of well F-03

From the pressure Vs. depth plot above, abnormal pressure (overpressure) was encountered at about 3689m to 3716m above the area of interest (Reservoir). Going below 3716m approaching the reservoir, a drop in pressure to about 5810psi at 3719m was observed. The pressure was within 5810- 6420psi range from 3719m to 3743m before increasing gradually again at 3744m,the pressure continued to increase downward to 3745m and reaching a high of 9736psi at 3783m.

Table 5.Summary of predicted pore pressure using various models and actual pore pressure

Well	Actual Pressure (psi)	Eaton Resistivity (psi)	Eaton Sonic (psi)	Eaton Modified (psi)	Mathew &Kelly (psi)	Bowers (psi)
F-01	7773psi@3719m	6078.8	5917	6078.8	6078.8	6078
F-02	7701psi@3635m	7861	6330	7861.6	7861	-
F-03	7982psi@3693m	8330	7419	8332	8332	-

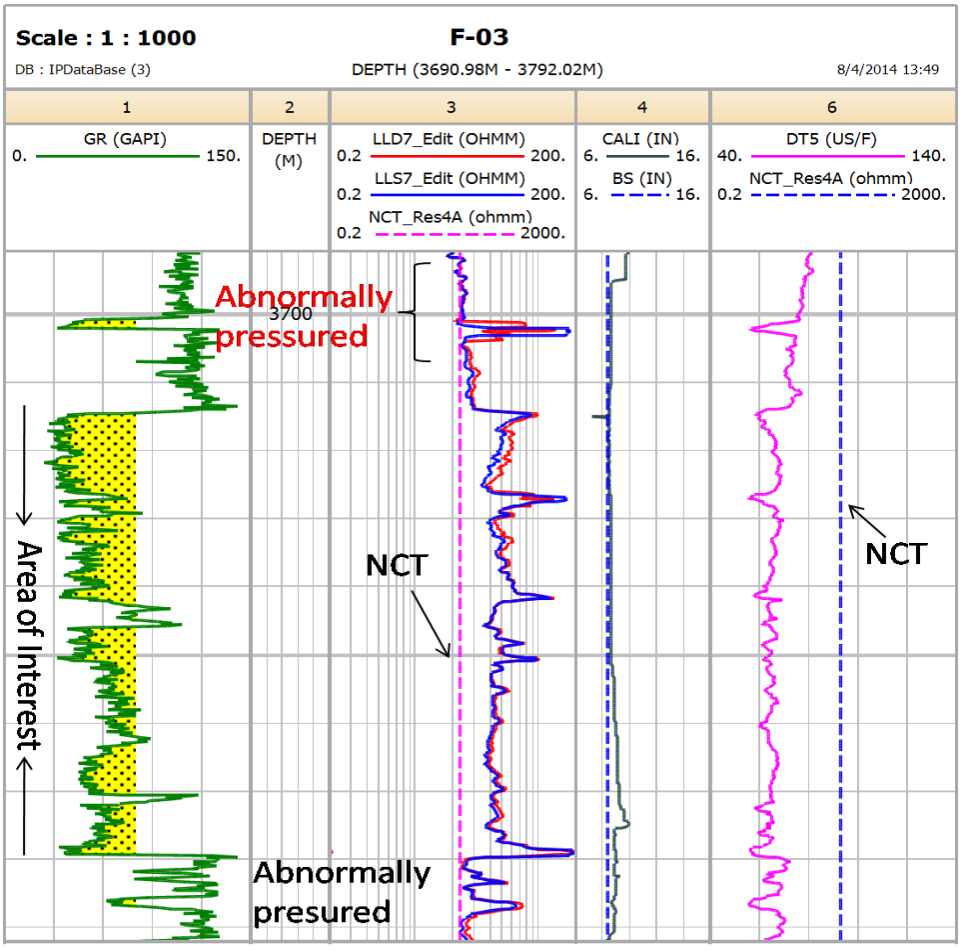

Figure 4.31 Normal compaction trend line, resistivity curve and sonic curve for well F-03

The resistivity curve increases in value moving away from the NCT line at 3700m in track 3 from the Figure above. From 3700m to 3780m the resistivity value is high as it deviates from the NCT line denoting that the area is not overpressured. The DT curve in track 3 also indicates this as it gives a low reading away from the NCT line (Chunduru, R., Ghosh, A., Kumar, M., 2009).

Areas above the reservoir are overpressured looking at the interval transit time (Dt) curve, resistivity (LLD) curve and normal compaction trend (NCT) line relation in track 3 and track 6 of the Figure above.

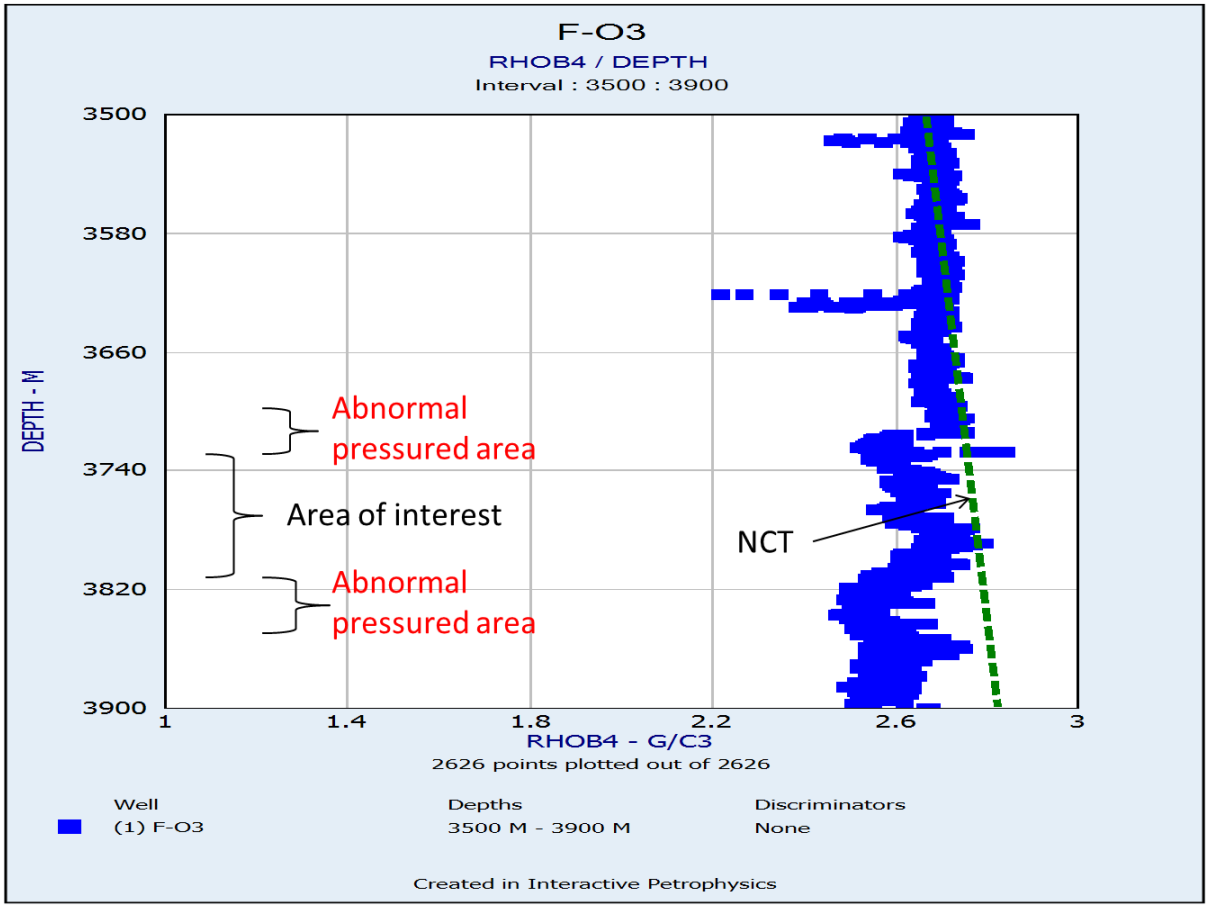

Figure 4.32 Density vs depth plot of well F-03

In well F-03 the density – depth plot indicates that at about 3690m – 3710m there is abnormal pressure due to the significant decrease in density. Around 3720m – 3770m the density

increases indicating normal compaction (normal pressure). At about 3780m it drops again, an indication of abnormal pressure.

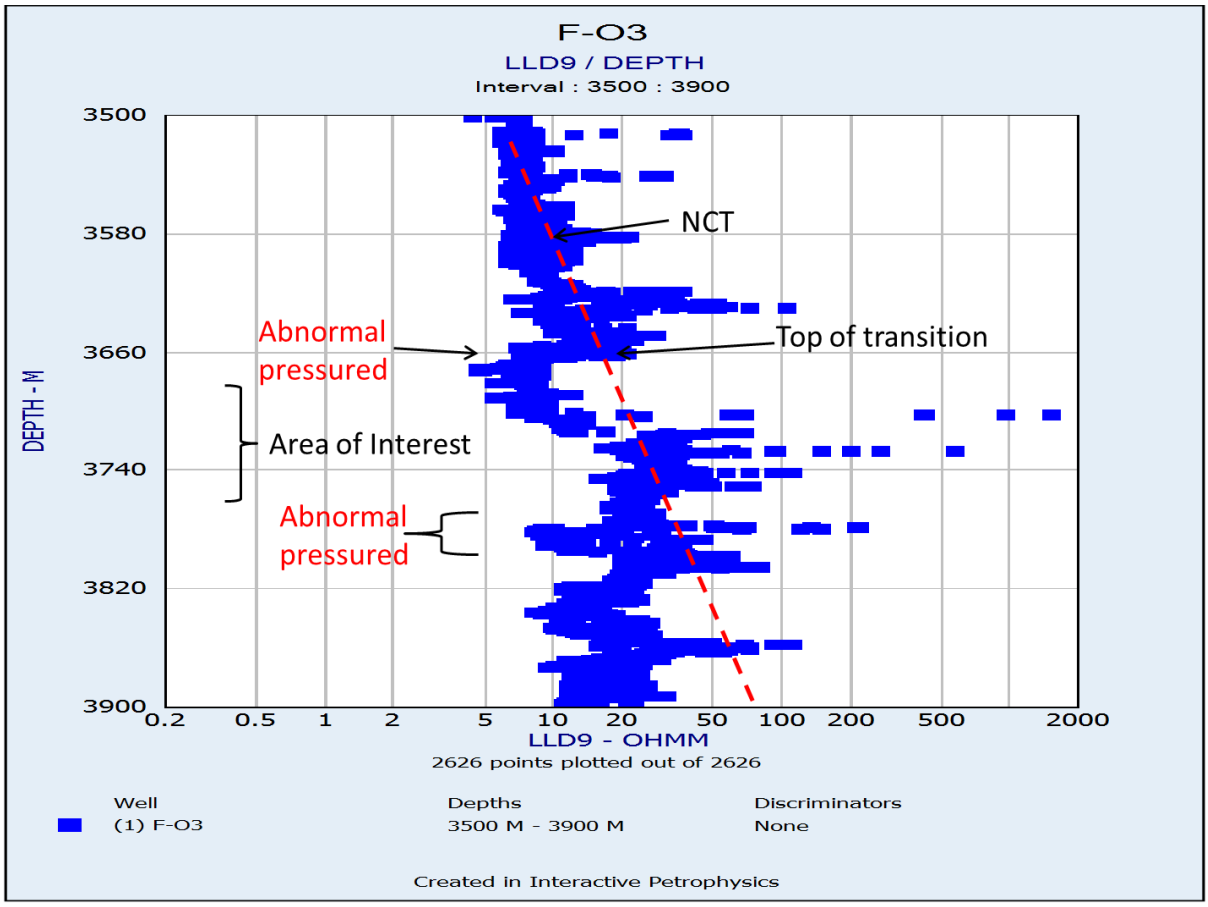

Figure 4.33 Resistivity vs depth plot of well F-03

At about 3670m – 3710m from the resistivity versus depth plot above there is a clear decrease in resistivity with depth, a property of abnormal pressure (undercompaction). From 3720m – 3770m the resistivity increases signifying normal compaction (normal pressure). There was another decrease in resistivity at about 3780m going down the formation, indicating abnormal pressure.

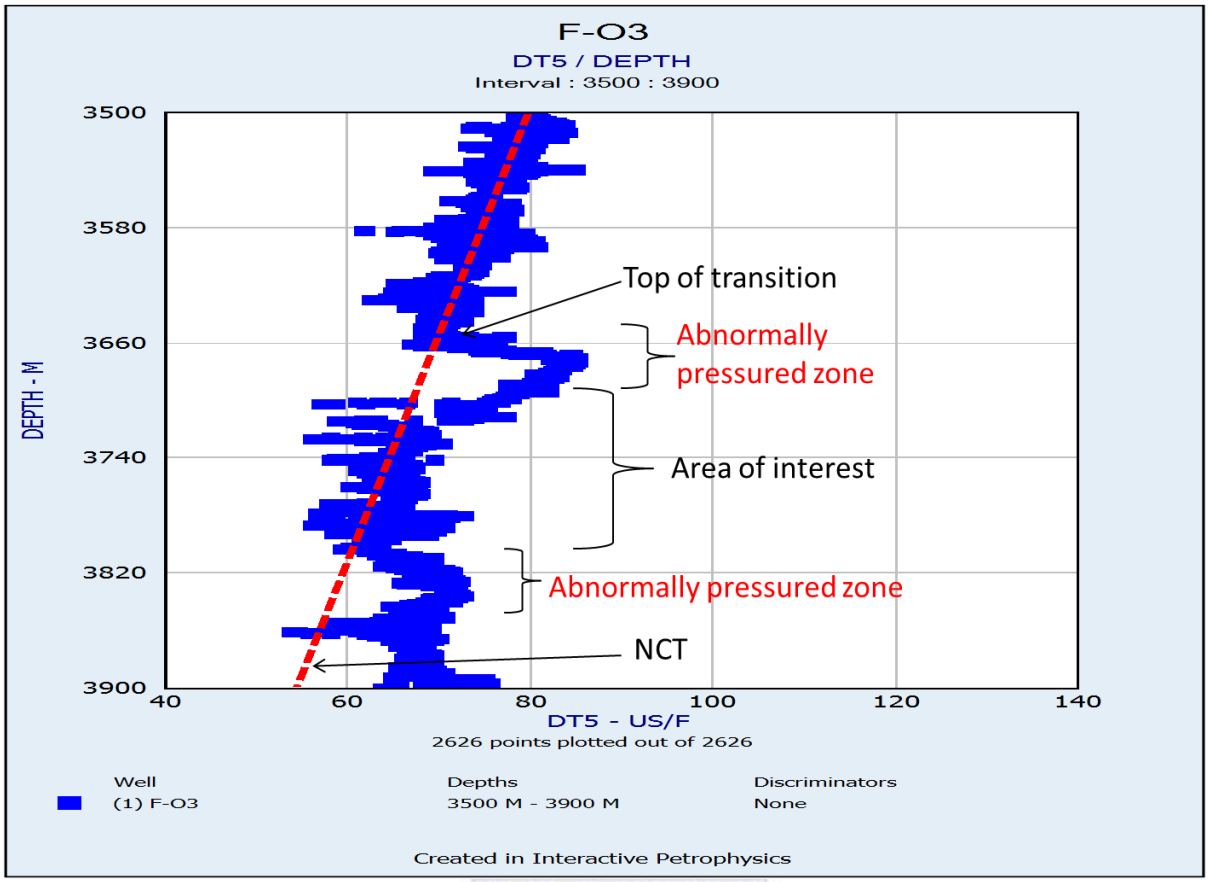

Figure 4.34 Sonic vs depth plot for well F-03

The sonic log in the figure above is in agreement with the density and resistivity plot versus depth as it indicates abnormal pressure at about the same intervals as the density and resistivity log plot.

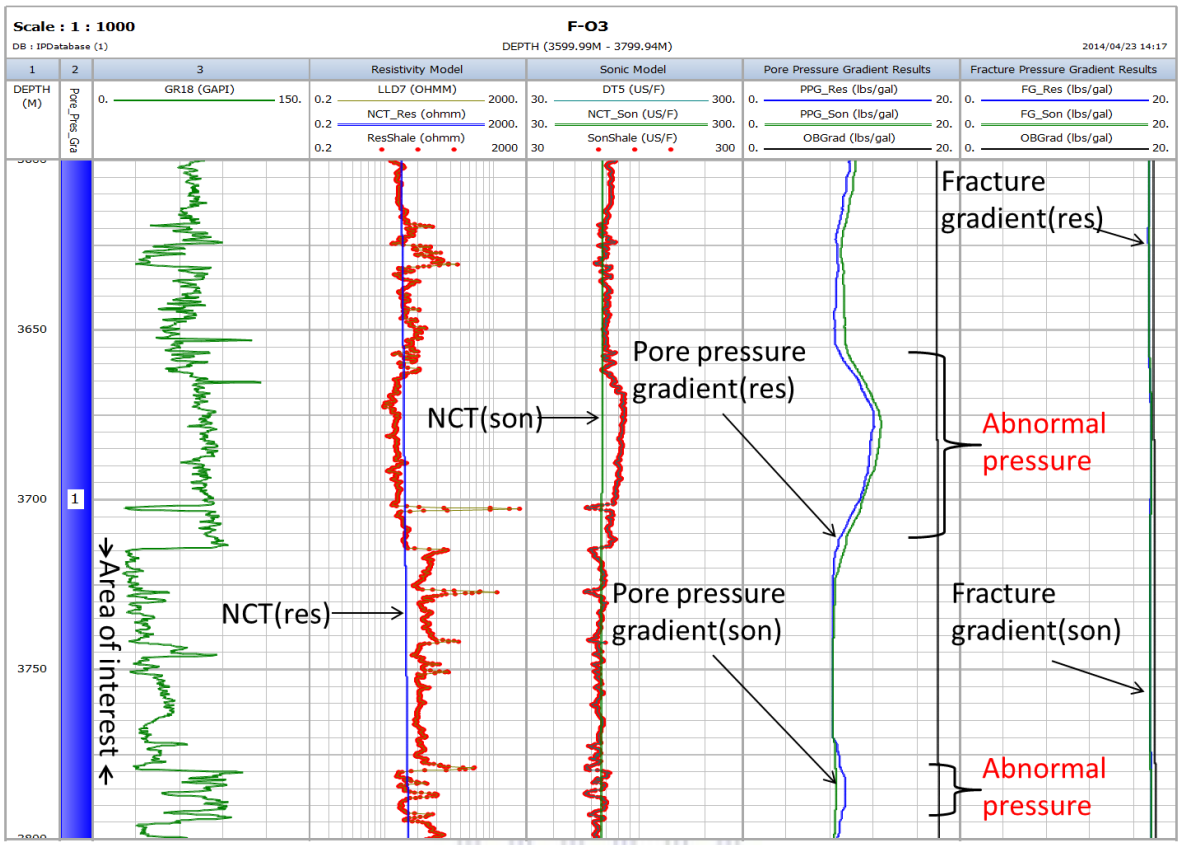

Figure 4.35 Pore pressure relationship with resistivity and sonic log for well F-03

Table 6. Typical features of pressured shales.

Normally Pressured Shales	
Porosity	Decreases with depth
Conductivity	Decreases with depth
Density	Increases with depth
Resistivity	Increases with depth
Sonic travel time	Decreases with depth
Temperature gradient	Relatively constant

(G.E.Omolaiye, E.A.Ayolabi, C.S.Ugwuabgo, 2013)

Table 7. Characteristics of abnormally pressured shale

Abnormally Pressured Shales	
Porosity	Higher than expected
Conductivity	Higher than expected
Density	Lower than expected
Resistivity	Lower than expected
Sonic travel time	Higher than expected
Temperature gradient	Increases with depth

(G.E.Omolaiye, E.A.Ayolabi, C.S.Ugwuabgo, 2013)

Table 8. Normal formation pressure gradients for several areas of active drilling.

Area	Pressure gradient (psi/ft)
West Texas	0.433
Gulf of Mexico coastline	0.465
North sea	0.452
Malaysia	0.442
Mackenzie delta	0.442
West Africa	0.442
Anadarko basin	0.433
Rocky mountains	0.436
California	0.439
South Africa	0.449

CHAPTER FIVE

5.0: CONCLUSION

The reservoir in the wells F-01 – F-03 of the Bredasdorp basin contains little or no hydrocarbon but more gas and seems to be a gas reservoir or potential gas reservoir. They all have overpressured zones around the area of interest with well F-03 having the highest pressure. Predictions using various models shows that the Ben Eaton Resistivity model is the closest to the actual pressure but doing some manual calculations using the Ben Eaton model and the Field Method shows that the field method was more accurate in calculating the pore pressures or that was the actual method used by the Engineers in calculating the pore pressure (actual) of the reservoir at the time. Areas within the reservoirs had pressures ranging from 5194psi to 6371psi with F-03 again having the highest .This is to say that the F-03 well is the most overpressured of all the wells having higher pressure readings within and around the reservoir. Pressure of 5329psi was encountered within the reservoir of well F-01, pressure of 5194psi, 5732psi (at 3631-34m), 6446psi, 6008psi (at 3661m) within F-02 and 6371psi (at 3950m) within F-03. In well F-01, low porosity values were gotten, some areas of the reservoir sandstone possess poor porosity(below 10%) qualities while some areas like the 3709m – 3728m are fairly good and possess fairly good porosity(above 10%) qualities. F-02 is not really a good reservoir at the time with a porosity of 10% but with the gas it contains, there is some potential. The gas although seems to be locked up by shale or tight formation. F-03 contains gas too but the sandstones are really over pressured. Abnormally pressured zones of the well F-01, F-02, and F-03 were easily identified using the proposed approach. Predicted abnormal pressure around the zone of interest for well F-01 is about 6078psi at 3719m while the actual pressure is 7773psi, for well F-02 it's about 7861psi(predicted) and 7701psi(actual) at 3635m, and for well F-03 about 8330psi(predicted) at 3693m and 7982psi(actual). Analysis of resistivity, sonic, and density log data shows that overpressure in the formation could be inferred to be generated by disequilibrium compaction based on porosity anomaly.

Limitations;

One of the limitations encountered is late provision of data for well F-03 which caused modifications here and there and slowed down the progress of this study. Also unavailability of data for well F-01 and F-03 towards the end of the study especially sonic/interval transit time data which lead to some improvising but in the end much of the work was done.

LIST OF ACRONYMS

NCT ……. Normal compaction trend

LWD……. Logging while drilling

GWC ……. Gas water contact

DST ……. Drill stem test

RFT ……. Repeat formation test.

KB ……. Kelly bushing

BS ……. Bit size log

m ……. Meters

ILD ……. Resistivity log

AAPG ……. American association of petroleum geologist

GR ……. Gamma ray log

Phi ……. Porosity log

CALi ……. Caliper log

Sw ……. Water saturation

NPHI ……. Neutron porosity log

RHOB ……. Neutron density log

DT ……. Sonic transit time log

FG …….. Fracture gradient

PPG …….. Pore pressure gradient

LOT …….. Lick off test

OBG …….. Overburden gradient

Png …….. Hydrostatic pore pressure

Rn …….. Normal shale resistivity

R …….. Resistivity

Mwd …….. Measurement while drilling

Dtn …….. Sonic travel time at normal pressure

QC …….. Quality control

LQC …….. Log quality control

Vsh …….. Volume of shale

TVD …….. True vertical depth

ITT …….. Interval transit time

Vcl …….. Volume of clay

Psi …….. Pound per square inch (unit for pressure)

TD …….. Total depth

5.1: REFRENCES

Baker, C. (1972): Aquathermal pressuring- role of temperature in the development of abnormal pressure zones. AAPG Bulletin, 72, 1334-1359.

Bowers, G.L. (2001): Determining an Appropriate Pore Pressure Estimation Strategy, Paper OTC 13042.

Bradley, J.S., (1975): Abnormal formation pressure, AAPG, vol. 59/6, PP. 967-973.

Burden, P.L.A., (1992): SOEKOR Partners explore possibilities in Bredasdorp basin off South Africa. Soekor (Pty.) Ltd. Parow, South Africa.

Cengiz, E. and Subhashis, M.(2004): Real time pore pressure prediction ahead of the Bit. Schlumberger Technology Corporation,110 Schlumberger drive,MD#4 Sugar land, Texas 77478,USA and WesternGeco,10001 Richmond Ave Houston, Texas 77042,USA. Report prepared for Research Partnership to Secure Energy of America, 1650 highway 6, suite 300 Sugar land, Texas, USA.

Dutta, N.C.(2002): Geopressure prediction using seismic data: Current status and road ahead: Geophysics, 67, 2012-2041.

Eaton, B.A. (1968): Fracture gradient prediction and its application in the oil field operations Paper SPE2 163 JPT 25-32.

Eaton, B.A. (1972): Graphical method predicts geopressures worldwide, World Oil, 182, 1972, 51-57.

Eaton, B.A. (1975): The Equation for geopressure prediction from well logs society of petroleum engineers of AIME. Paper SPE 5544.

Gutierrez, M.A, Braunsdore, N.R., Couzens, B.A. (2006): Calibration and ranking of pore pressure prediction models. The leading Edge, Dec., 2006, pp. 1516-1523.

Haney, M.M, Hofmann, H. and Snieder R*:* Well-log analysis of pore pressure mechanisms near a minibasin-bouding growth fault at South Eugene Island field, offshore Louisiana. Center of wave phenomenon, Center of Rock abuse and Sandia National Laboratories, Department of Geophysics and Geophysical technology Department, Colorado School of Mines, Golden, Colorado, USA.

Hussain Rabia : Well Engineering and construction. [Online] Available

http://faculty.ksu.edu.sa/shokir/PGE472/Textbook%20and%20References/RABIA%20-%20WELL%20ENGINEERING%20%20CONSTRUCTION.pdf

Iain Hillier, Baker Hughes, INTEQ: Origins of Abnormal Pore Pressure. [Online] Available

http://www.lps.org.uk/dialogweb/current_articles/hillier_abnormal_pressure/abnormal_pressure.htm

Jeffrey, S.F. (2009): The development of a pore pressure and fracture gradient prediction model for Ewing Banks 910 area in the Gulf of Mexico.

Jincai, Z. (2011): Earth science reviews: pore pressure prediction from well logs; methods, modifications, and new approaches. Shell Exploration and Production Company, Houston, Texas, USA.

Jincai, Z. (2013): Effective stress, porosity, velocity and abnormal pore pressure prediction accounting for compaction disequilibrium and unloading. Shell Upstream Americas, USA.

Lopez, J.L., Rappold, P.M., Ugueto, G.A., Wieseneck, J.B., Vu, K. (2004): Intergrated shared earth model : 3D pore pressure prediction and uncertainty analysis. The Leading Edge, Jan., 2004, pp. 52-60.

McMillan, I.K., McLachlan, I.R. (1979): Microfaunal biostratigraphy, chronostratigraphy and history of the Mesozoic and Cenozoic sediments on the coastal margin of South Africa.Spec. Publ.geol.Soc.S.Afr., 6, 161-182.

Mouchet, J.P., Mitchell, A. (1988): Abnormal pressures while drilling published by Elf aqutainemanuel techniques 2.

Omolaiye, G.E, Ayolabi, E.A., Ugwuagbo, C.S. (2013): Pore pressure evaluation and prediction in Esenam field, Nothern Depobelt Niger delta, Nigeria.

Paul, S., Chatterjee, R., Kundan, A. (2009): Estimation of pore pressure gradient and fracture gradient from well logs: A theoretical analysis of techniques in use, Indian Oil and Gas review symposium and international exhibition (IORS 2009) September 11-12, Mumbai, India.

Petroleum Agency SA., (2008): Petroleum Exploration: Information and opportunities 2008. Petroleum Agency SA, 30pp.

Petroleum Agency SA., (2008b): Exploration opportunities with the Arniston half-graben and Western Bredasdorp Basin. Petroleum Agency SA.Www.petroleumagencysa.com

Pritambera: Estimation of pore pressure from well logs: a theoretical analysis and case study from an offshore basin, North Sea. Indian School of Mines, Dhanbad Jharkhand-826004, India.

Quijada, M.F, Stewart, R.R.(2007): Petrophysical analysis of well logs from Manitou lake, Saskatchenwan.

Richard, E.S.(2002): Challenges of porosity-based pore pressure prediction. University of Durham, Department of Geological Sciences, England.

Richard, S. (2012): Review of pore pressure prediction challenges in high temperature areas. IkonGeopressure.

Sara, B. and Anirbid, S. (2011): A comparative study of predicted and actual pore pressures in Tripur,India. School of Petroleum Technology,Raisan, Gandhinagar-382007, Gujarat, India.

Satinder, C. and Alan, R.H.(2006): Velocity determination for pore pressure prediction. Acis Corporation, Calgary, Canada and Fusion Petroleum Technologies, Houston, USA.

Shuling, L., Cary, P. and Shinguo, W. (2012): Pore pressure and fracture gradient prediction in shale gas formations: Accounting for complex rock properties and anisotropies. Halliburton, Asia.

Van der Spuy, D. (1990): Organic maturity and burial history modelling in petroleum exploration, offshore South Africa. Geol. Soc. S. Afr., Geocongress '90, abstracts, 742-744.

Van der Spuy, D. (2003): Aptian source rocks in some South African Cretaceous basins.Geol. Soc. London, Spec Pub, 181-198.

Van Wagoner, J.C., Mitchum, R.M., Campion, K., and Rahmanian, V.D., (1990): Siliciclastic Sequence Stratigraphy in well Logs, Cores and Outcrops: American Association of Petroleum Geologists, Tulsa, pp. 55.

RELATED WEBSITES:

http://www.senergyworld.com/software/interactive-petrophysics-overview

http://www.mxcad.com/ip/advanced-interpretation/205-pore-fracture-pressure-gradient-calculations-962

http://www.metu.edu.tr/~kok/pete322/322CHAPTER-2.pdf

http://www.lps.org.uk/dialogweb/current_articles/hillier_abnormal_pressure/abnormal_pressure.htm

http://petrowiki.spe.org/Methods_to_determine_pore_pressure

http://www.metu.edu.tr/~kok/pete322/322CHAPTER-3.pdf

http://www-odp.tamu.edu/publications/161_SR/chap_10/c10_4.htm

http://faculty.ksu.edu.sa/shokir/PGE472/Textbook%20and%20References/RABIA%20-%20WELL%20ENGINEERING%20%20CONSTRUCTION.pdf

http://www.sciencedirect.com/science/article/pii/S0264817213000913?np=y